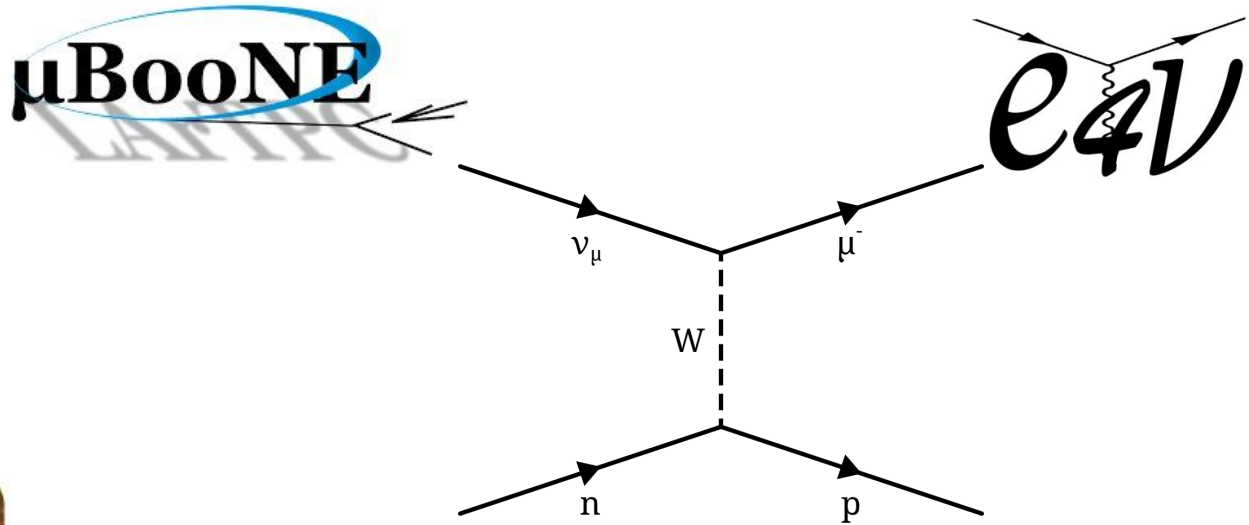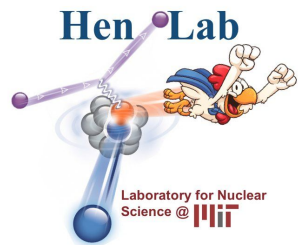# Exclusive Quasielastic-like ν_μ-^{40}Ar Interactions in MicroBooNE and Connections with Electron Scattering

Wine & Cheese Seminar, Oct 30 2020

A.Papadopoulou (apapadop@mit.edu)
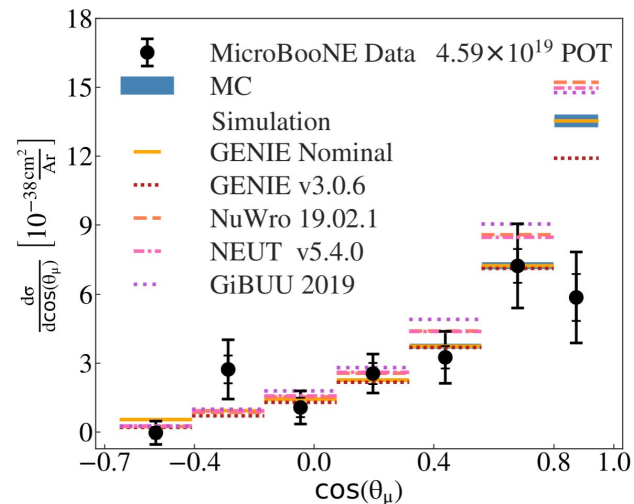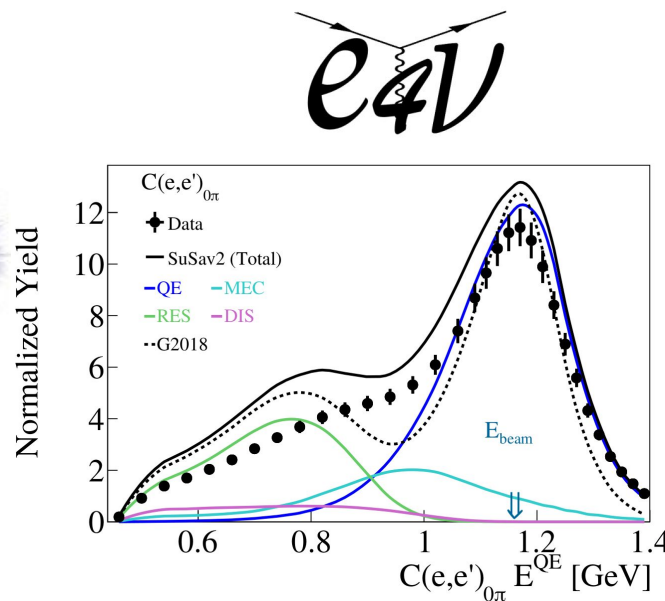on behalf of the MicroBooNE & e4ν collaborations

Overview

- Era of high precision neutrino oscillation measurements

- Liquid Argon Time Projection Chambers (LArTPCs)
  are state-of-the-art detectors in neutrino physics

- Demand for highly precise ν cross section measurements
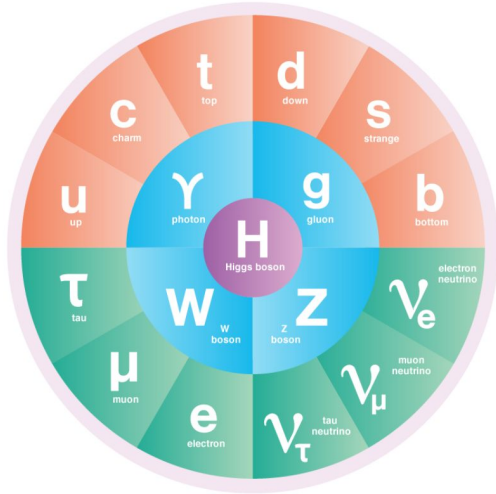
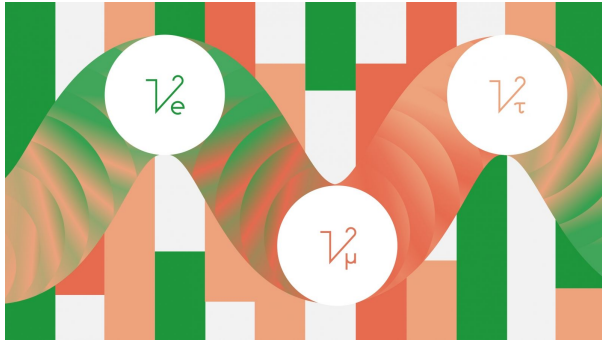# Outline

μBooNE

Modeling Input

e4ν

- First exclusive measurement of Quasielastic-like interactions using the MicroBooNE detector

- Connections with electron scattering

3

Neutrinos

Standard Model
- 3 (anti-)neutrinos of 3 flavours
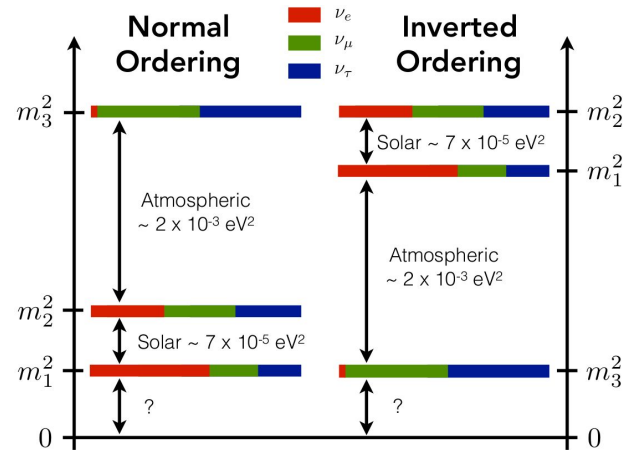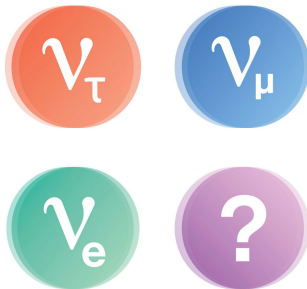- Massless
- Interact weakly
  (W / Z exchange)

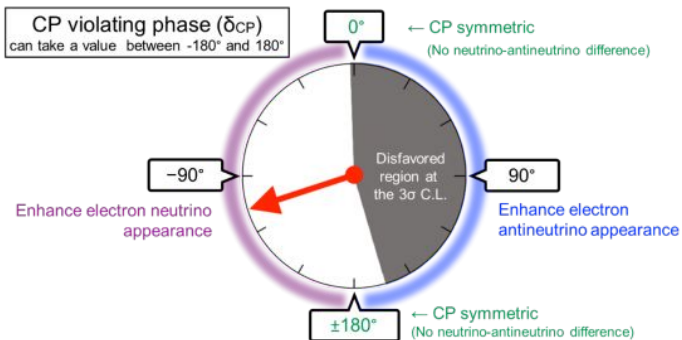**Beyond Standard Model**
- Neutrino oscillate → have mass

Yet a lot of open questions …

Open Questions

- Absolute mass
- Mass ordering
- CP violation
- Nature of neutrinos (Dirac vs Majorana)
- Sterile neutrinos

ν_τ ν_μ

ν_e ?

Normal Ordering   Inverted Ordering

ν_e ν_μ ν_τ

m_3^2 m_2^2

Solar ~ 7 x 10⁻⁵ eV²

m_1^2

Atmospheric ~ 2 x 10⁻³ eV²

Atmospheric ~ 2 x 10⁻³ eV²

m_2^2 Solar ~ 7 x 10⁻⁵ eV²

m_1^2 m_3^2

?   ?

0   0

A.Himmel, Neutrino 2020

T2K *Nature* **580**, 339–344 (2020)

CP violating phase (δCP) can take a value between -180° and 180°

0°   ← CP symmetric (No neutrino-antineutrino difference)

−90°   Disfavored region at the 3σ C.L.   90°

Enhance electron neutrino appearance   Enhance electron antineutrino appearance

±180°   ← CP symmetric (No neutrino-antineutrino difference)

NOvA Preliminary

Normal Hierarchy

$\sin^2\theta_{23}$

T2K, Nature 580: ■ BF — ≤ 90% CL ⋯ ≤ 68% CL
NOvA: ✦ BF □ ≤ 90% CL ■ ≤ 68% CL
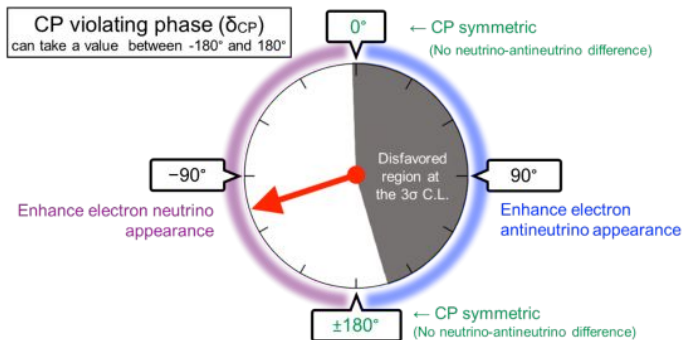
0 $\frac{\pi}{2}$ π $\frac{3\pi}{2}$ 2π

δ_{CP}

- Absolute masses
- **Mass ordering**
- **CP violation**
- Nature of neutrinos (Dirac vs Majorana)
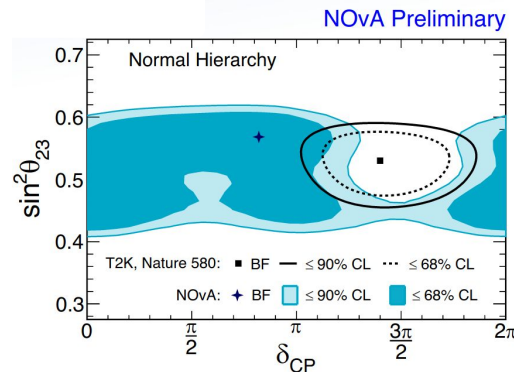- **Sterile neutrinos**

Investigated with short- & long-baseline oscillation experiments
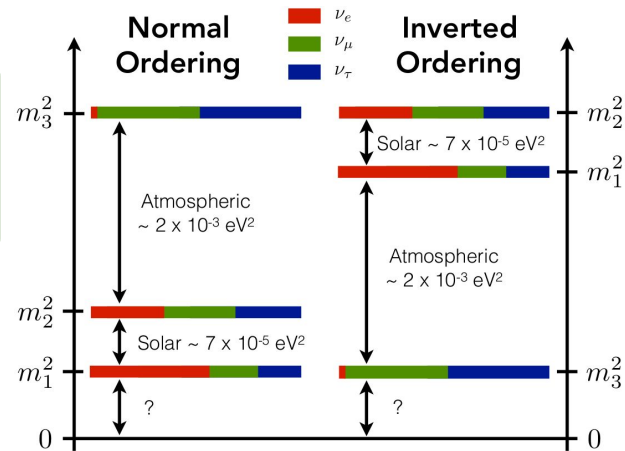
T2K *Nature* **580**, 339–344 (2020)

A.Himmel, Neutrino 2020

Neutrino Oscillation Experiments

ν_α

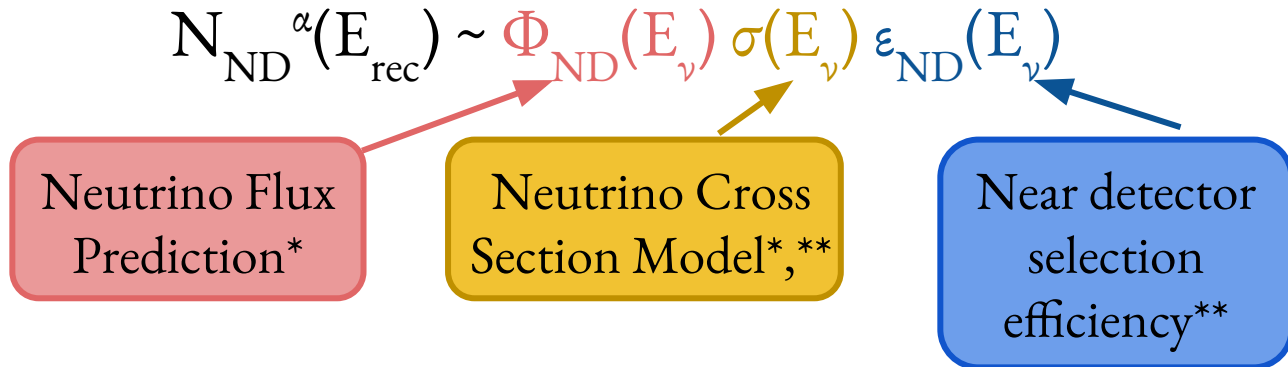High precision appearance / disappearance measurements

Near Detector

Detect ν_α

$N_{ND}{}^{\alpha}(E_{rec})$
Number of events
of flavor α

Appearance
Measurement

Far Detector

E_{rec} = Reconstructed ν energy

Near Detector
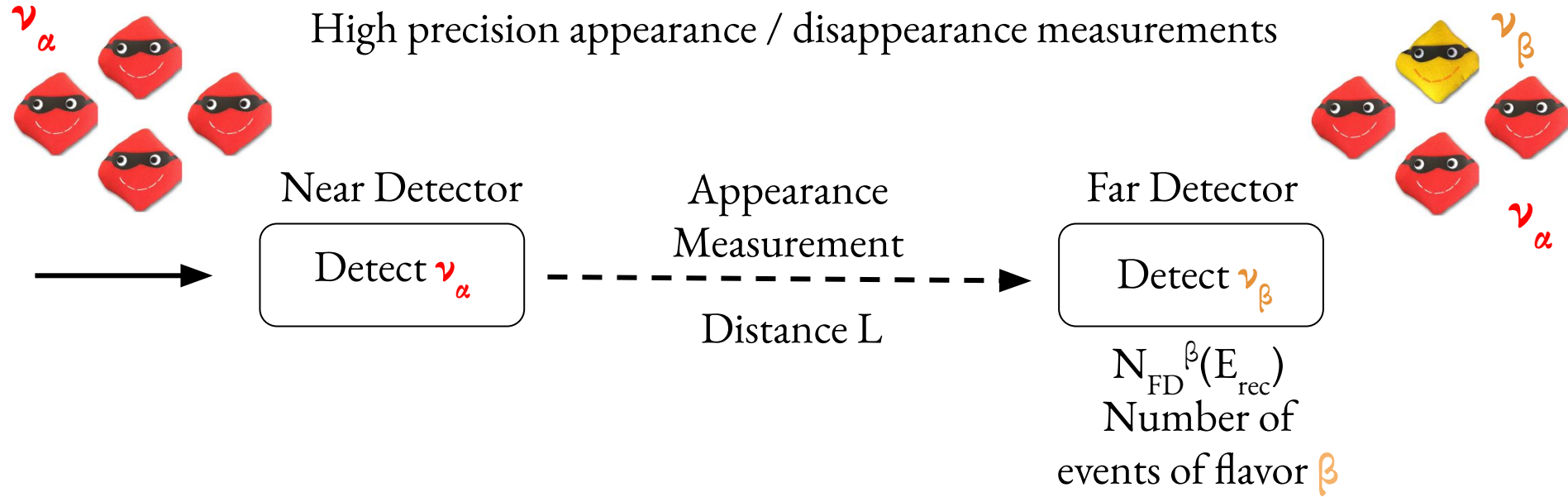
$$N_{ND}{}^{\alpha}(E_{rec}) \sim \Phi_{ND}(E_{\nu})\,\sigma(E_{\nu})\,\varepsilon_{ND}(E_{\nu})$$

Neutrino Flux Prediction*

Neutrino Cross Section Model*,**

Near detector selection efficiency**

*E_{ν} = True ν energy   **σ also depends on observables like muon momentum

Neutrino Oscillation Experiments

High precision appearance / disappearance measurements

ν_α

ν_β

ν_α

Near Detector

Detect ν_α

Appearance Measurement

Distance L

Far Detector

Detect ν_β

$N_{FD}^{\beta}(E_{rec})$
Number of events of flavor β

E_{rec} = Reconstructed ν energy

Far Detector

$$N_{FD}^{\beta}(E_{rec}) \sim \Phi_{FD}(L, E_{\nu}) \; \sigma(E_{\nu}) \; \varepsilon_{FD}(E_{\nu}) \; P(\nu_{\alpha} \rightarrow \nu_{\beta})$$

$\propto L / E_{\nu}$

Oscillation probability

Neutrino Flux Prediction

Neutrino Cross Section Model

Far detector selection efficiency
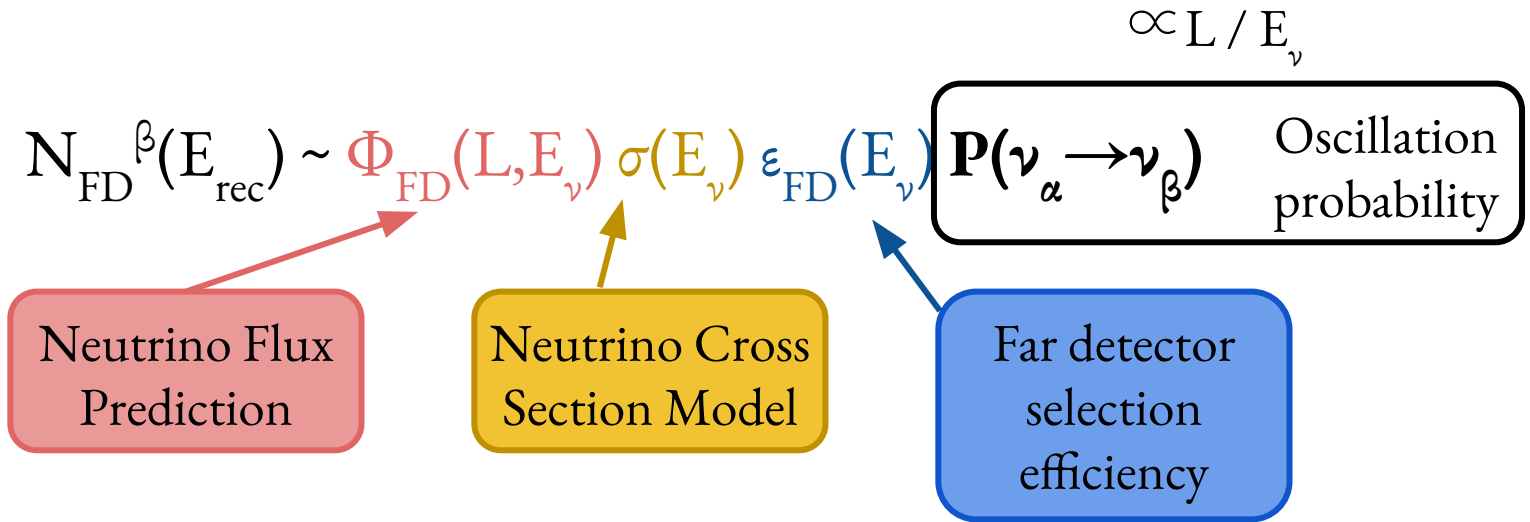
Far Detector

$$N_{FD}{}^{\beta}(E_{rec}) \sim \Phi_{FD}(L,E_\nu)\ \sigma(E_\nu)\ \varepsilon_{FD}(E_\nu)\ \mathbf{P}(\nu_\alpha \rightarrow \nu_\beta)$$

Oscillation probability

Modeling Input

- Smearing relating E_ν/E_{rec}
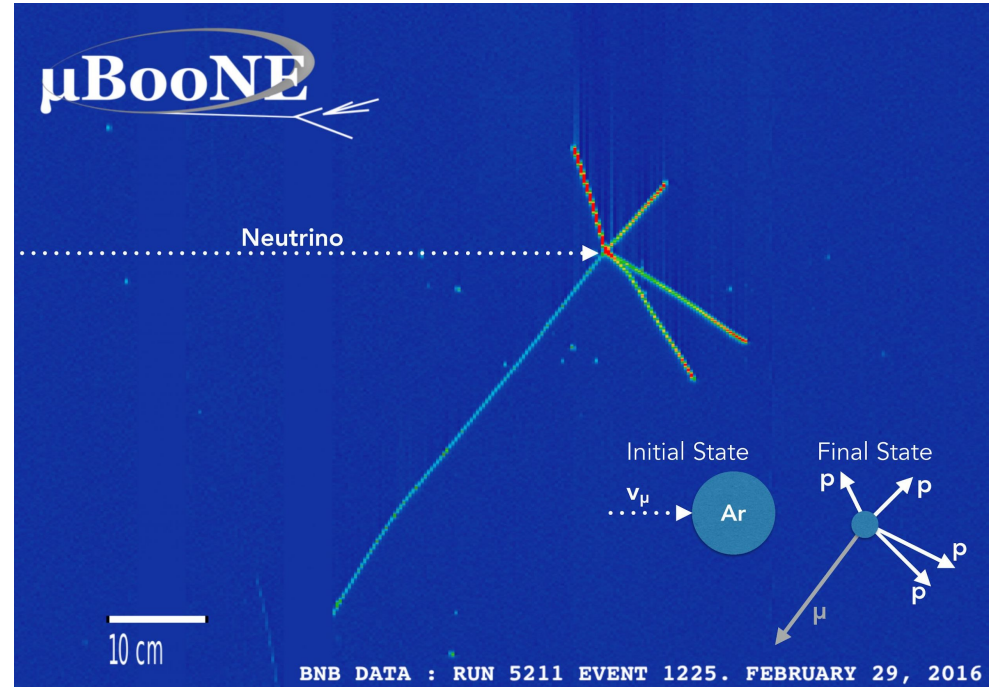- Signal / background topologies
- ...

Far Detector

$$N_{FD}^{\beta}(E_{rec}) \sim \Phi_{FD}(L, E_\nu)\, \sigma(E_\nu)\, \varepsilon_{FD}(E_\nu)\, P(\nu_\alpha \rightarrow \nu_\beta) \quad \text{Oscillation probability}$$

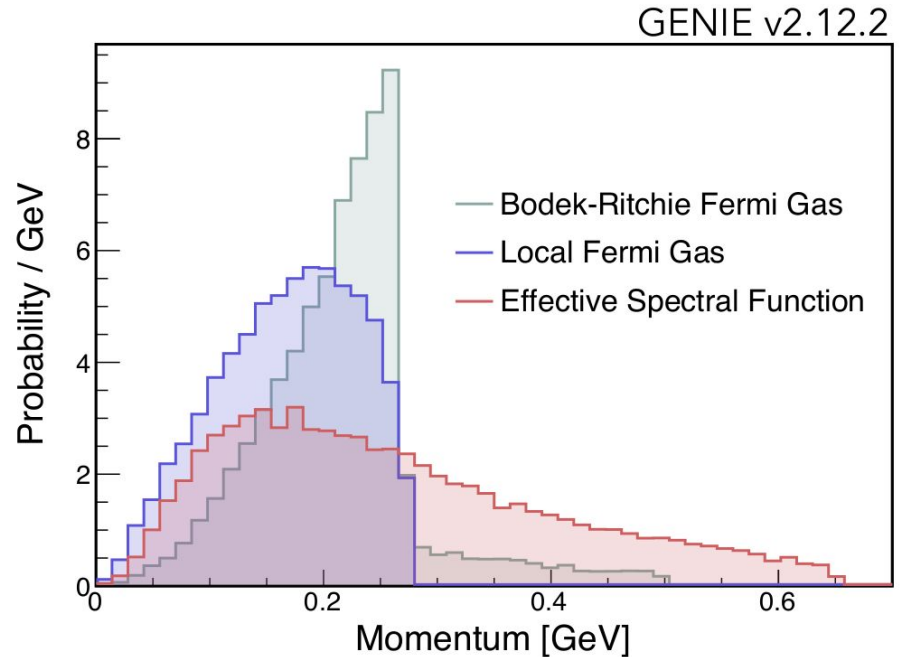Need for high precision ν cross section measurements & for state-of-the-art detectors

Neutrino Interactions

Nuclear effects not well understood especially on heavy elements

Fermi Motion

Neutrino scattering off nucleon in complex nuclear system
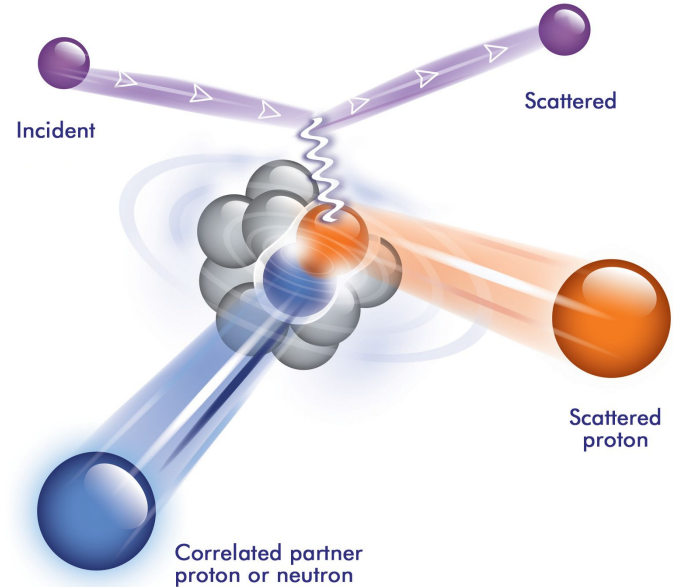

GENIE v2.12.2

Credit: M. Del Tutto

Nucleon-nucleon Correlations

- Meson Exchange Current (MEC)
- Short Range Correlations

  Rev. Mod. Phys. 89, 045002 (2017)

Need to measure outgoing particles

Possible in LArTPCs!

Incident

Scattered

Scattered proton
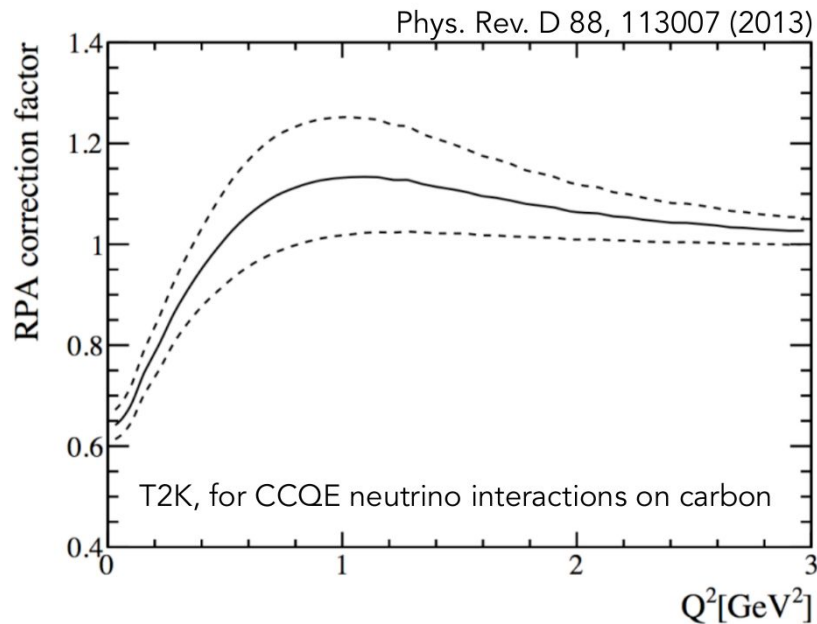
Correlated partner proton or neutron

RPA Effects

Use random phase approximation method (RPA)

Suppression at low Q^2

Calculations on carbon & extrapolation to argon

Phys. Rev. C 97 044616 (2018)
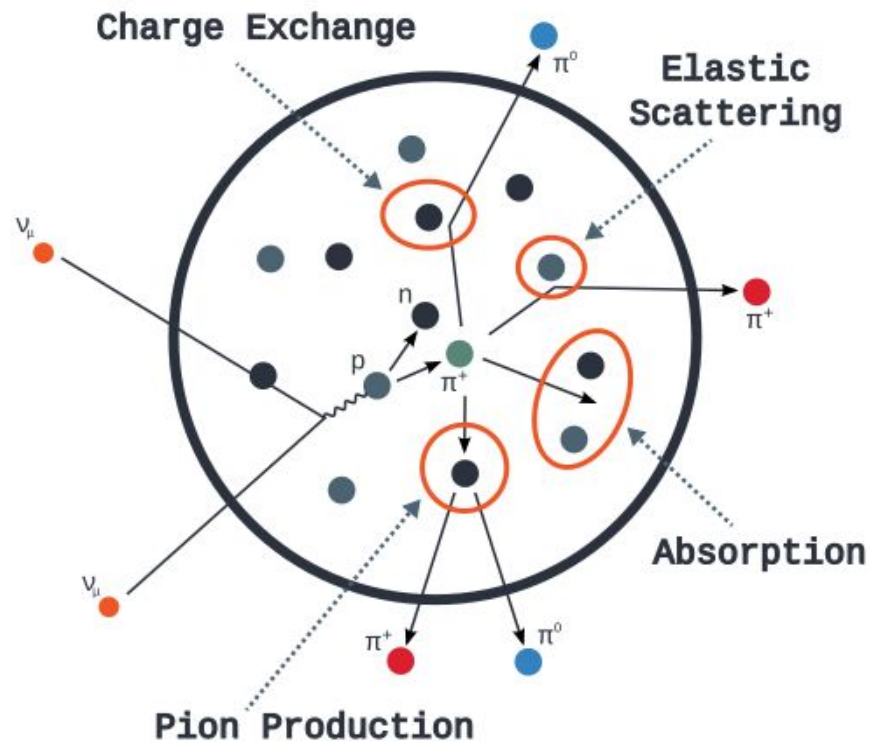Phys. Rev. C 92 024606 (2015)

Phys. Rev. D 88, 113007 (2013)

T2K, for CCQE neutrino interactions on carbon

Final State Interactions

Re-absorption or multiple hadron production in final state

Credit: T. Golan

Cross Section Uncertainty Dominate

T2K *Nature* **580,** 339–344 (2020)

| Type of Uncertainty	$\nu_e/\bar{\nu}_e$ Candidate Relative Uncertainty (%)
Super-K Detector Model	1.5
Pion Final State Interaction and Rescattering Model	1.6
Neutrino Production and Interaction Model Constrained by ND280 Data	2.7
Electron Neutrino and Antineutrino Interaction Model	3.0
Nucleon Removal Energy in Interaction Model	3.7
Modeling of Neutral Current Interactions with Single γ Production	1.5
Modeling of Other Neutral Current Interactions	0.2
Total Systematic Uncertainty	6.0

5% out of 6%!
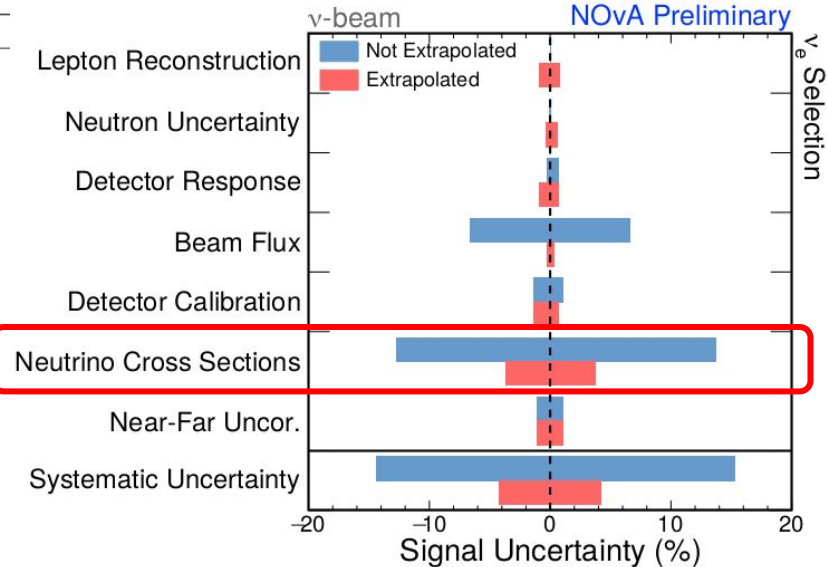
Future Experiments

- Oscillation parameter extraction with percent level uncertainties

- Demand for precise ν cross section modelling
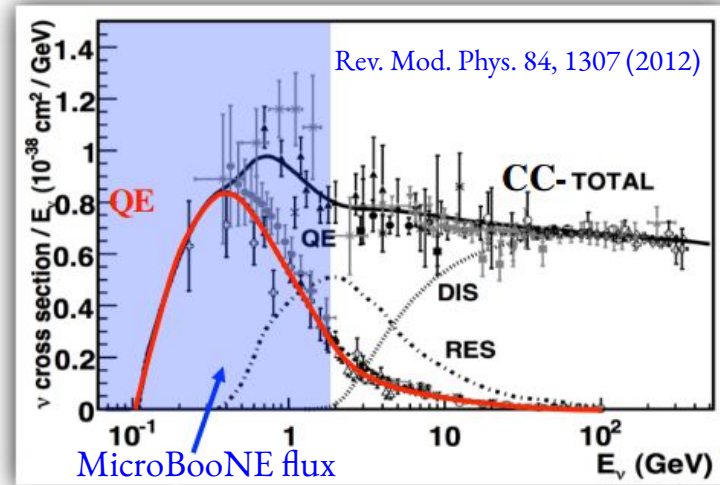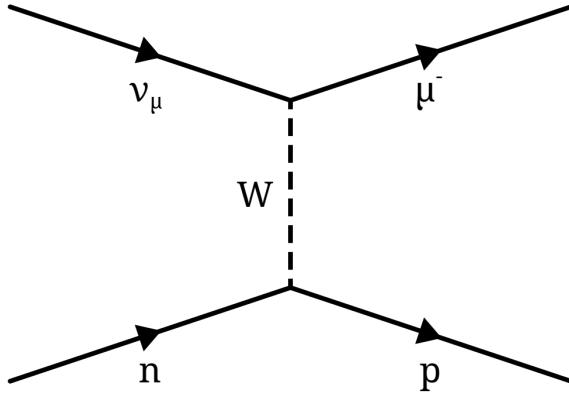
- Head start with Short-Baseline Neutrino (SBN) Program
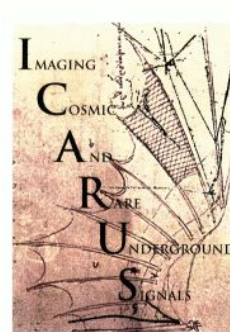
LArTPC Experiments
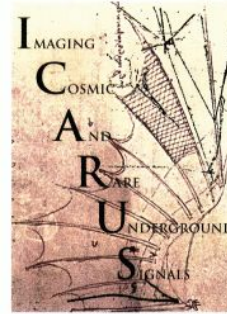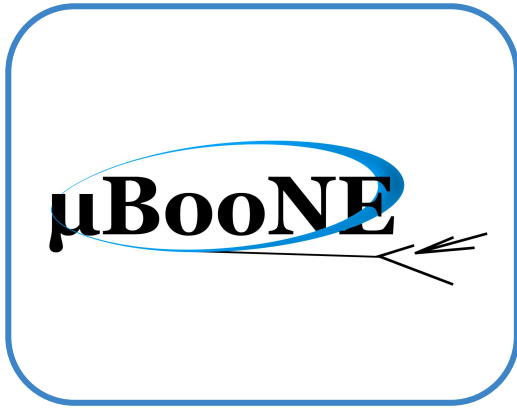
Ideal for more detailed topology measurements

MicroBooNE has already recorded ~500k ν scattering events over the past 5 years
(an initial ~5% data set used in this analysis)

Charged Current Quasi-elastic Interactions

Simple 1p0π topology

Dominant at energies relevant for MicroBooNE
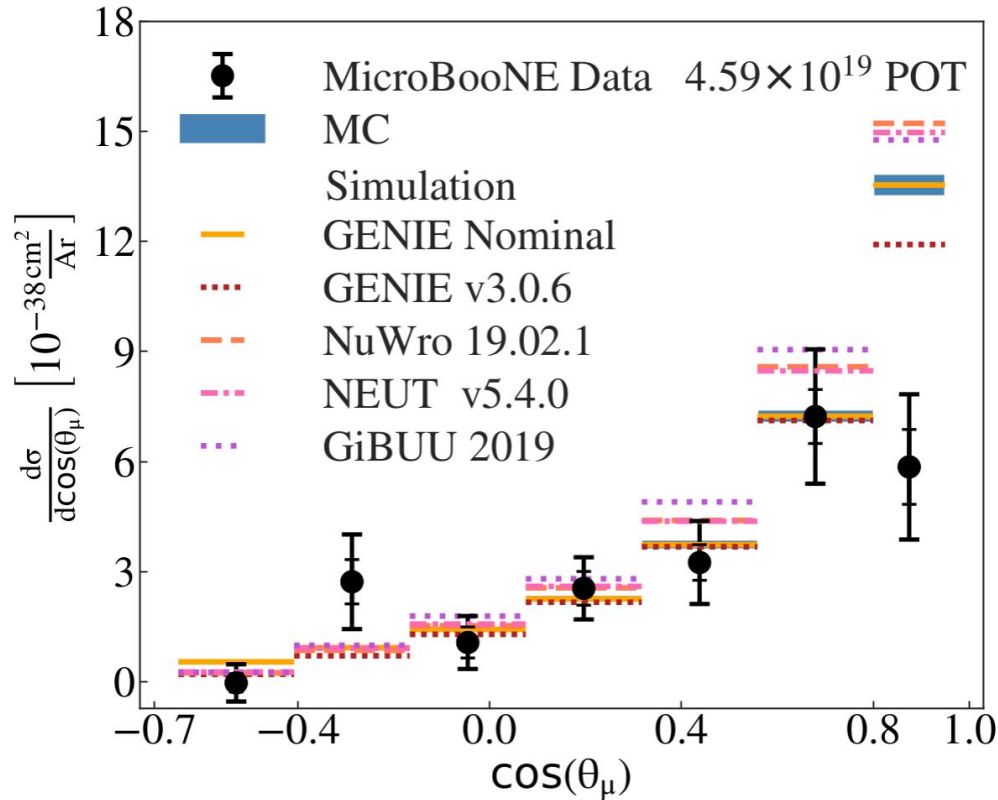
Previous Measurements

Experiment	Target
ArgoNeuT	Ar
MINERvA	CH, C/CH, Fe/CH, Pb/CH
MINOS	Fe
NOMAD	C
SciBooNE	CH
T2K	CH, H_2O
NOvA	CH
MiniBooNE	CH
MicroBooNE	Ar

No CCQE-like measurement

Different nuclei

Large data sets for exclusive measurements
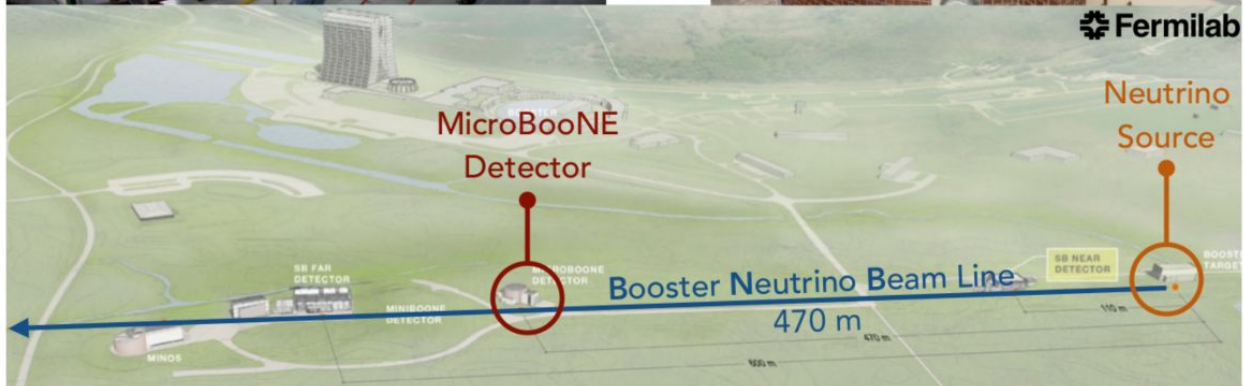
First measurement of differential charged current quasielastic–like ν_μ-^{40}Ar scattering cross sections using the MicroBooNE detector
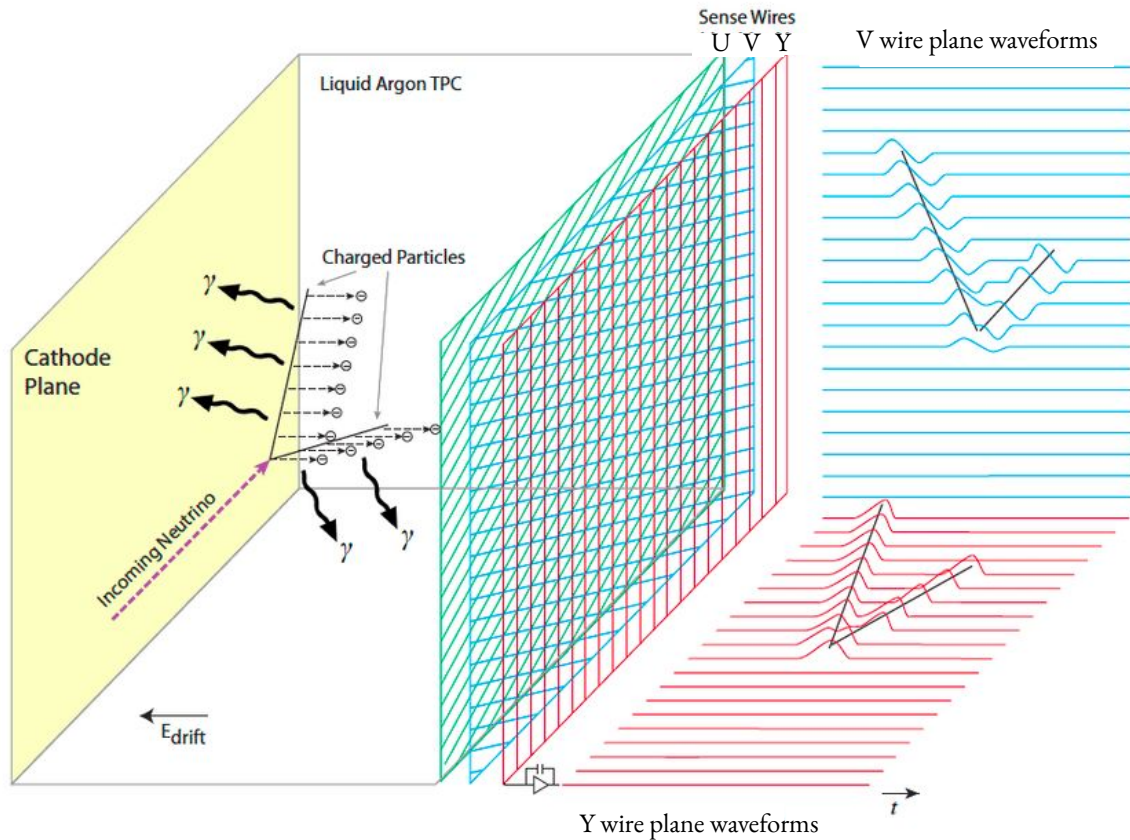
Phys. Rev. Lett. 125, 201803 (2020)

MicroBooNE

JINST 12, P02017 (2017)
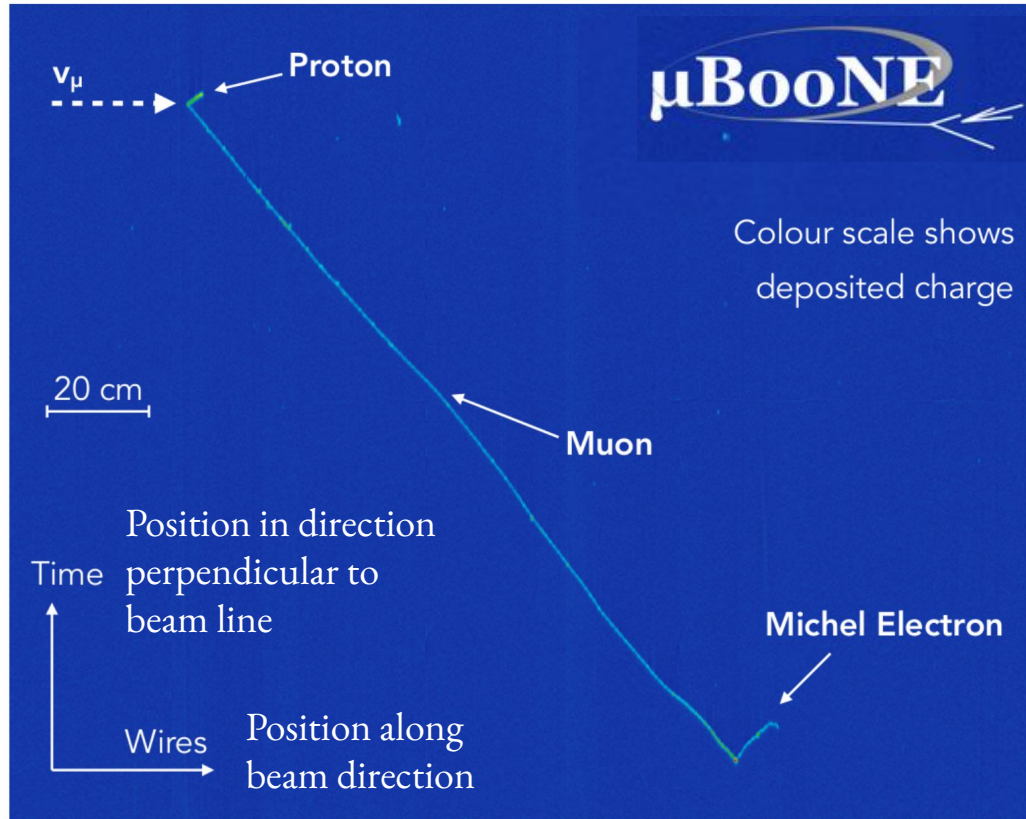
Time Projection Chambers

Sense Wires
U V Y

V wire plane waveforms

Liquid Argon TPC

Cathode Plane

γ
γ
γ

Charged Particles

Incoming Neutrino

E_drift

Y wire plane waveforms

- 3 wire planes
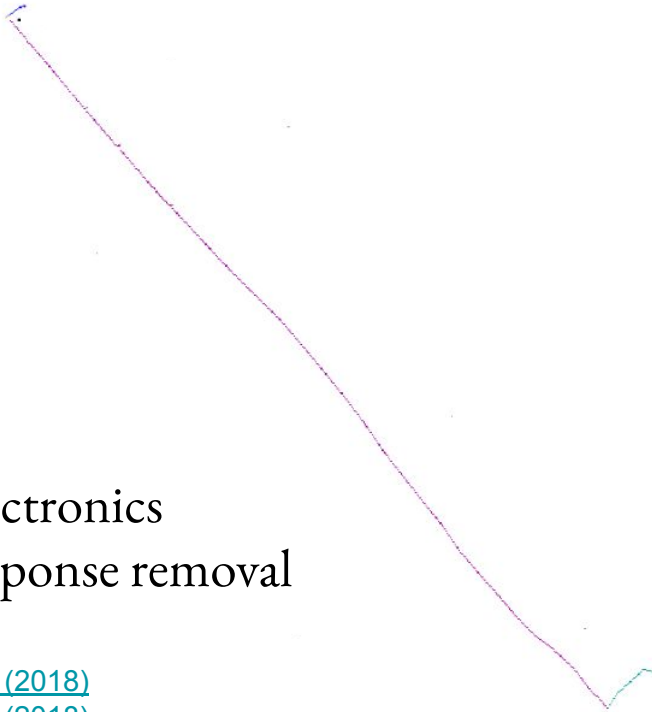- 8192 gold coated wires
- 3 mm wire spacing
- 32 PMTs

Event Displays

From raw hits to
particle reconstruction

Pandora Pattern Recognition

Eur. Phys. J. C78, 1, 82 (2018)

Readout electronics
and field response removal

JINST 13, P07006 (2018)
JINST 13, P07007 (2018)

Event Reconstruction
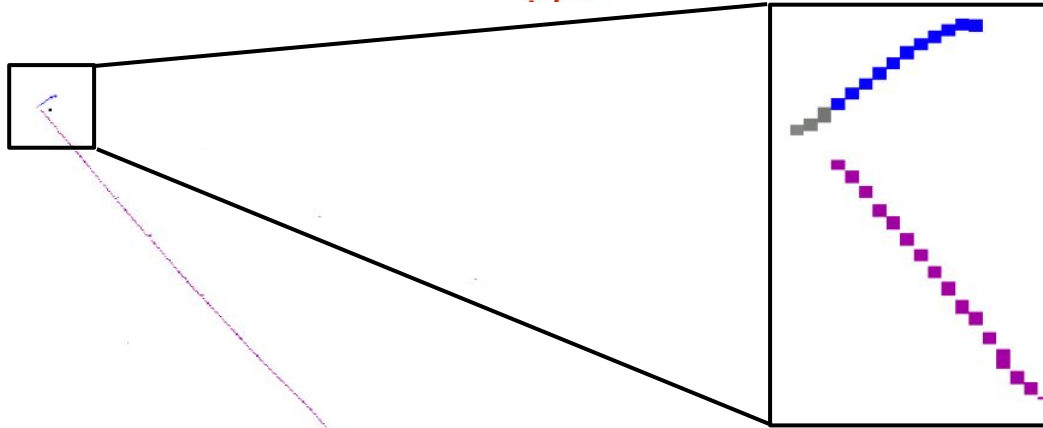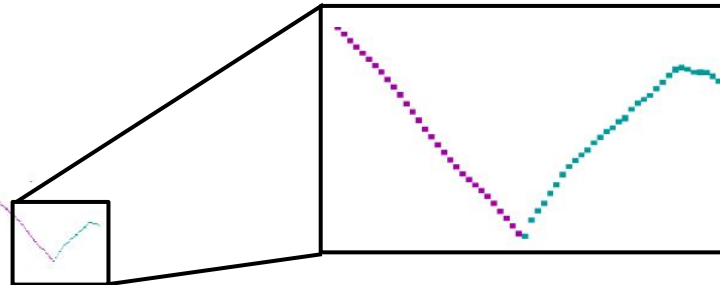

From raw hits to
particle reconstruction

**Pandora Pattern
Recognition**
Eur. Phys. J. C78, 1, 82 (2018)

Readout electronics
and field response removal

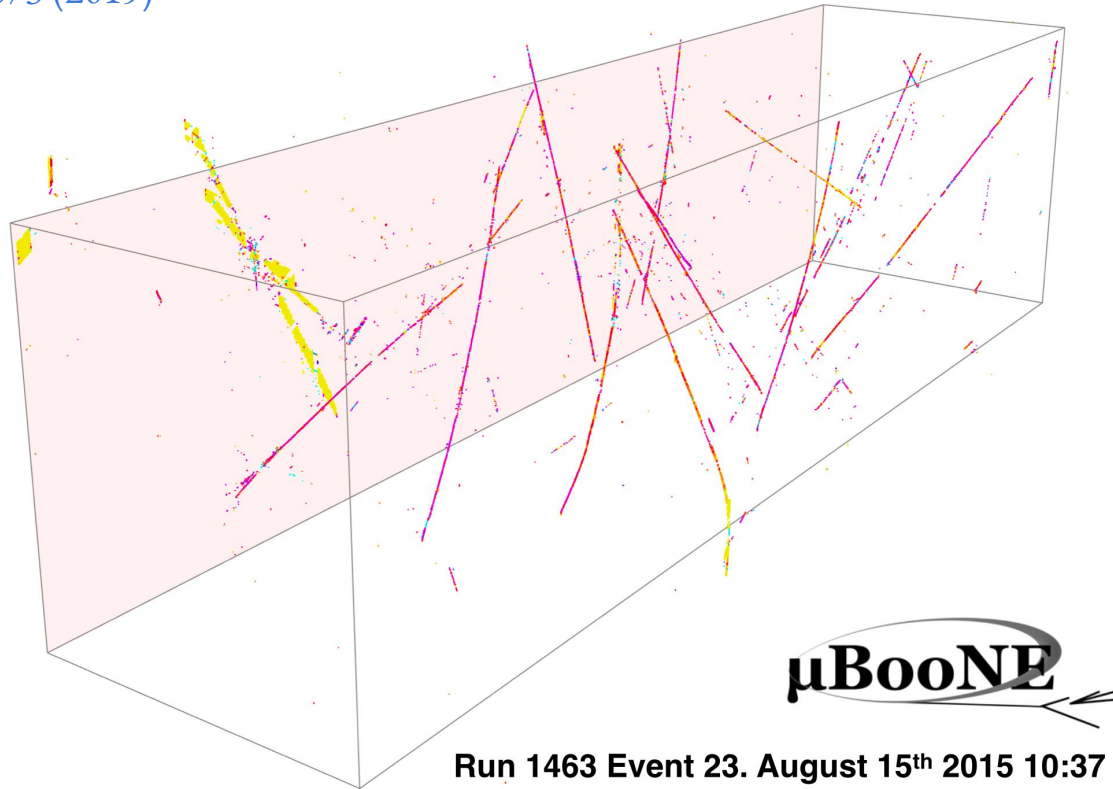JINST 13, P07006 (2018)
JINST 13, P07007 (2018)

μBooNE
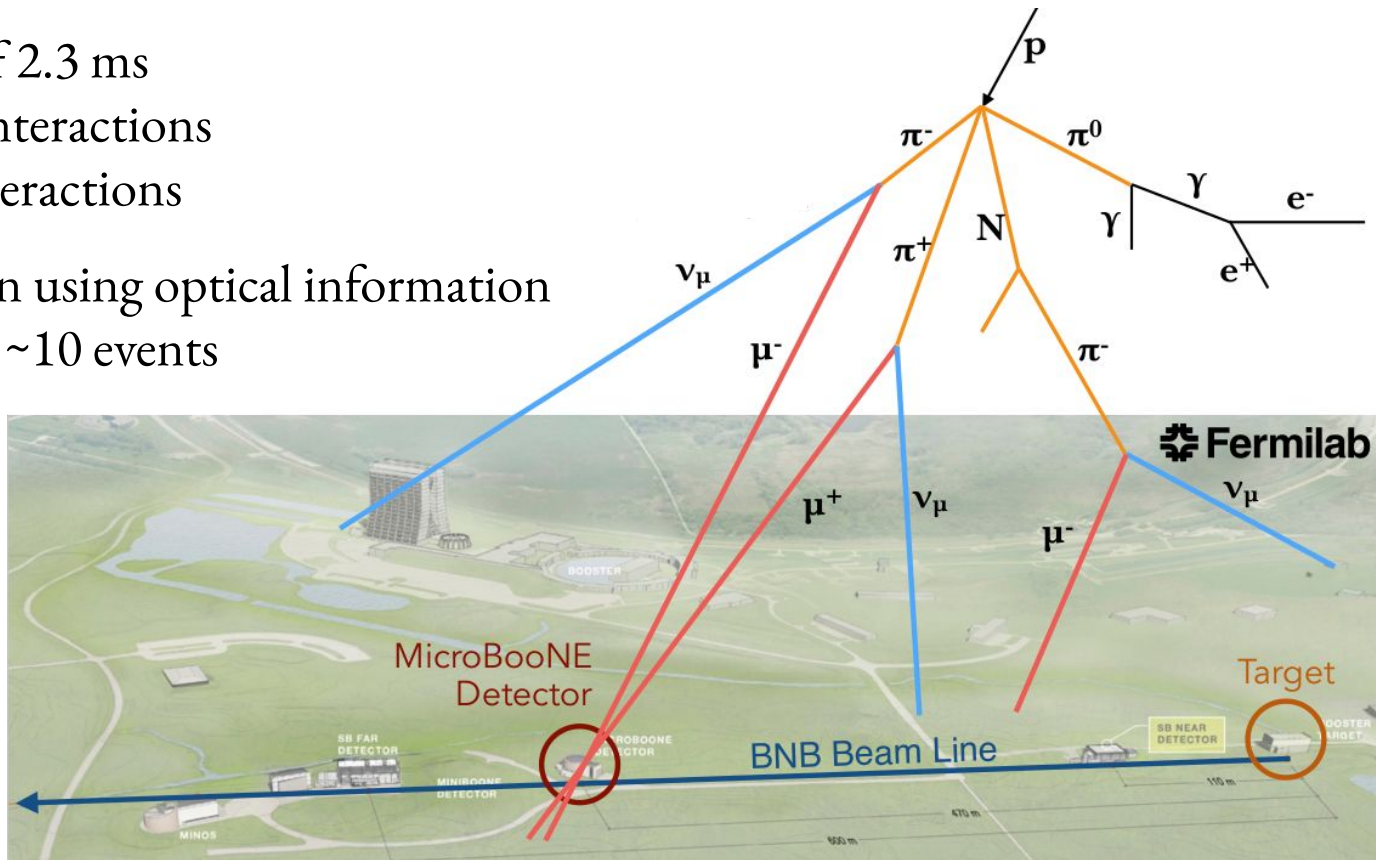
Run 1463 Event 23. August 15th 2015 10:37

# Cosmic Background Dominance

Readout window of 2.3 ms
- ~20 cosmic interactions
- ~0.0017 ν interactions

Significant reduction using optical information to 1 ν interaction in ~10 events

Overlay Samples
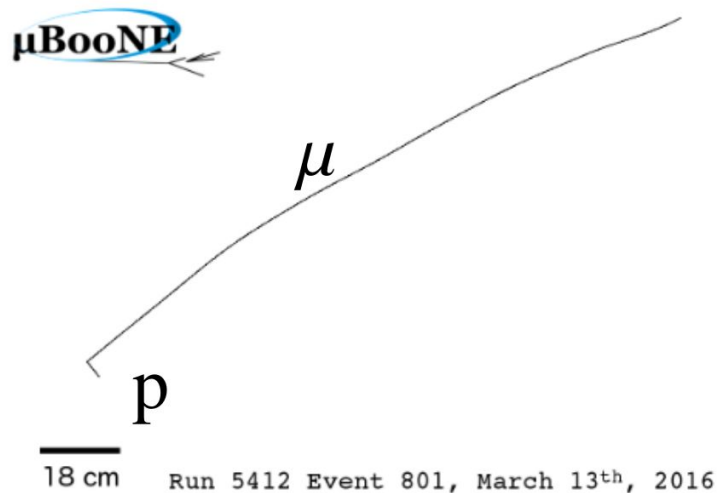

- First MicroBooNE analysis using novel technique in the LArTPC community

- Simulated events on top of real cosmic events

- Will be used as default simulation technique by MicroBooNE
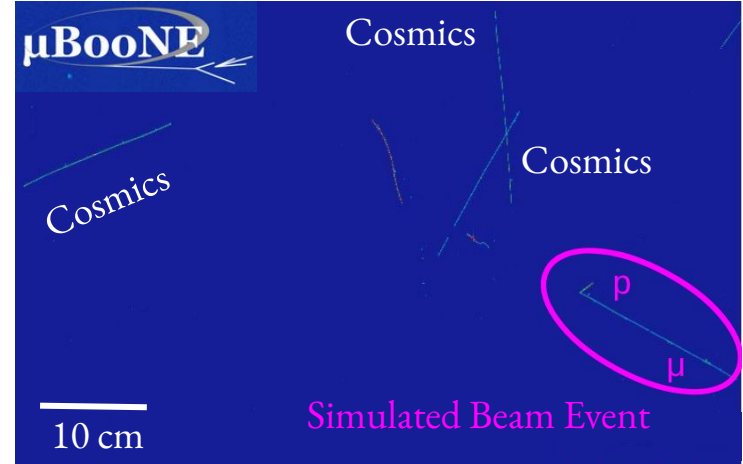
Signal Definition

Vertex of two tracks

- 1 muon (> 100 MeV/c)
- 1 proton (> 300 MeV/c)
- No $\pi^{\pm}$ (> 70 MeV/c)

μBooNE

μ

p

18 cm   Run 5412 Event 801, March 13th, 2016

CC1p0π topology

All reconstructed tracks

Zooming out

Neutrino induced tracks

ν_μ
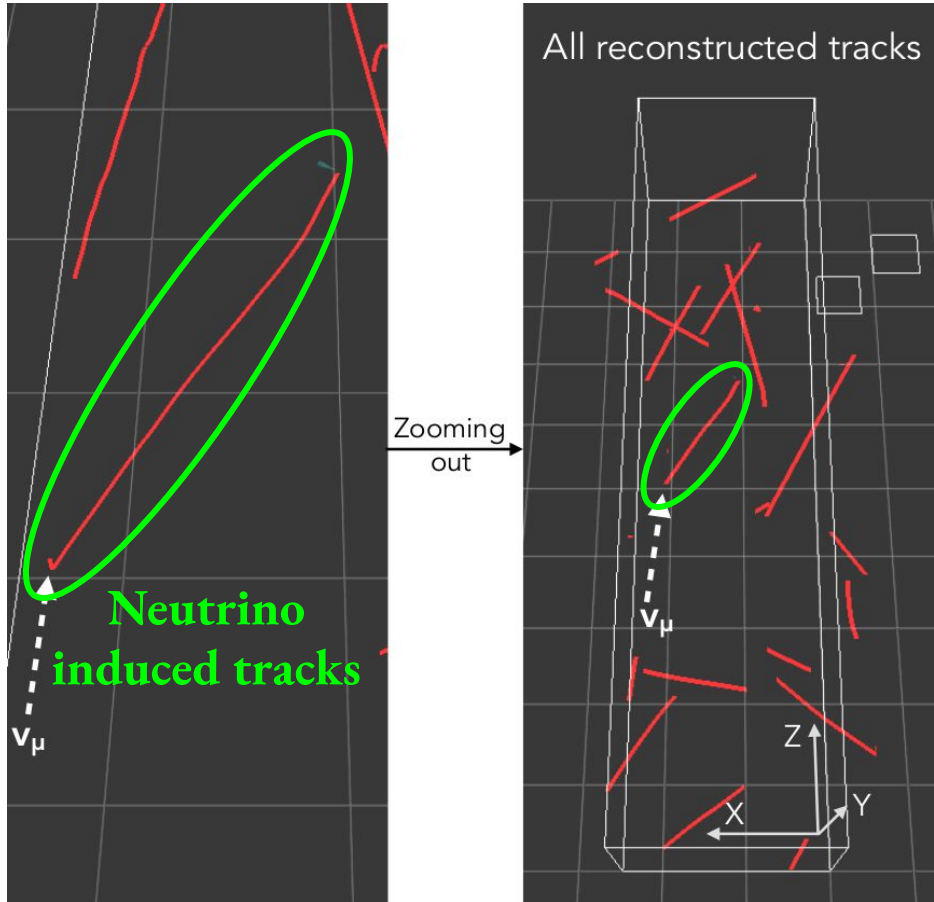
Detector and kinematics–based cuts to reject cosmics & to enhance signal

Eur. Phys. J. C 79 673 (2019)

Credit: M. Del Tutto

33

Cosmic Rejection

- Energy deposition profile (particle identification)

- Track length

- Scintillation light at vertex

- Non-collinearity
  $$|\Delta\theta_{\mu p} - 90^o| < 55^o$$

- Charge deposition at vertex

μBooNE

Candidate μ

Candidate p

18 cm   Run 5412 Event 801, March 13th, 2016
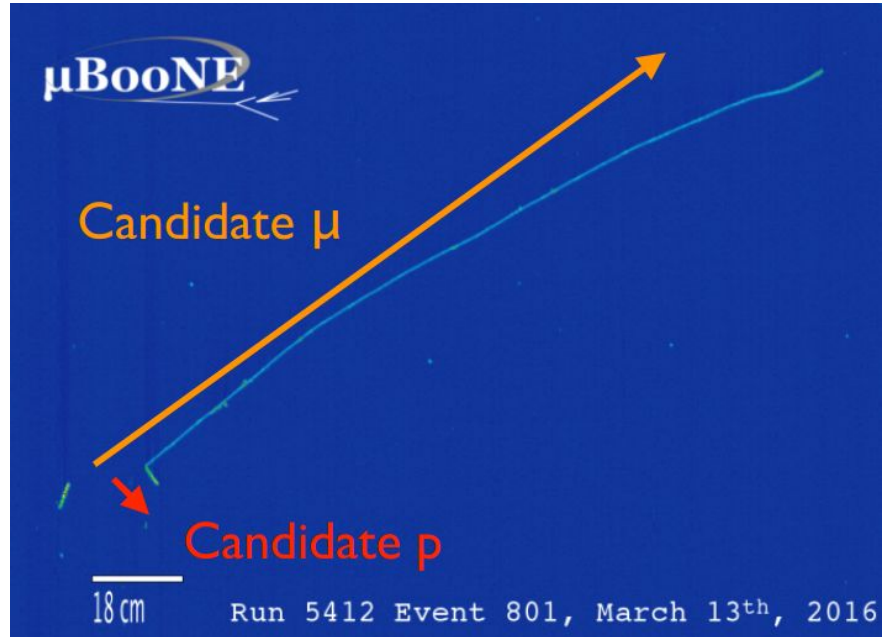
Energy Deposition Profile

Protons identified by Bragg peak
in last 30 cm of track

Low proton threshold @ **300 MeV/c**

JINST 15, P03022 (2020)

Coplanarity

$$|\Delta\phi_{\mu p} - 180^o| < 35^o$$

Transverse imbalance
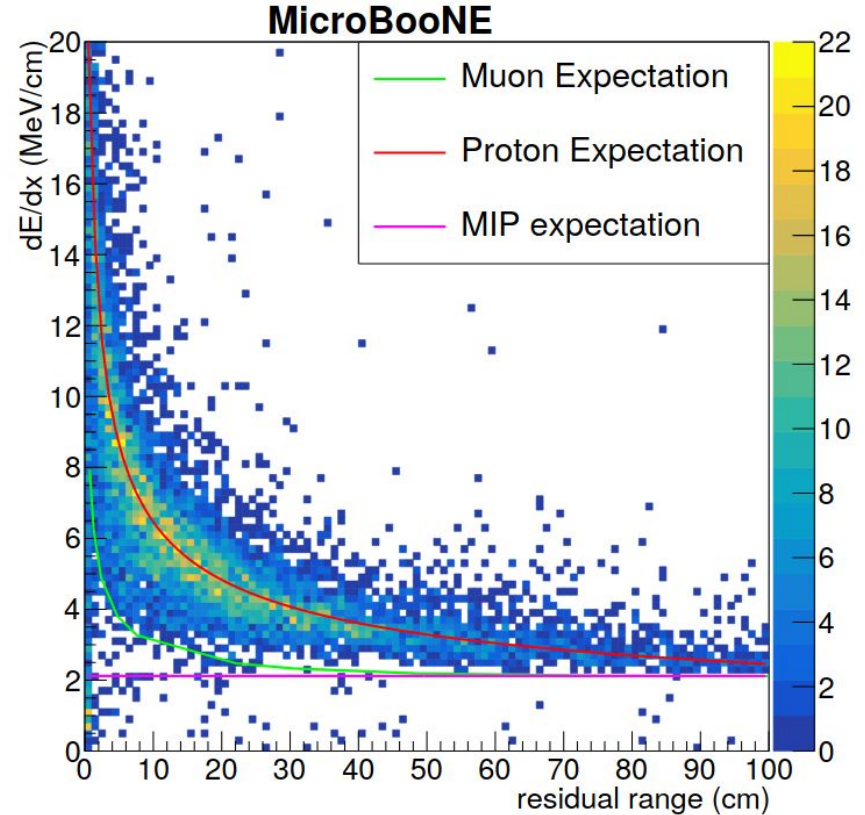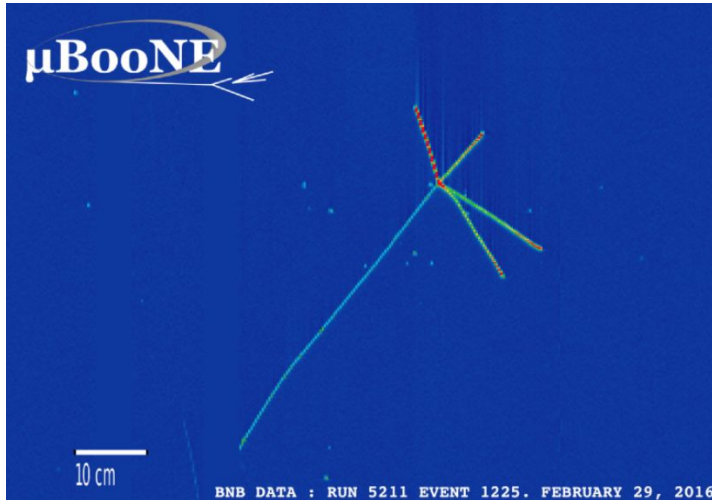
$$P_T = |\vec{P}_\mu + \vec{P}_p|_T < 0.35\,GeV/c$$

CCQE Enhancement

Coplanarity

$$|\Delta\phi_{\mu p} - 180^o| < 35^o$$

Transverse imbalance

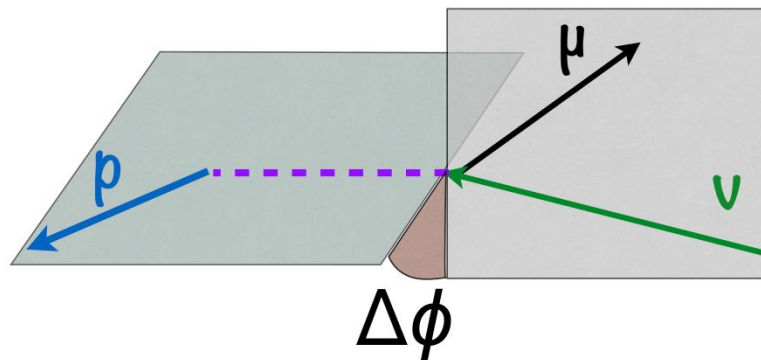$$P_T = |\vec{P}_\mu + \vec{P}_p|_T < 0.35\,GeV/c$$
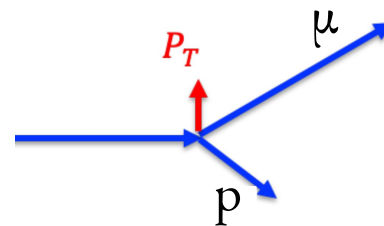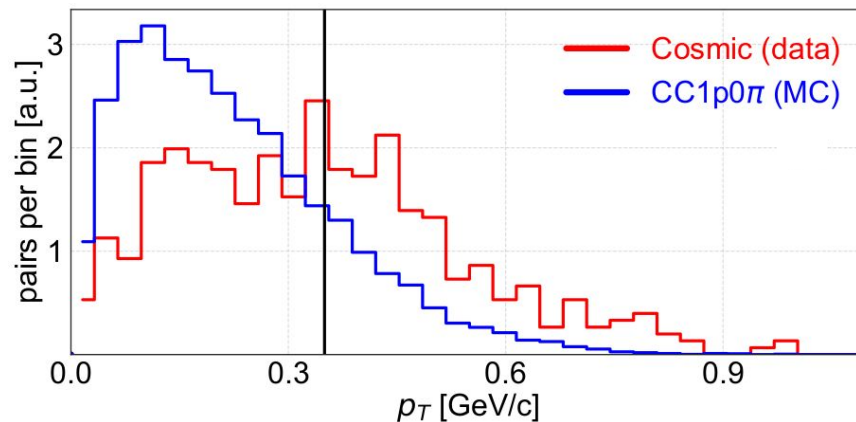
Statistics

After selection cuts

data events: 410

Using our MC, we report
a CC1p0π topological signal purity ~84%

CCQE Dominance

MicroBooNE Simulation
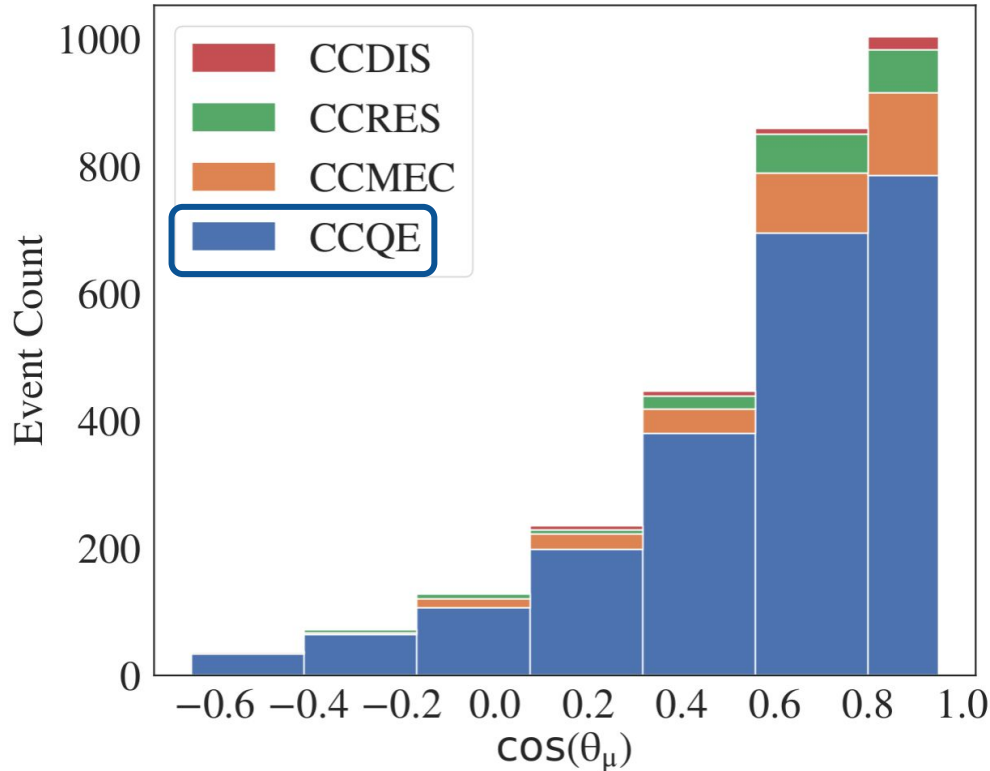
Interaction Mode	Fractional Contribution (%)
CCQE	81.1
CCMEC	10.9
CCRES	6.6
CCDIS	1.4

GENIE v2.12.2

Cross Section Extraction

- Event selection in data sample

- Cosmic background subtraction

- Beam related MC background subtraction

- Detection efficiency correction

$$\frac{\mathrm{d}\sigma}{\mathrm{d}X_n} = \frac{\mathrm{N}_n^{\mathrm{on}} - \mathrm{N}_n^{\mathrm{off}} - \mathrm{B}_n}{\epsilon_n \cdot \Phi_\nu \cdot \mathrm{N}_{\mathrm{target}} \cdot \Delta_n}$$

X = kinematic variable of interest

Cross Section Extraction

$$\frac{\mathrm{d}\sigma}{\mathrm{d}X_n} = \frac{N_n^{on} - N_n^{off} - B_n}{\epsilon_n \cdot \Phi_\nu \cdot N_{target} \cdot \Delta_n}$$

$N^{on} \rightarrow$ # events in beam-on data

(ν interactions in beam spill time)

$N^{off} \rightarrow$ # events in beam-off data

(cosmic activity)

Data

Constants

$\Phi_\nu \rightarrow$ integrated neutrino flux

$N_{targets} \rightarrow$ number of target nuclei

$\Delta \rightarrow$ bin width

Cross Section Extraction

$$\frac{\mathrm{d}\sigma}{\mathrm{d}X_n} = \frac{N_n^{\mathrm{on}} - N_n^{\mathrm{off}} - \mathbf{B_n}}{\mathbf{\epsilon_n} \cdot \Phi_\nu \cdot N_{\mathrm{target}} \cdot \Delta_n}$$

B → beam related MC background

(mimic 1μ1p signal but not true CC1p0π)

ε → effective detection efficiency

MC

Effective Efficiency

$$\epsilon_n = \frac{\text{true CC1p0}\pi \text{ reconstructed in bin n}}{\text{true CC1p0}\pi \text{ generated in bin n}}$$

Reconstruction effects

Resolution effects

Bin migration effects

Unfolding technique

Results reported as a function of **true variables**

Systematic Uncertainties

$$Syst = Flux \oplus XSec \oplus Detector$$

Framework from
MiniBooNE collaboration
PRD 79, 072002, 2009

More than 40 reweightable
GENIE parameters

MICROBOONE-NOTE-1074-PUB

- Longitudinal & transverse diffusion
- Light yield outside the TPC
- Electron lifetime
- Recombination model
- Space charge map
- Electronic response

MICROBOONE-NOTE-1045-PUB

MICROBOONE-NOTE-1032-PUB

Integrated Cross Section Uncertainty Breakdown

Source Of Uncertainty	Relative Uncertainty (%)
Beam Flux & POT	19
Cross Section Modelling	7
Detector Response	18
Efficiency μ-p decoupling	6
Statistical	16
Total	32

Already significant improvements for future analyses on MicroBooNE
to reduce detector & cross section systematic uncertainties

MICROBOONE-NOTE-1075-PUB   K.Duffy Neutrino 2020   MICROBOONE-NOTE-1074-PUB
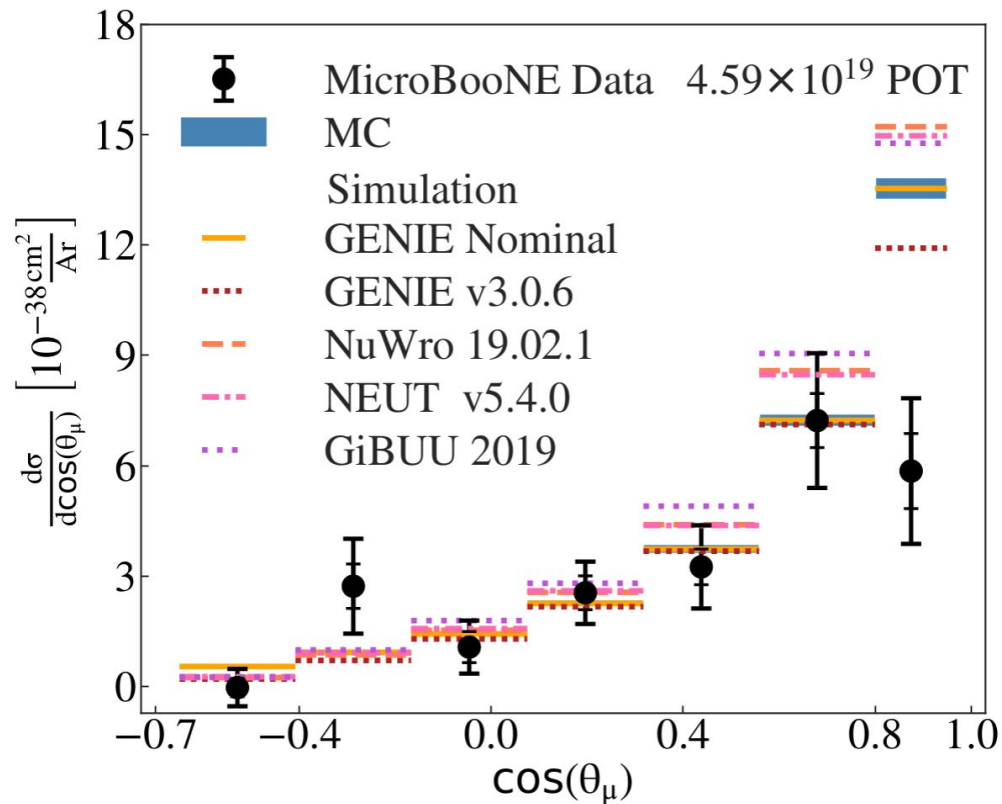
Good agreement with models, except at very forward muon scattering angles

GENIE Nominal = GENIE v2.12.2
GENIE v3.0.6 = G18_10a_02_11a

Model Comparisons

Model Component	GENIE Nominal v2.12.2 This work	GENIE v3.0.6 G18_10a_02_11a Future analyses	NuWro (19.02.1)	NEUT (v5.4.0)	GiBUU (2019)
Nuclear Model	Bodek-Ritchie Fermi Gas [1]	Local Fermi Gas [2, 3]	Local Fermi Gas [2, 3]	Local Fermi Gas [2, 3]	Consistent nuclear medium corrections
Quasi-elastic	Llewellyn-Smith [4]	Nieves [2, 3]	Nieves [2, 3]	Nieves [2, 3]	LFG model for nucleon momenta
MEC	Empirical [5]	Nieves [2, 3]	Nieves [2, 3]	Nieves [2, 3]	Separate MEC model [11]
Resonant	Rein-Seghal [6]	Berger-Seghal [7]	Berger-Seghal [7]	Berger-Seghal [7]	
Coherent	Rein-Seghal [6]	Berger-Seghal [7]	Berger-Seghal [7]	Rein-Seghal [6]	Propagates final state particles according to the BUU equations [11]
FSI	hA [8]	hA2018 [8]	Oset [10]	Oset [10]	

Significant differences in model components used
in GENIE Nominal and other generators

Model Comparisons

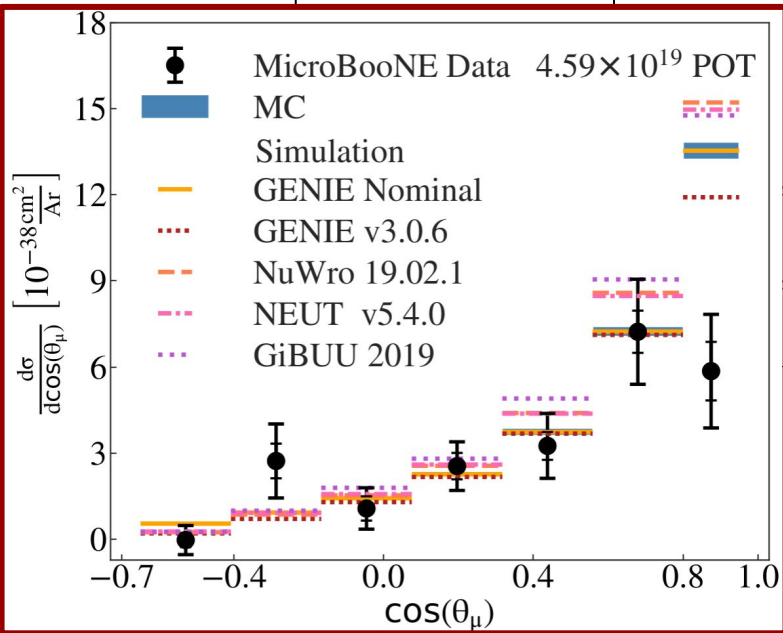| Model Component	GENIE Nominal v2.12.2 This work	GENIE v3.0.6 G18_10a_02_11a Future analyses	NuWro (19.02.1)	NEUT (v5.4.0)	GiBUU (2019)
Nuclear Model	Bodek-Ritchie Fermi Gas [1]	Local Fermi Gas [2, 3]	Local Fermi Gas [2, 3]	Local Fermi Gas [2, 3]	Consistent nuclear medium corrections
		[2, 3]	Nieves [2, 3]	Nieves [2, 3]	LFG model for nucleon momenta
		[2, 3]	Nieves [2, 3]	Nieves [2, 3]	Separate MEC model [11]
		ghal [7]	Berger-Seghal [7]	Berger-Seghal [7]	
		ghal [7]	Berger-Seghal [7]	Rein-Seghal [6]	Propagates final state particles according to the BUU equations [11]
		8 [8]	Oset [10]	Oset [10]	

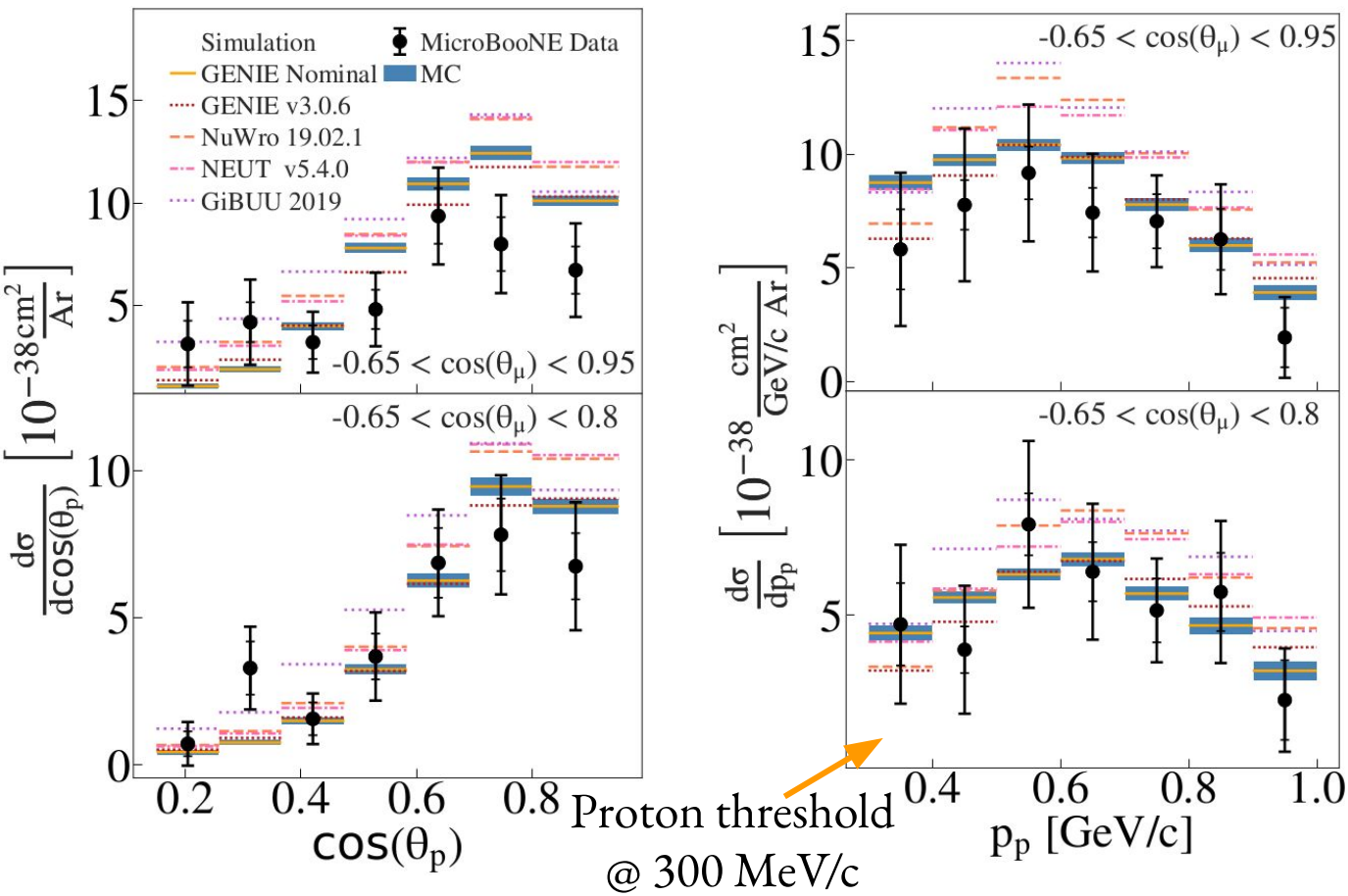**None of them reproduces deficit in forward direction**

Full
phase-space

Excluding
forward region
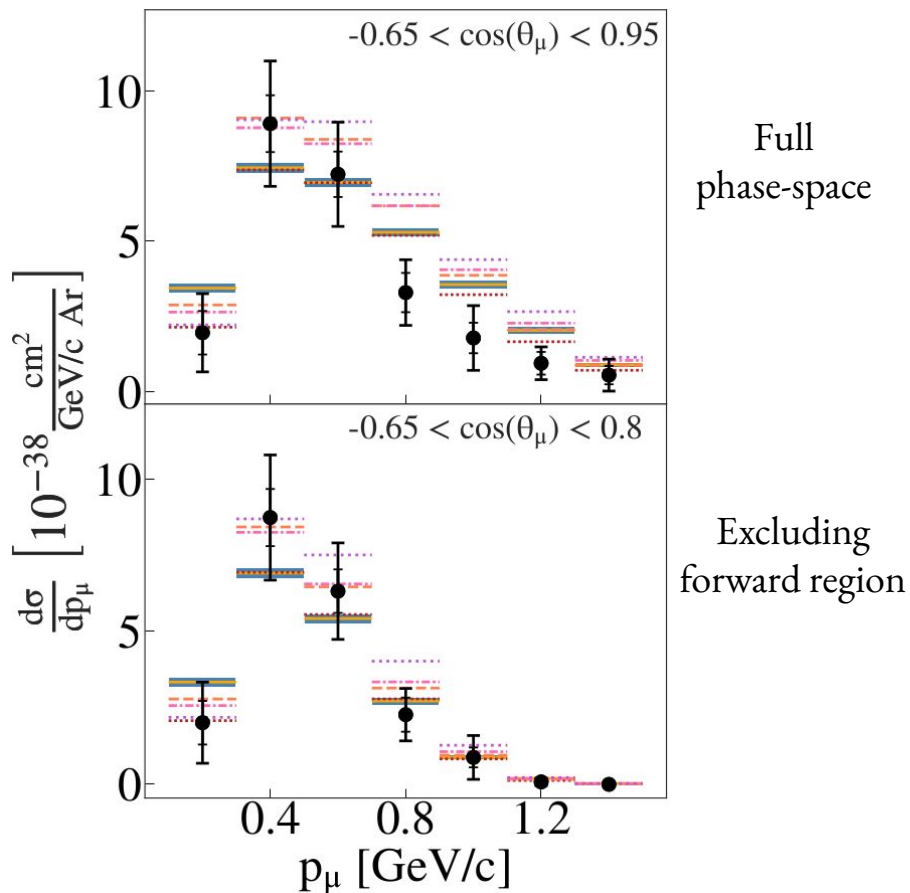
Improved agreement
if forward muon angles
are excluded

Proton Results

Full
phase-space

Improved agreement
if forward muon angles
are excluded

Excluding
forward region

Proton threshold
@ 300 MeV/c

χ^2 Comparisons

Linear sum of 1D χ^2's

Not accounting for correlations between distributions

		Differential Cross Section χ^2/d.o.f	
		$-0.65 < \cos(\theta_\mu) < 0.95$	$-0.65 < \cos(\theta_\mu) < 0.8$
Generators	GENIE Nominal	63.2/28	30.1/27
	GENIE v3.0.6	34.6/28	21.4/27
	NuWro 19.02.1	76.7/28	29.9/27
	NEUT v5.4.0	78.5/28	32.2/27
	GiBUU 2019	82.2./28	40.0/27

GENIE v3.0.6 results in the lowest χ^2 /d.o.f.

Same conclusion as in inclusive analysis Phys. Rev. Lett. 123, 131801 (2019)
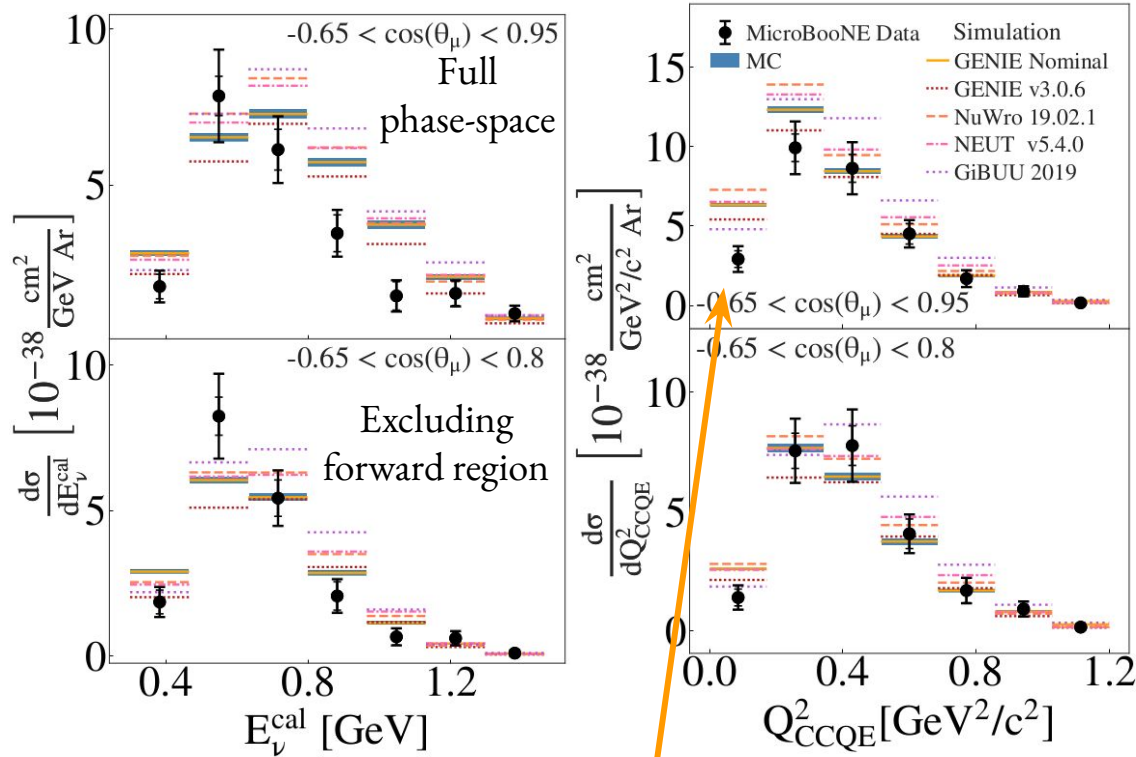
$$\mathrm{E}_{\nu}^{cal} = \mathrm{E}_{\mu} + \mathrm{T}_p + 40\,\mathrm{MeV}$$

$$\vec{p}_{\nu} = (0, 0, \mathrm{E}_{\nu}^{cal})$$

$$Q^2_{CCQE} = (\mathrm{E}_{\nu}^{cal} - \mathrm{E}_{\mu})^2 - (\vec{p}_{\nu} - \vec{p}_{\mu})^2$$

Expected low Q^2 deficit given $\cos\theta_{\mu}$ result

52

Model Comparisons

| Model Component	GENIE Nominal v2.12.2 μBooNE This work	GENIE v3.0.6 G18_10a_02_11a Future analyses	NuWro (19.02.1)	NEUT (v5.4.0)	GiBUU (2019)
Nuclear Model	Bodek-Ritchie Fermi Gas [1]	Local Fermi Gas [2, 3]	Local Fermi Gas [2, 3]	Local Fermi Gas [2, 3]	Consistent nuclear medium corrections
Quasi-elastic	Llewellyn-Smith [4]	Nieves [2, 3]	Nieves [2, 3]	Nieves [2, 3]	LFG model for nucleon momenta
MEC	Empirical [5]	Nieves [2, 3]	Nieves [2, 3]	Nieves [2, 3]	
Resonant	Rein-Seghal [6]	Berger-Seghal [7]	Berger-Seghal [7]	Berger-Seghal [7]	Separate MEC model [11]
Coherent	Rein-Seghal [6]	Berger-Seghal [7]	Berger-Seghal [7]	Rein-Seghal [6]	Propagates final state particles according to the BUU equations [11]
FSI	hA [8]	hA2018 [8]	Oset [10]	Oset [10]	

Differences in coulomb corrections, parameter tuning and implementation of RPA correction

Our data indicates that these seemingly small differences can have a highly significant impact

MicroBooNE Wrap Up

- First measurement of ν_μ - ^{40}Ar CCQE-like cross sections

- Powerful cosmic background rejection and high topological signal purity

- Improvement of theoretical models is required in forward region
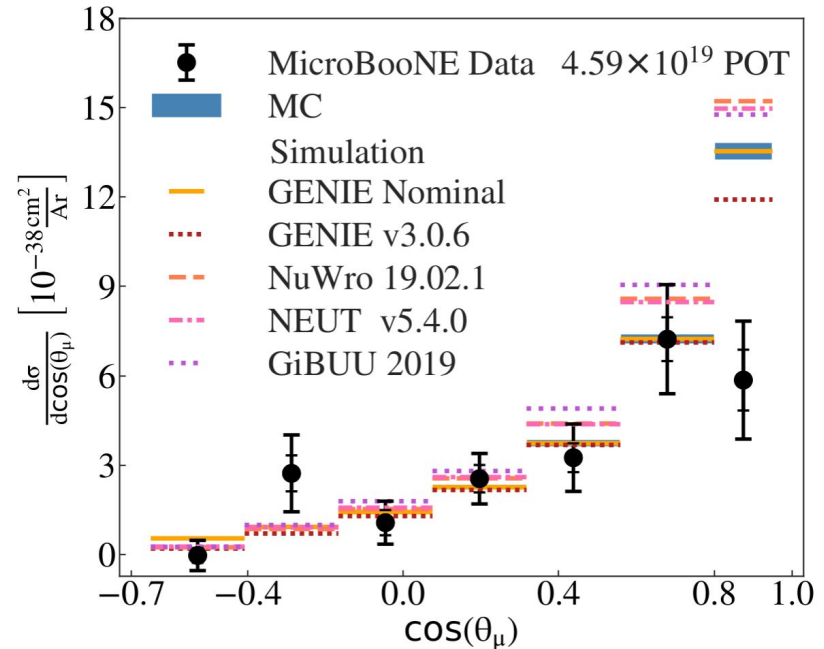
Phys. Rev. Lett. 125, 201803 (2020)

$$N_{FD}^{\beta}(E_{rec}) \sim \Phi_{FD}(E_{\nu})\, \sigma(E_{\nu})\, \varepsilon_{FD}(E_{\nu})\, P(\nu_{\alpha} \to \nu_{\beta})$$
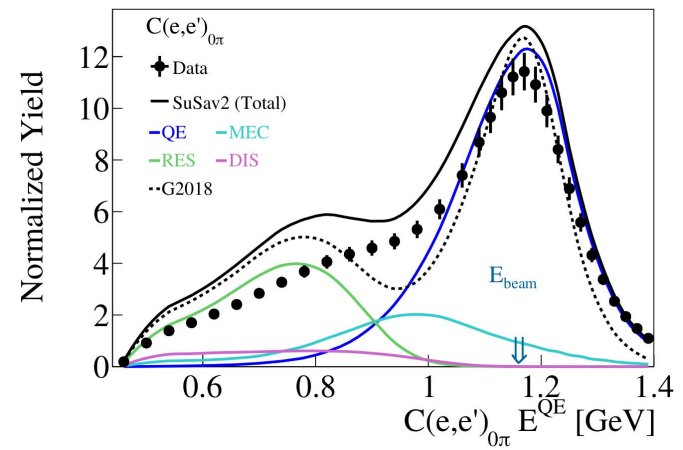
Oscillation probability

Modeling Input

How To Improve Modeling?

ν near detector constraints

Improved theory
in event generators

External Data

Why electrons?

- Very similar interactions

- Nuclear effects practically identical

- Known electron beam energy

- Benchmark ν event generators

Exclusive 1p0π Analysis With CLAS

- **Data Mining**

- Complementary to the one performed on

  μBooNE

- Large acceptance with $\theta_e > 15°$, investigation of forward deficit

- Charged particle detection threshold comparable to neutrino experiments

Jefferson Lab
Thomas Jefferson National Accelerator Facility

CEBAF
Large
Acceptance
Spectrometer

EC

Torus

DC

CC

SC

EC
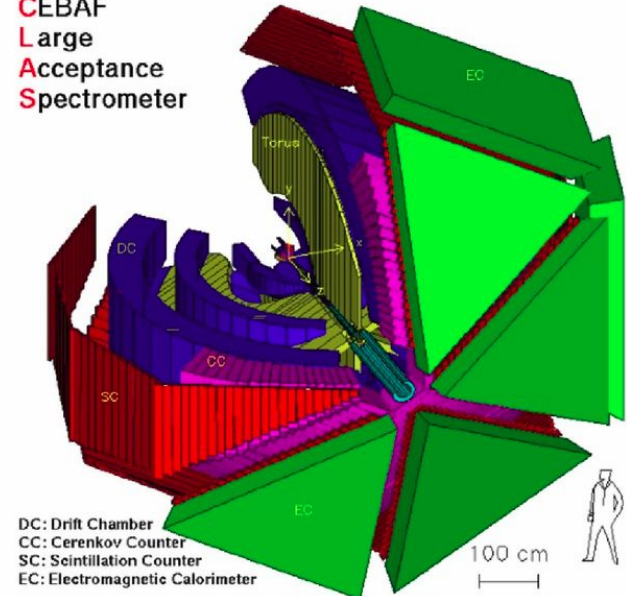
DC: Drift Chamber
CC: Cerenkov Counter
SC: Scintillation Counter
EC: Electromagnetic Calorimeter

100 cm

Playing The Neutrino Game

μBooNE

- 1 muon (> 100 MeV/c)
- 1 proton (> 300 MeV/c)
- No $\pi^\pm$ (> 70 MeV/c)

e4ν

- Select "clean" (e,e'p) events
  1 proton (> 300 MeV/c)
  No $\pi^\pm$ (> 150 MeV/c)

- Scale electron data by Q^4

- Study energy reconstruction
- Benchmark event generators

CLAS Available Data Sets

- Targets
  ^{4}He, ^{12}C, ^{56}Fe

T2K H_2O

NOvA   CH

DUNE / SBN Program   Ar

- Energies
  1, 2 & 4 GeV

Legend: T2K ND, BNB @ MiniBooNE, DUNE ND, MINERνA L.E.

Neutrino Flux (A.U.) vs E_ν (GeV)
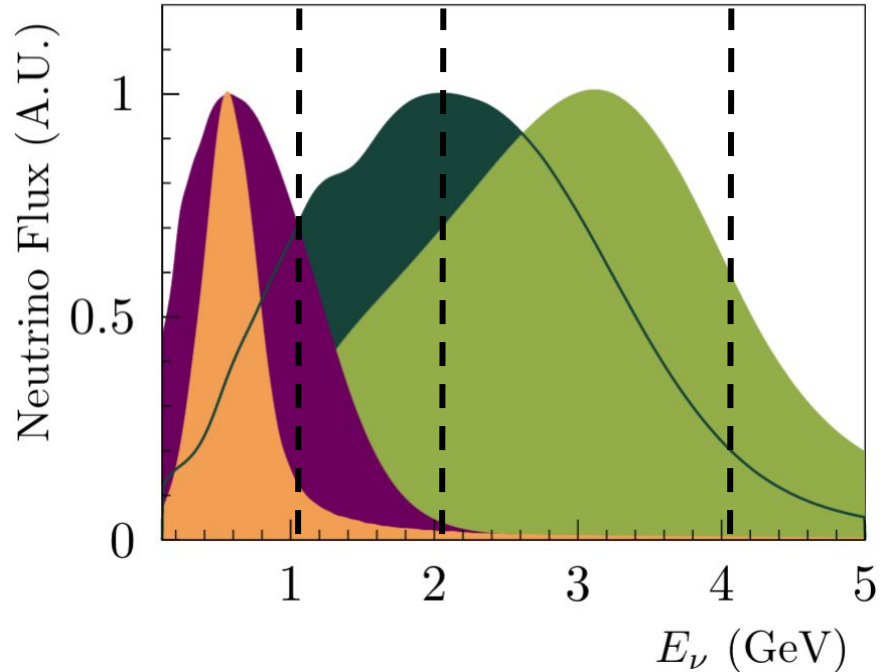
Credit: L. Pickering

Energy Reconstruction
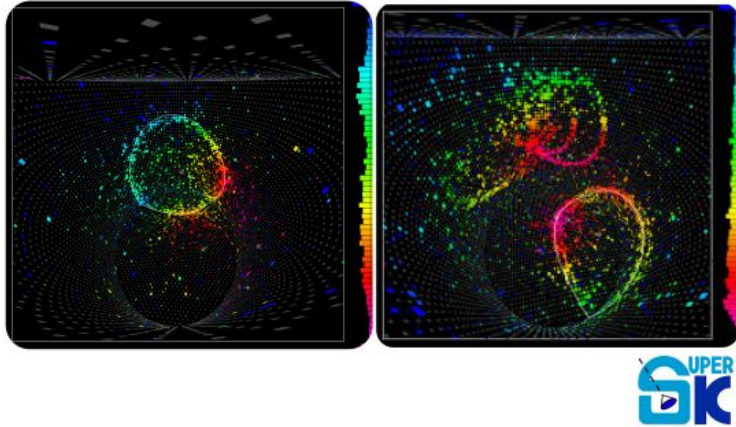
Cherenkov detectors
Assuming QE interaction
Using lepton kinematics

$$E_{QE} = \frac{2M\epsilon + 2ME_l - m_l^2}{2(M - E_l + |k_l|\cos\theta_l)}$$

Tracking detectors
Calorimetric sum
Using all detected particles

$$E_{cal} = E_l + T_p + \epsilon$$

nucleon separation energy $\epsilon \sim 20$ MeV

Inclusive 0π E^QE Reconstruction
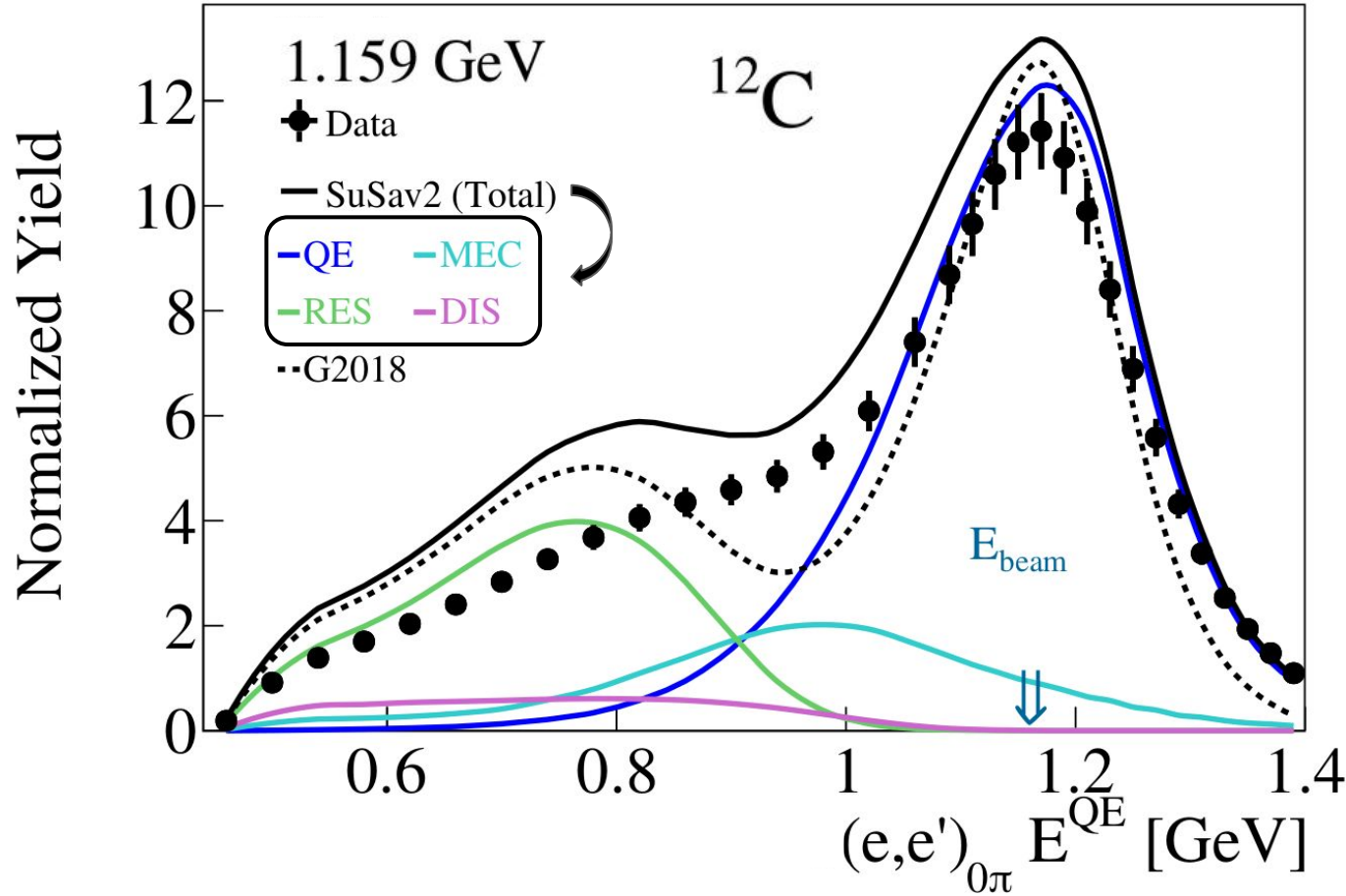
Simulation fails
to capture details

G2018 = GENIE v3 G18_10a_02_11a

SuSav2 = Superscaling model
Phys. Rev. D 94, 013012 (2016)
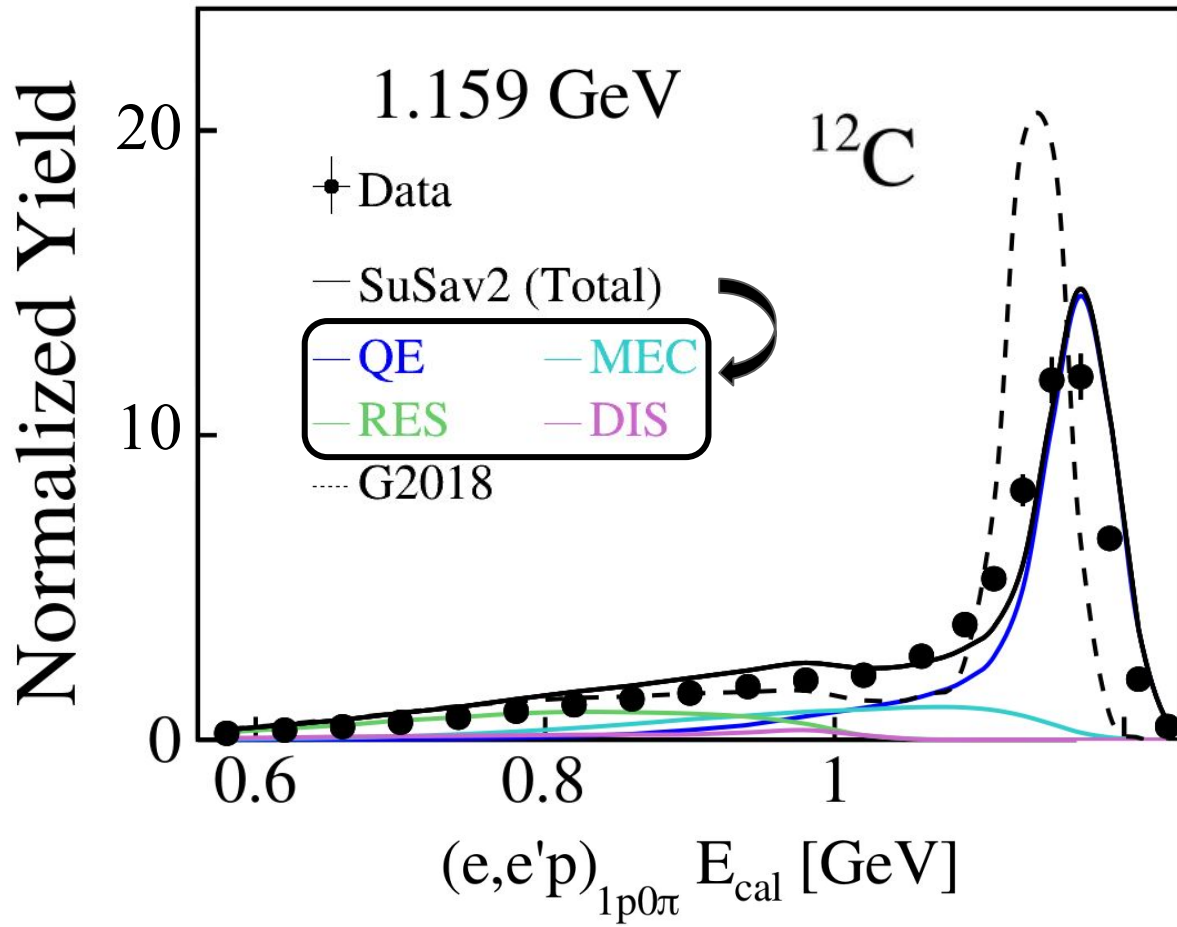
SuSav2 captures QE peak
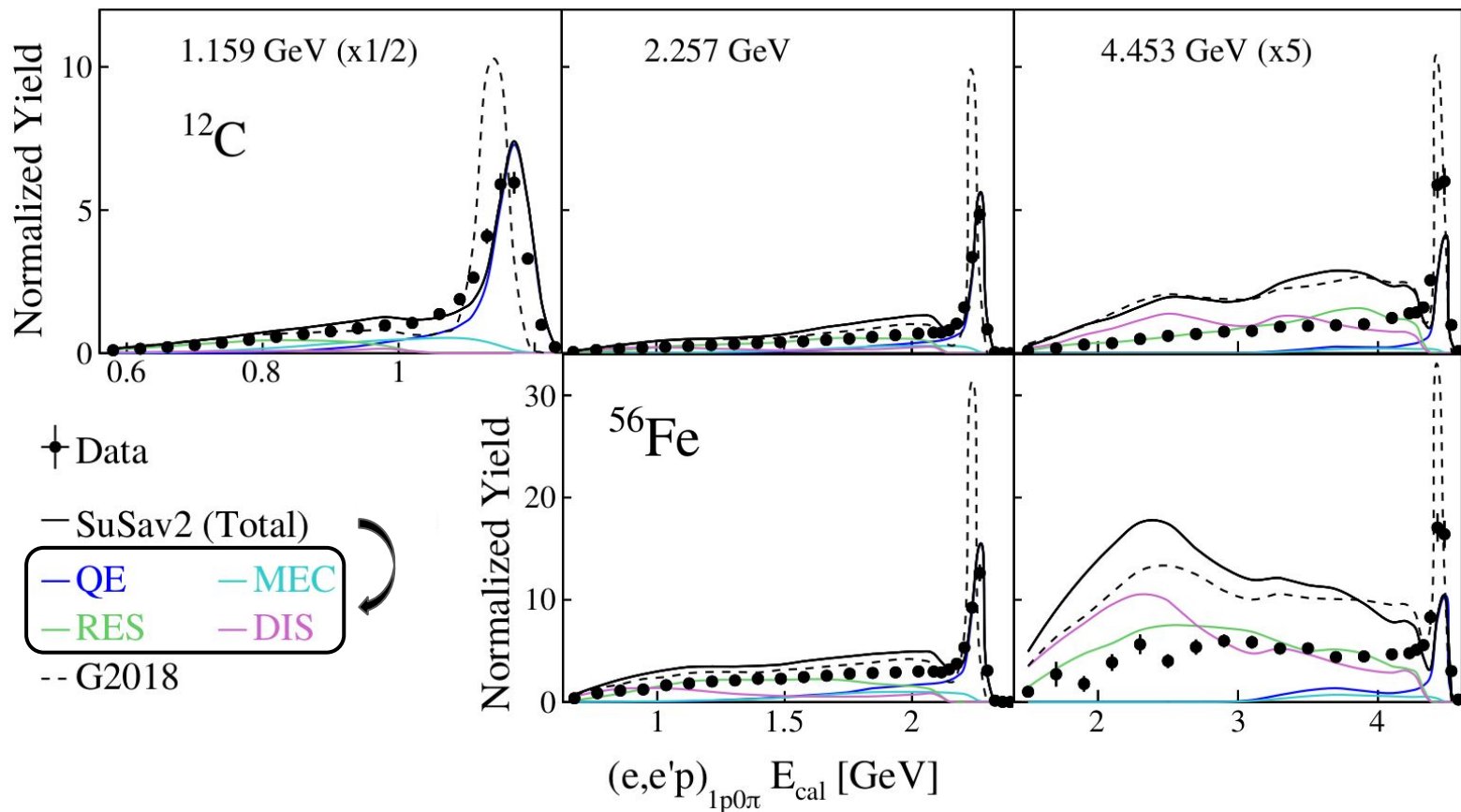
Simulation fails at high energies & on heavier nuclei

Future Plans @ CLAS12

- Acceptance down to 5°

- x10 luminosity [10^{35} cm^{-2} s^{-1}]

- Targets
  ^{2}D, ^{4}He, ^{12}C, ^{16}O, **^{40}Ar**, ^{120}Sn
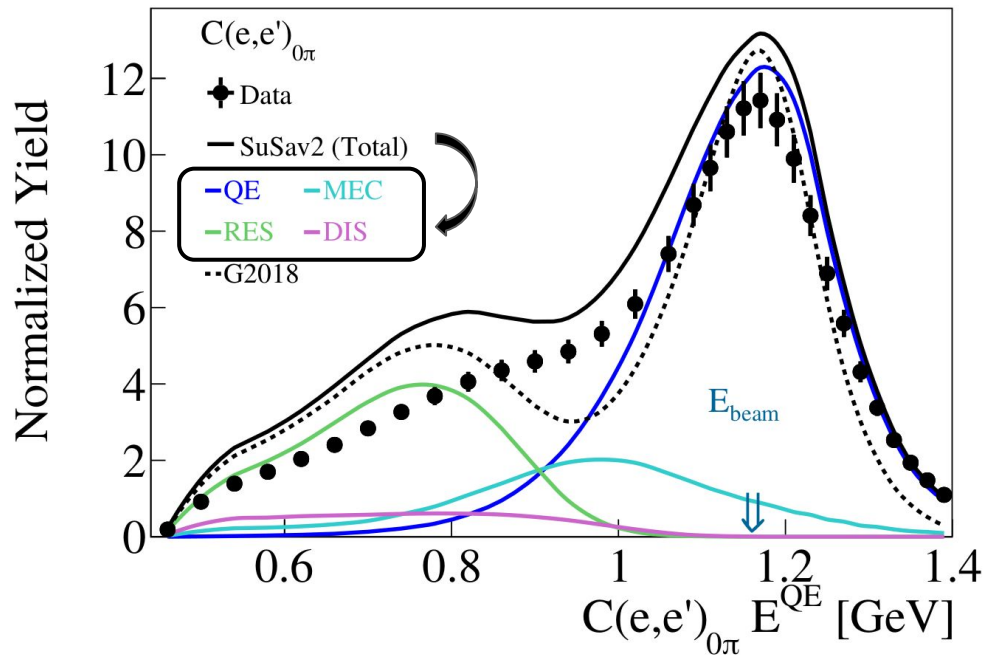
- 1 - 7 GeV beam energies

- Data taking in 2021
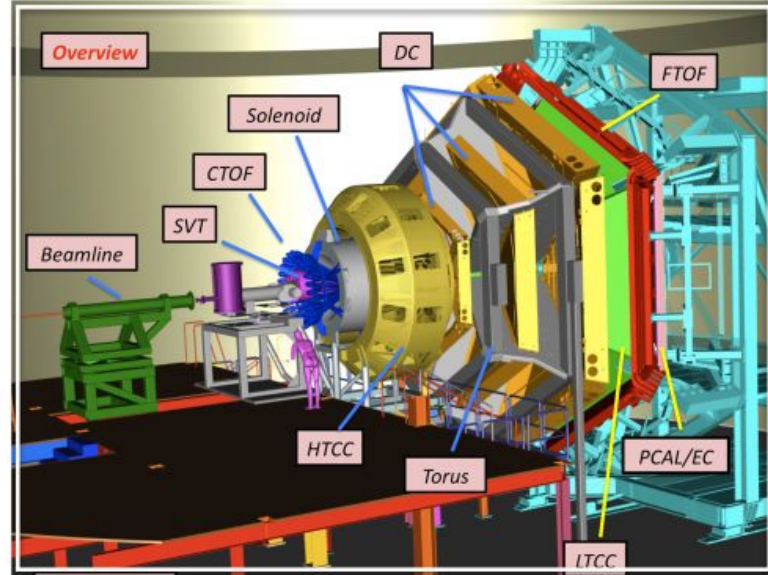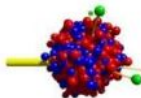
- Benchmarking *ν* models against wide phase-space electron data sets

- Data/MC disagreements even for QE-like topologies

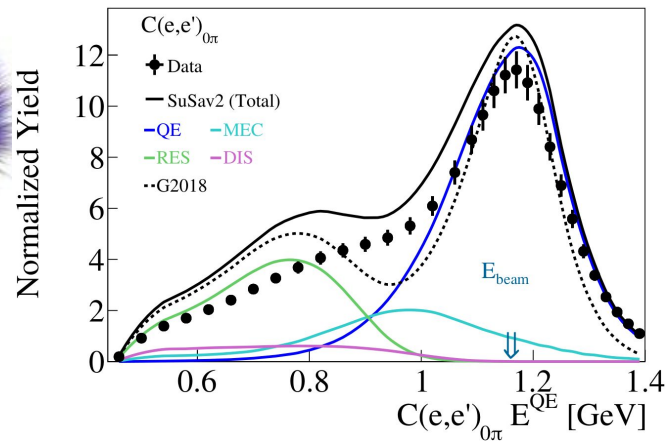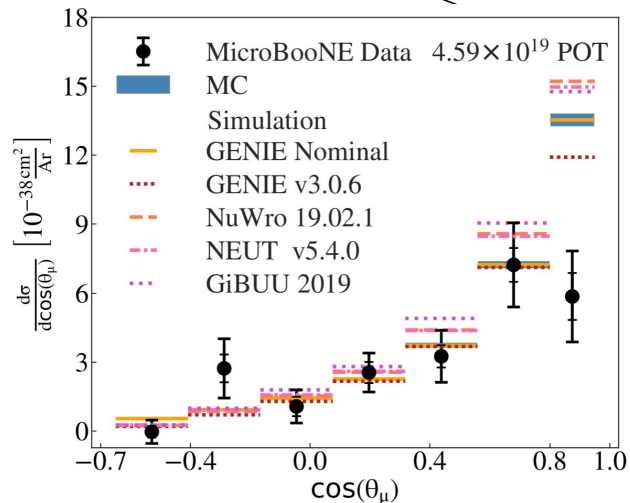- Need for more electron scattering data sets to constrain neutrino models
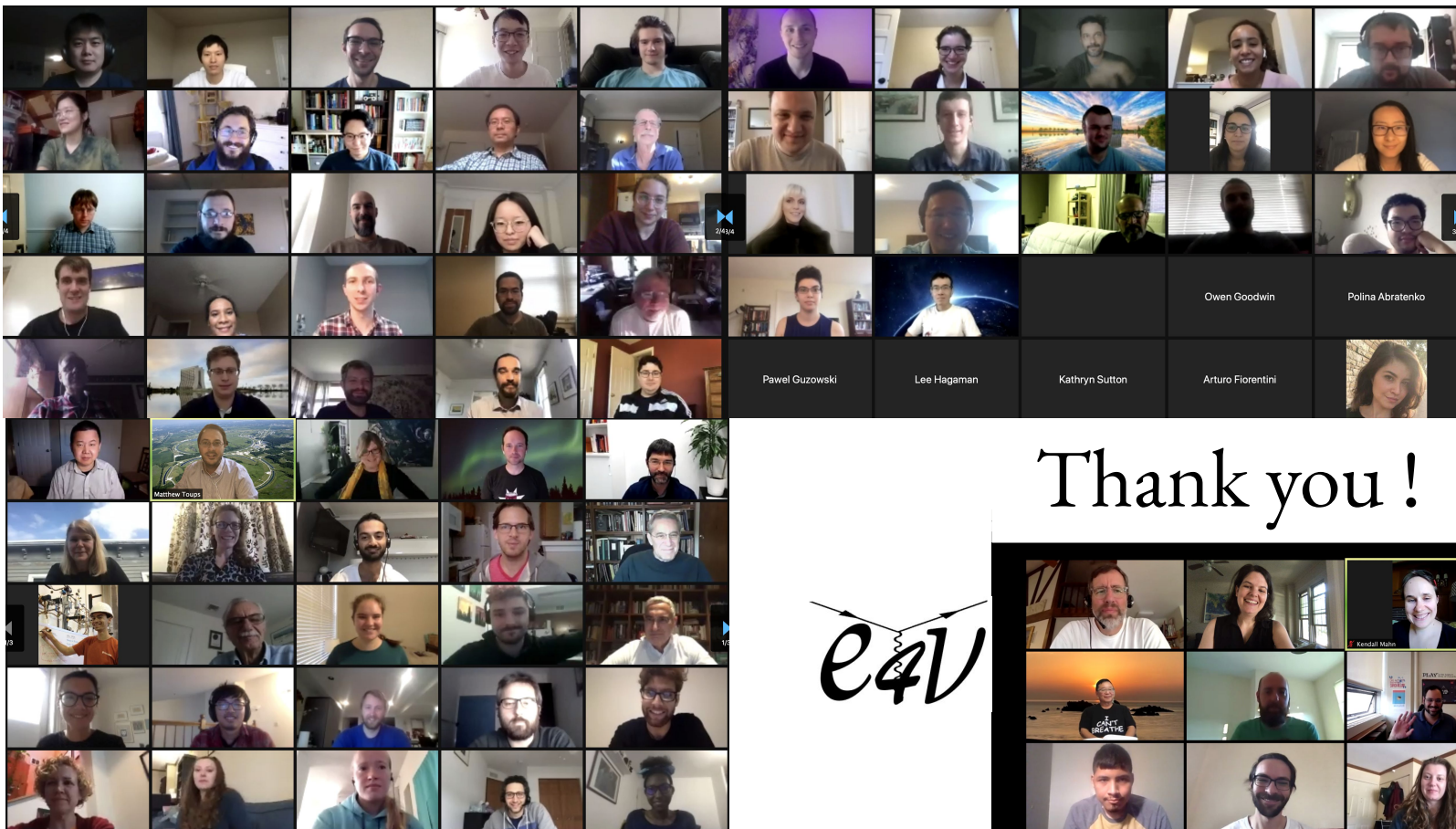
Potential impact on DUNE

μBooNE

Modeling Input

e4ν

- First exclusive measurement of Quasielastic-like interactions using the MicroBooNE detector

- First head-to-head comparison between neutrino & electron scattering

Thank you !
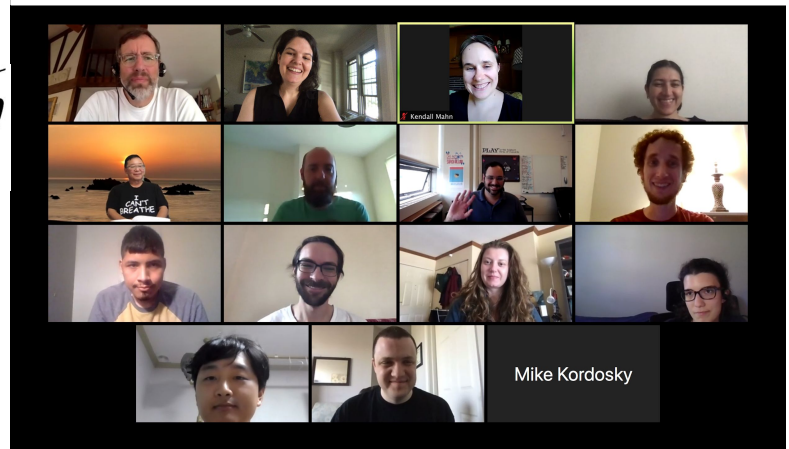
Questions ?

Backup Slides

References

[1] Phys. Rev. D.24 (1981), p. 1400
[2] Phys. Rev. C.83 (2011), p. 045501
[3] Phys. Rev. D.88 (2018), p. 113007
[4] Phys. Rept. 3 (1972), p. 261
[5] AIP Conf. Proc. 1663 (2015), p. 030001
[6] Ann. Phys. 133 (1981), p. 79
[7] Phys. Rev. D.79 (2009), p. 053003
[8] arXiv:1510.05494
[9] Phys. Rev. D 80, 093001 (2009)
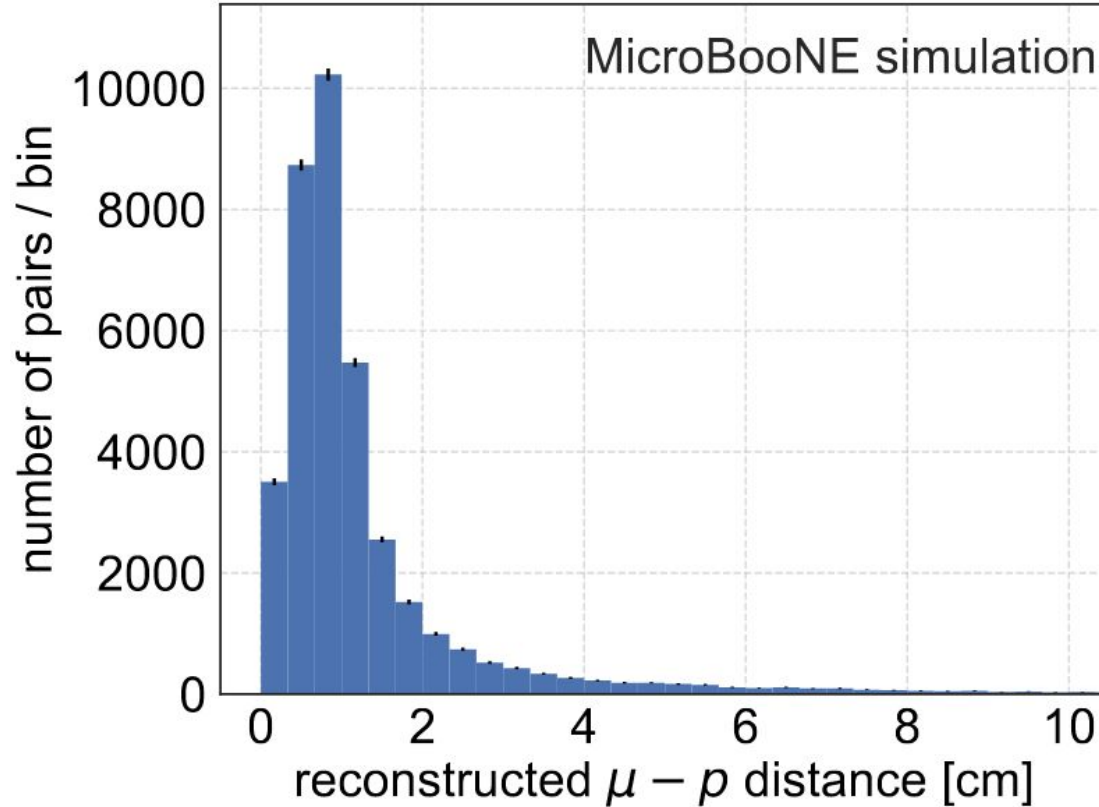[10] Nuclear Physics A 484, 557 (1988)
[11] Physics Reports 512, 1 (2012)

Preselection

Pairs of tracks at close proximity with a distance < 11 cm between any two edges (start-start, start-end, end-start, end-end)
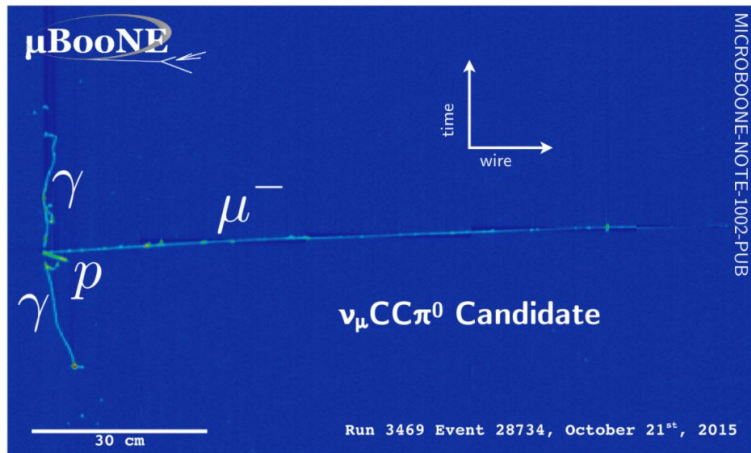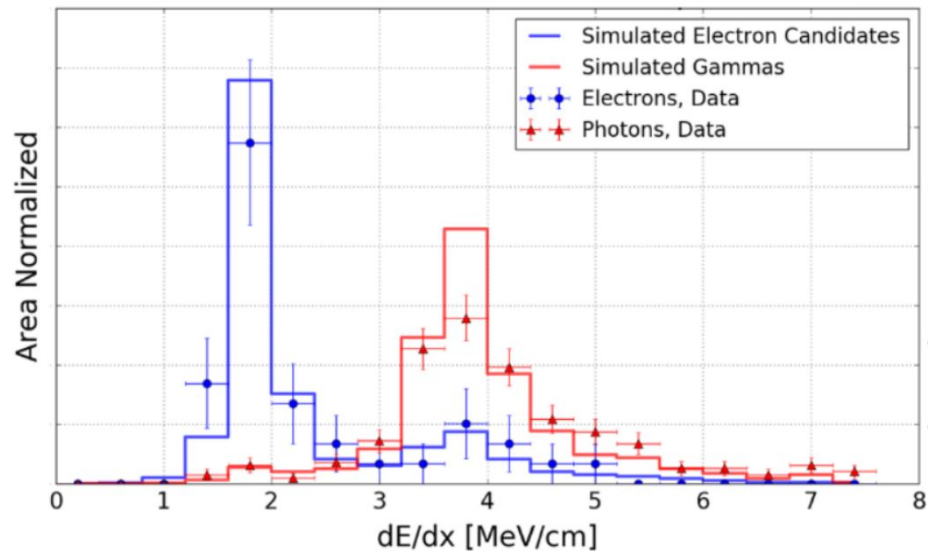
Preselection
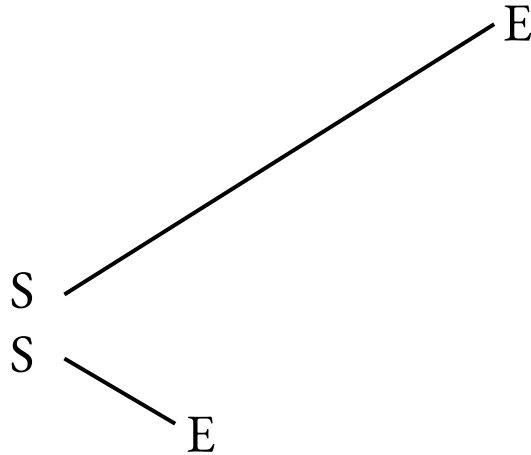
MicroBooNE simulation

Particle Identification In LArTPCs

- Detailed 3D imaging of ν interactions
- Electron / photon discrimination

ArgoNEUT

CC1p0π Topological Signal Definition

Vertex of two tracks

- 1 muon (> 100 MeV/c)

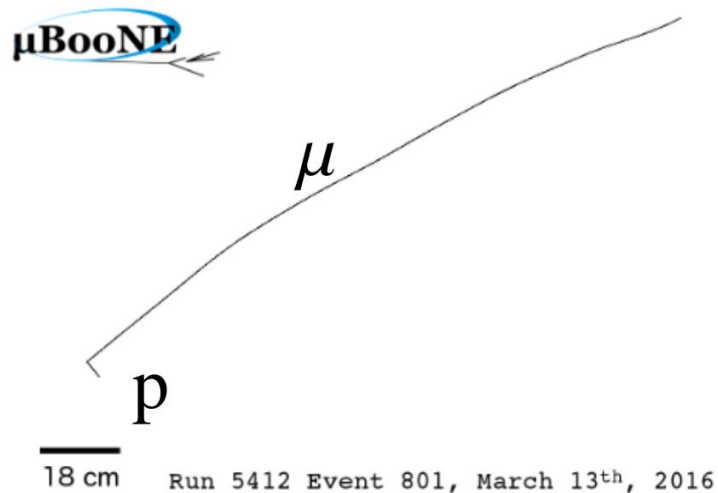Either semi-contained or fully contained

[Multiple Coulomb Scattering]

[JINST 12 P10010 (2017)](#)

- 1 proton (> 300 MeV/c)

Fully contained

[Momentum from range*]

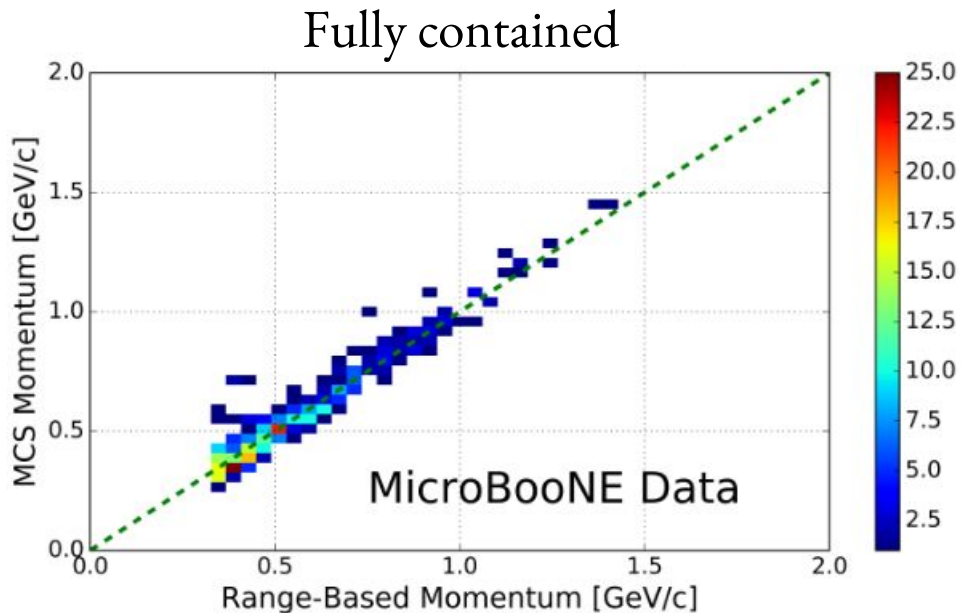- No $\pi^{\pm}$ (> 70 MeV/c)

μBooNE

μ

p

18 cm   Run 5412 Event 801, March 13th, 2016

* Table 289: Muons in Liquid argon (Ar)
   http://pdg.lbl.gov/2012/AtomicNuclearProperties/MUON_ELOSS_TABLES/muonloss_289.pdf

Multiple Coulomb Scattering (MCS)

Fully contained

Figure 7. MCS-computed momentum versus range momentum for the automatically selected beam neutrino-induced fully contained muon sample in MicroBooNE data after hand scanning to remove poorly reconstructed tracks and obvious mis-identification topologies. The color (z) scale indicates number of tracks.

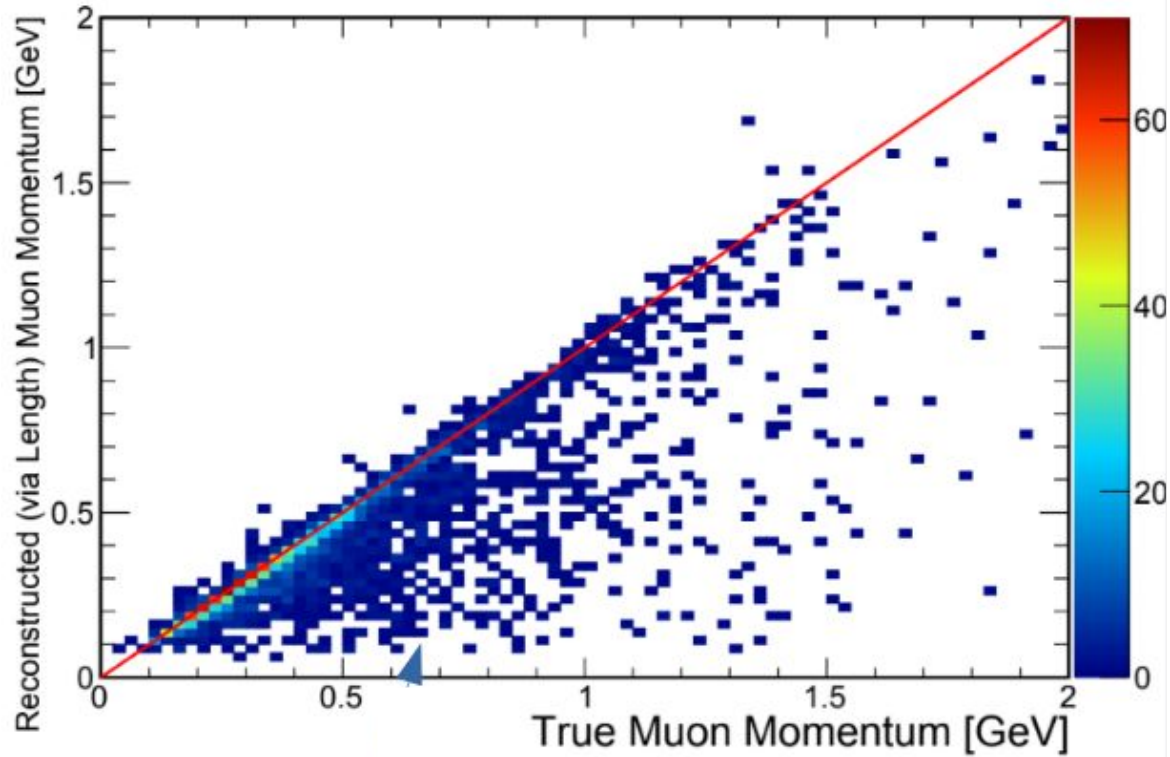JINST 12 P10010 (2017)

Multiple Coulomb Scattering (MCS)
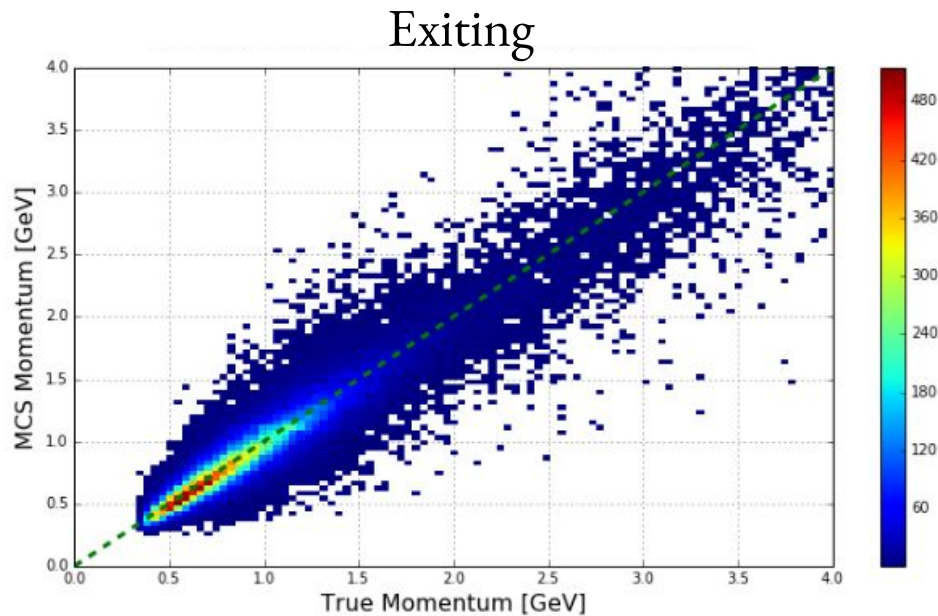
Exiting

Figure 10. MCS-computed momentum versus true momentum for the MCTRACKS (truth-based) sample of simulated exiting muons from BNB ν_μCC interactions in MicroBooNE with at least one meter of track contained within the TPC. The color (z) scale indicates number of tracks.

JINST 12 P10010 (2017)

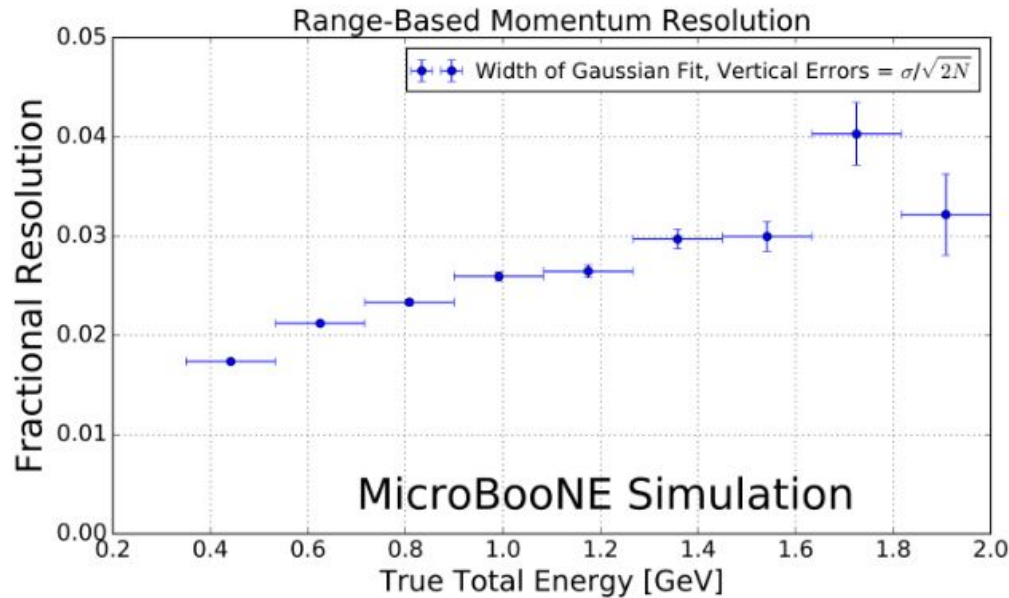# Multiple Coulomb Scattering (MCS)
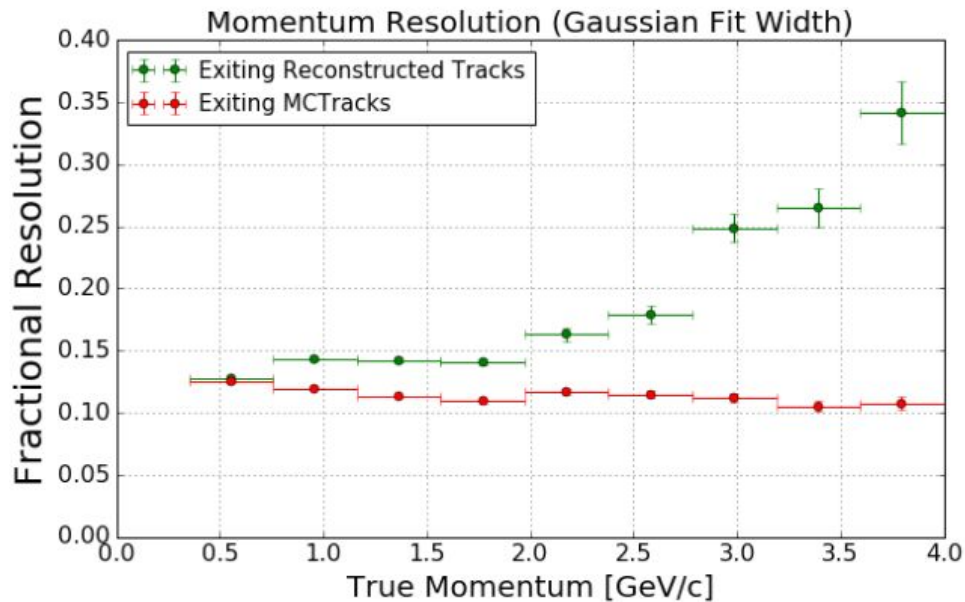
Figure 12. MCS momentum fractional bias (top) and resolution (bottom) from Gaussian fits to the reconstructed momentum as a function of true momentum for the exiting muon using the MCTRACKS (truth-based) sample and using the fully-simulated sample.

JINST 12 P10010 (2017)

Momentum From Range

# Momentum From Range

Figure 5. Range-based energy fractional bias (top) and resolution (bottom) from a sample of simulated fully contained BNB neutrino-induced muons using true starting and stopping positions of the track. The bias is less than 1% and the resolution is better than 4%.

JINST 12 P10010 (2017)

MicroBooNE Public Note 1031

MicroBooNE Simulation Preliminary
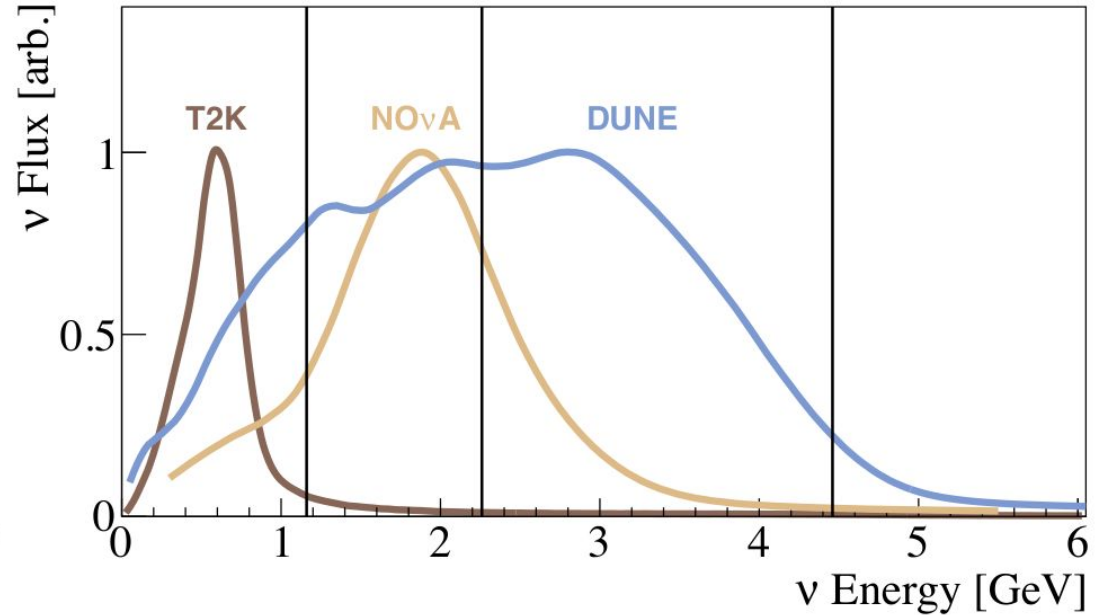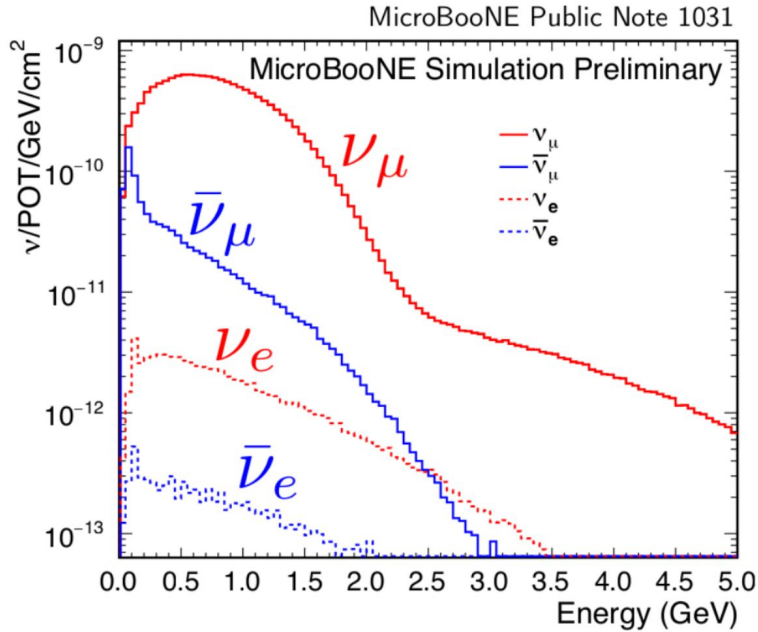
• Low energy & wide spectrum

Liquid Argon TPCs
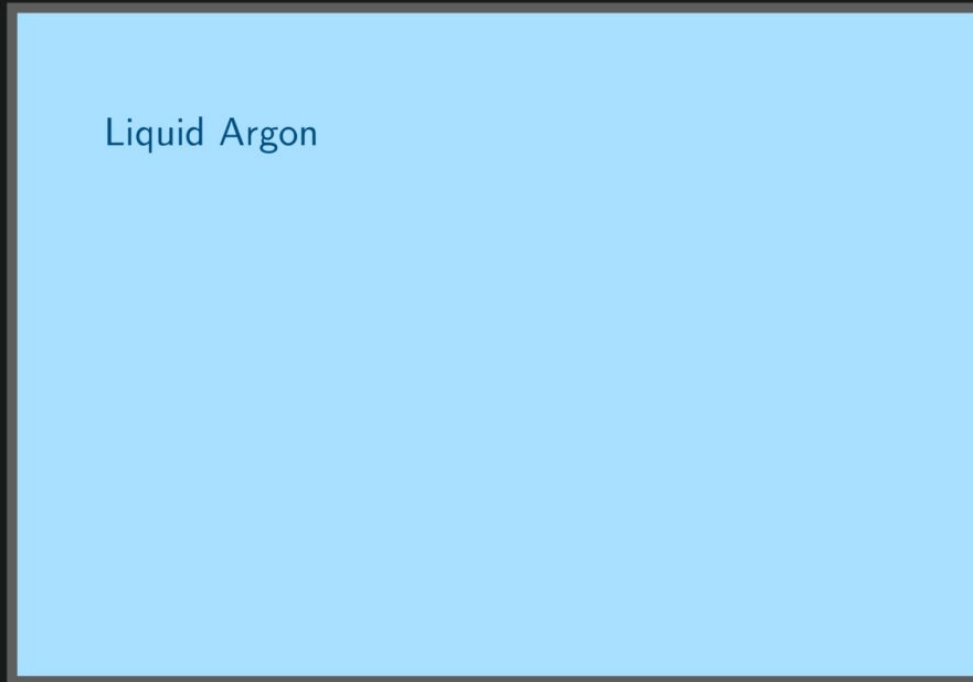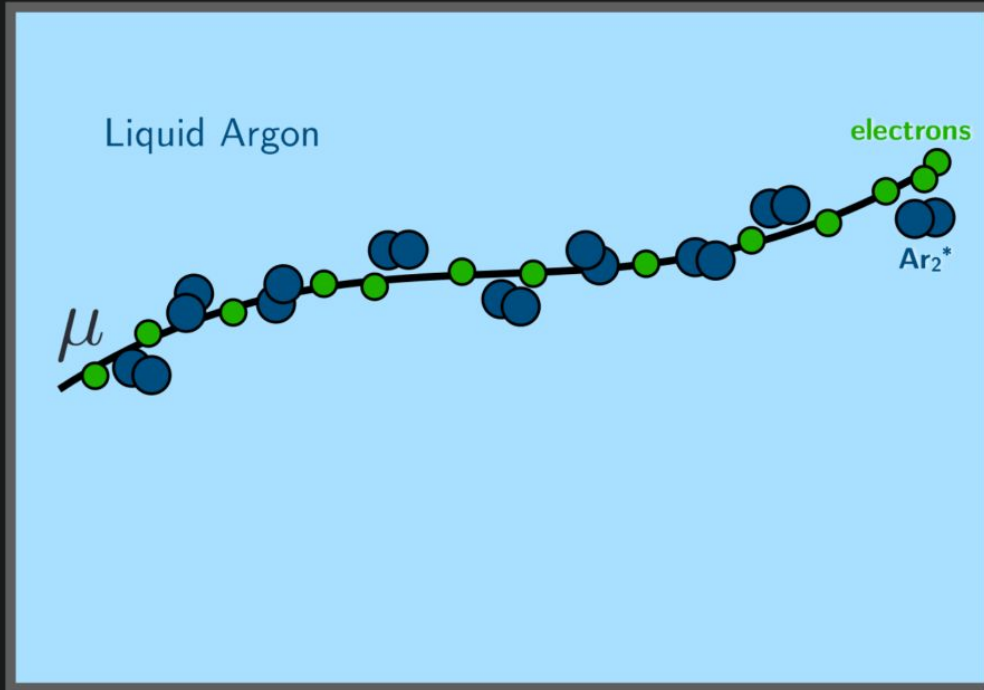
LAr
87K

Liquid Argon

Liquid Argon TPCs
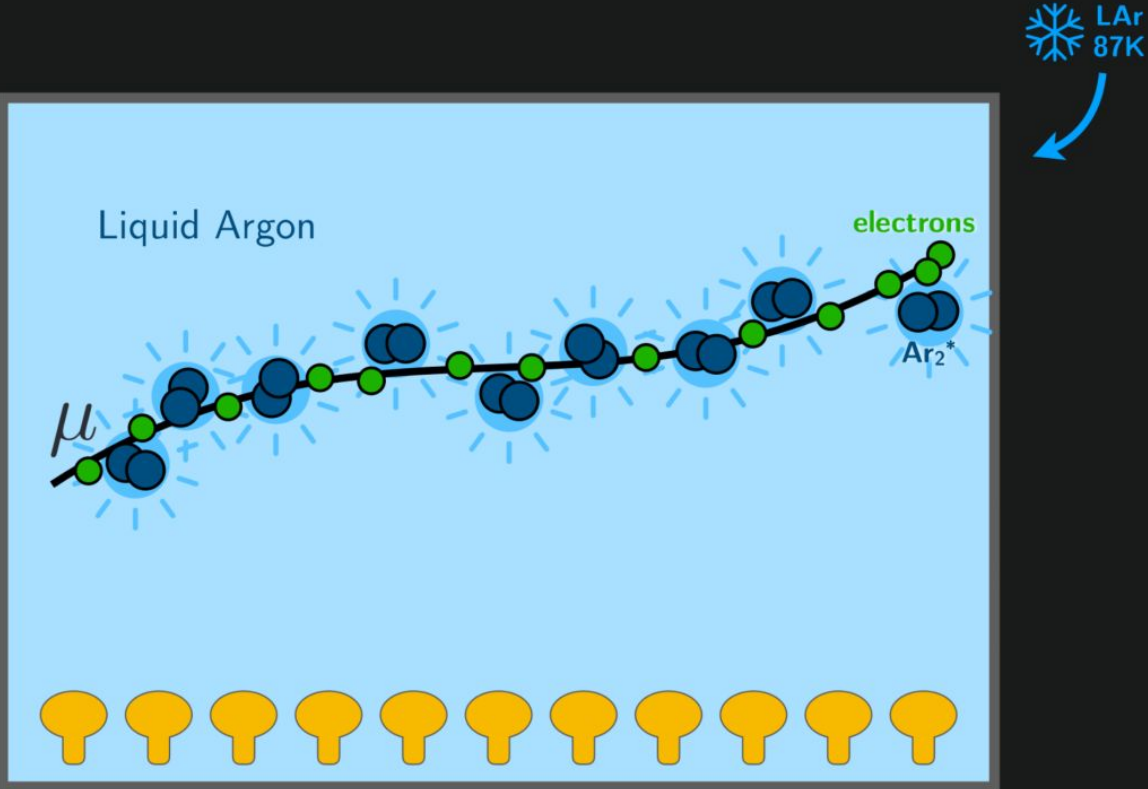
Liquid Argon TPCs
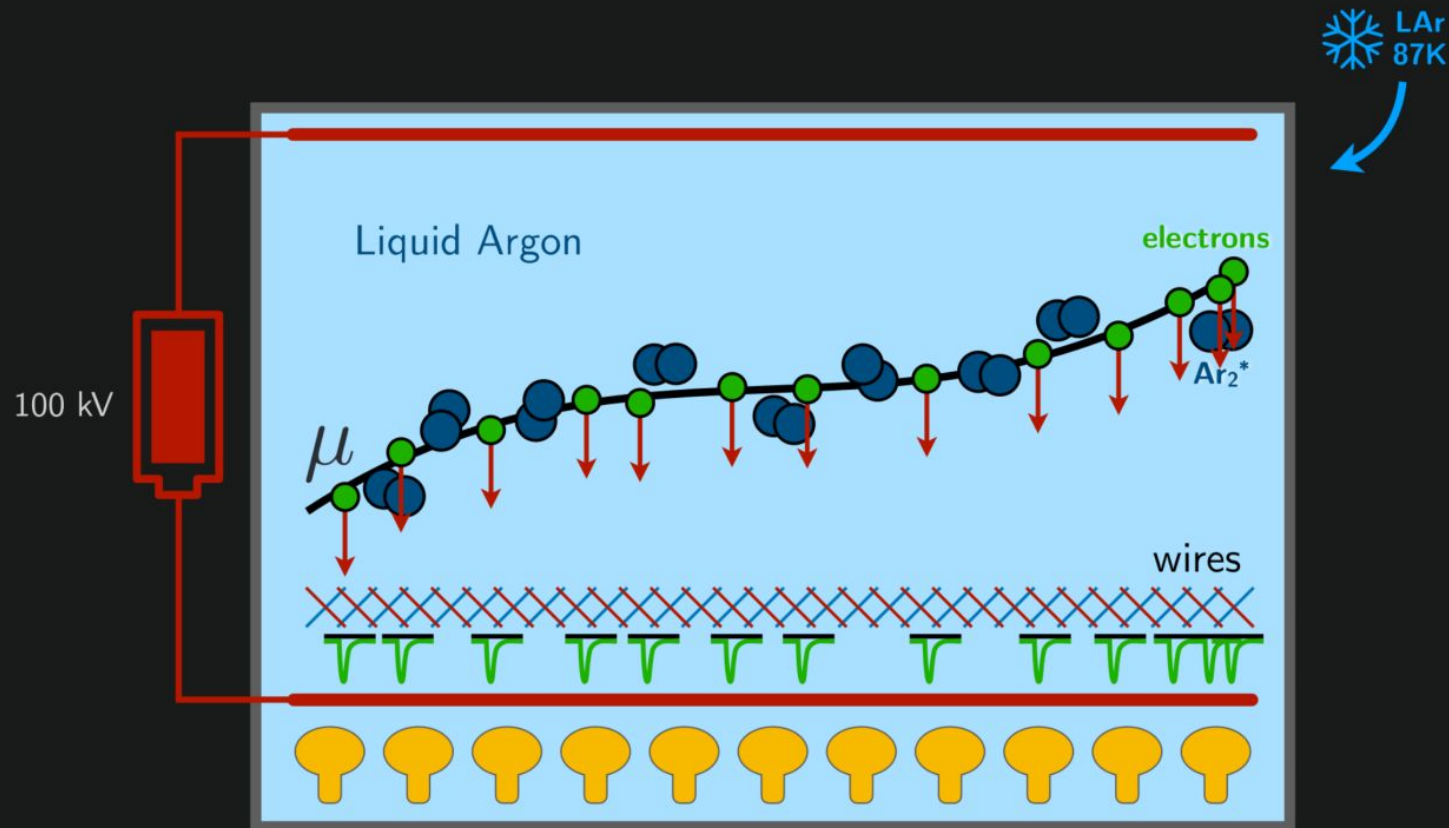
Liquid Argon TPCs

Liquid Argon TPCs
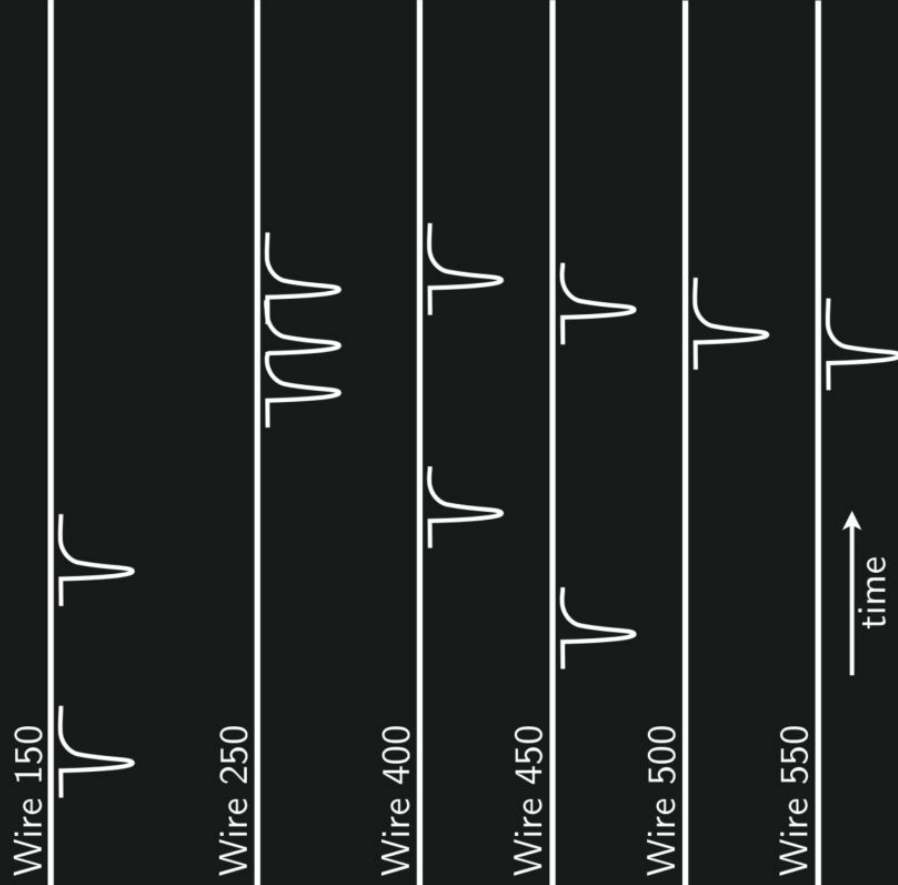
μBooNE

13 cm

Wire 150   Wire 250   Wire 400   Wire 450   Wire 500   Wire 550

time

BNB DATA : RUN 5536 EVENT 1612. MARCH 22, 2016
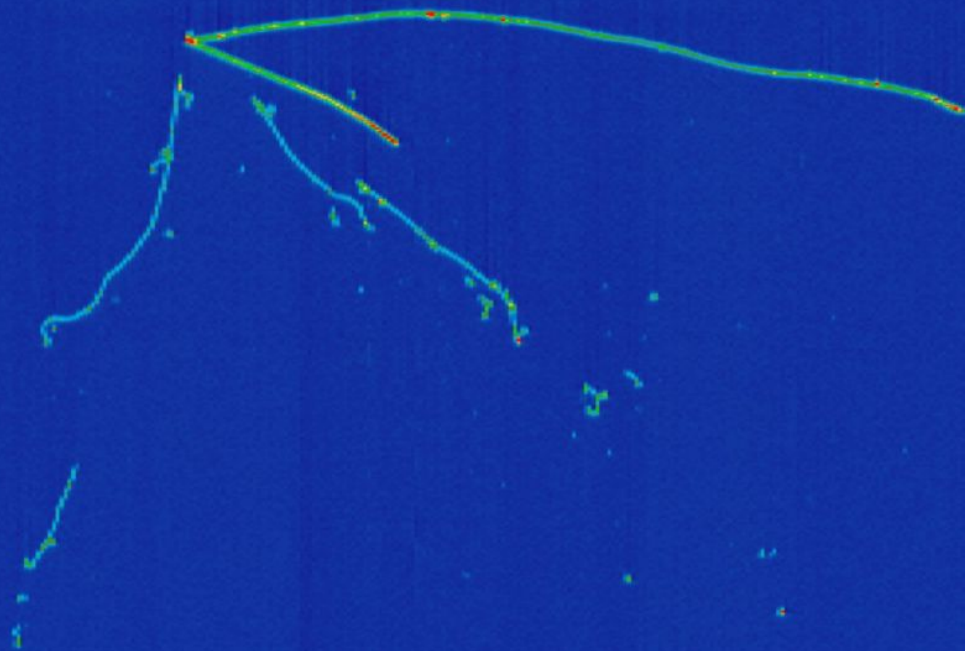
87

μBooNE

13 cm

BNB DATA : RUN 5536 EVENT 1612. MARCH 22, 2016
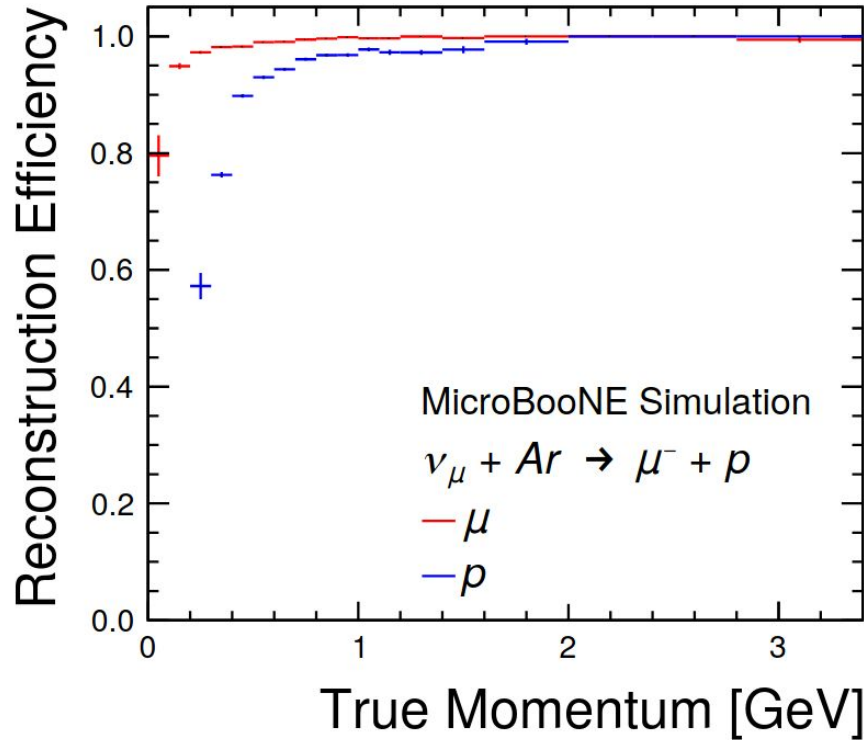
88

Pandora Reconstruction

MicroBooNE Simulation

$\nu_\mu + Ar \rightarrow \mu^- + p$

— μ

— p

- High efficiency & accuracy

- Spatial resolution ~1 cm

Eur. Phys. J. C 78, 82 (2018)

Pandora Reconstruction

MicroBooNE Simulation
$\nu_\mu + Ar \rightarrow \mu^- + p$
— μ
— p

- High efficiency & accuracy

- Spatial resolution ~1 cm

Data/Sim. Response Comparison: U Plane, Normal Region
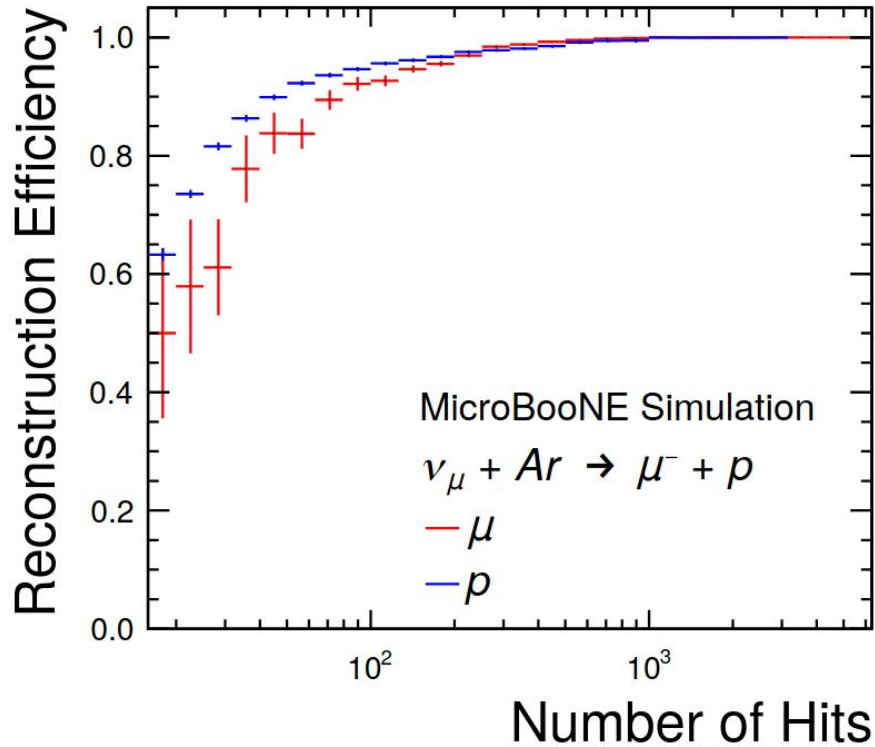
Data/Sim. Response Comparison: V Plane, Normal Region

JINST 13, P07007 (2018)
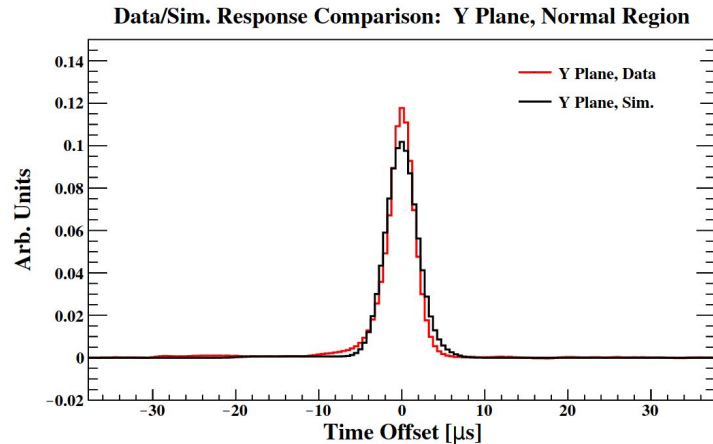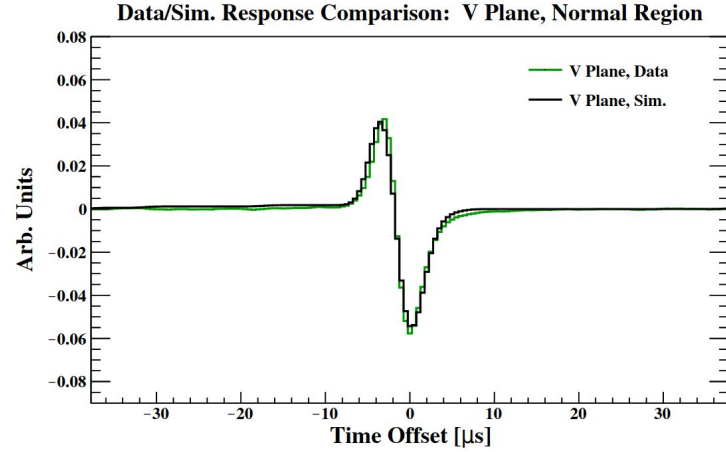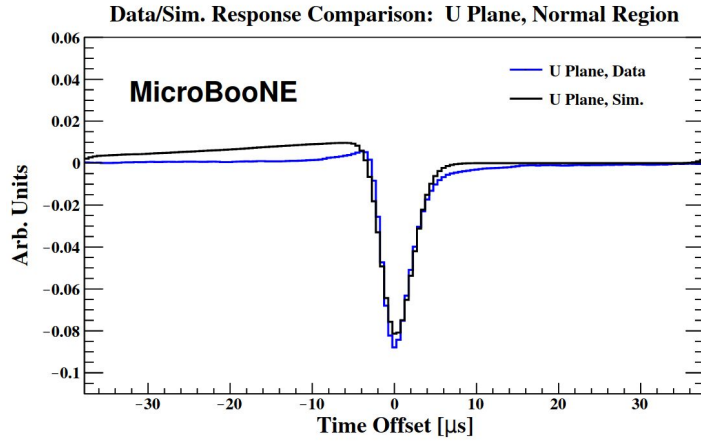
Data/Sim. Response Comparison: Y Plane, Normal Region

Data/Sim. Response Comparison: U Plane, Normal Region
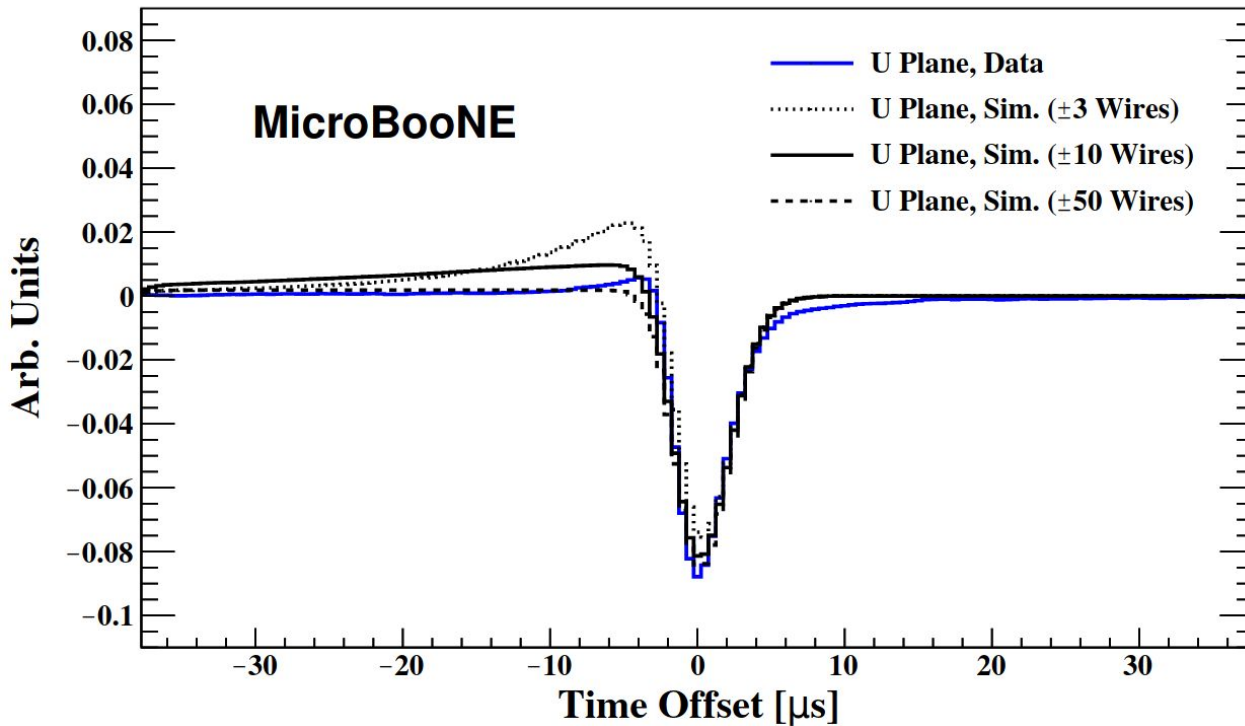
Signal Processing

- Wires further away also see a weaker induction signal
- Different points in the charge distribution give signals at different times
- Correct simulation needs to sum **all** the contributions of all signals with time offsets
- Improved signal processing over past 3 years
- **For this analysis**, we are still using the "simple" nearest-wire treatment & the collection plane

cumulative effect of the space charge in track reconstruction leads to squeezing of the reconstructed track in transverse directions and bending towards the cathode. See Figure 3.
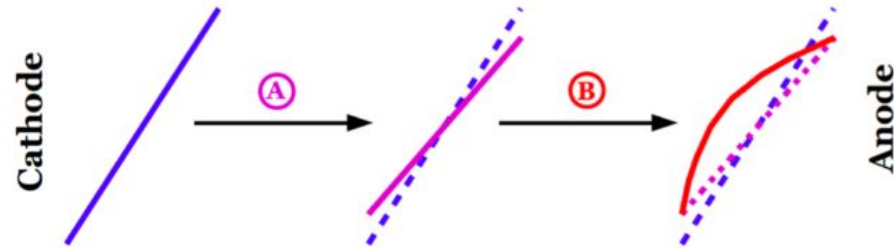
Figure 3. Diagram showing the effects of space charge on track reconstruction. The impact is two-fold: the reconstructed track could be squeezed by two extremes in the transverse directions of the TPC, as indicated in the rotation A, and bent towards cathode, as indicated by transformation B. (Image from Ref. [6] used by permission of its creator.)

Recombination

- Ionisation electrons can "recombine" with argon ions
- The rate at which they do this depends on the local density of argon ions
- Non-trivial conversion from observed charge to deposited energy

Recombination

(a) Data (b) MC simulation
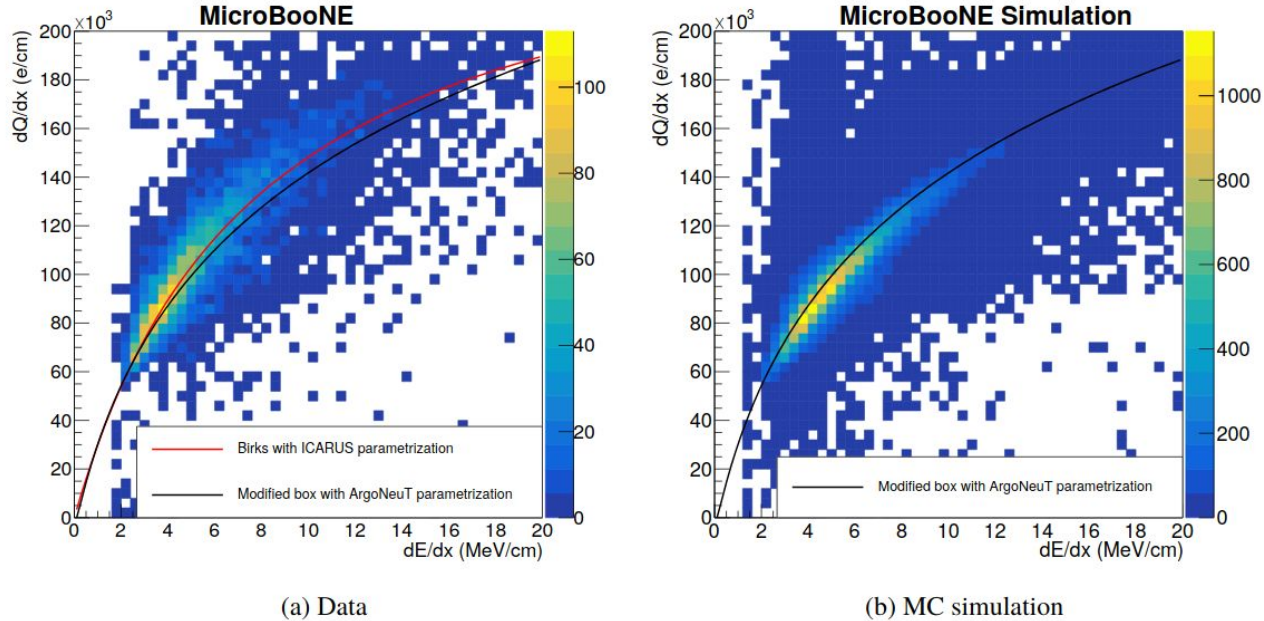
Figure 21. (a) Comparison of the measured dQ/dx vs. $(dE/dx)_{range}$ distribution with recombination models for selected proton tracks in data; (b) same comparison for selected protons in the MC simulation. The red curve corresponds to Birks' law and the black curve corresponds to the modified box model, using the parameters measured by the ICARUS and ArgoNeuT collaborations. Both model predictions are calculated at the nominal electric field of 0.273 kV/cm for MicroBooNE.

Recombination

- Modified box model

$$\left(\frac{dE}{dx}\right)_{\text{calibrated}} = \frac{\exp\left[\frac{\left(\frac{dQ}{dx}\right)_{\text{calibrated}}}{C_{\text{cal}}} \frac{\beta' W_{\text{ion}}}{\rho\mathscr{E}}\right] - \alpha}{\frac{\beta'}{\rho\mathscr{E}}}, \tag{3.1}$$

with

C_{cal} is a calibration constant used to convert ADC values to number of electrons,

W_{ion} = 23.6 x 10^{-6} MeV/electron (work function of argon),
$\mathscr{E}$ = 0.273 kV/cm (MicroBooNE drift electric field),
ρ = 1.38 g/cm^3 (liquid argon density at a pressure 124.106 kPa),
β' = 0.212 (kV/cm)(g/cm^2)/MeV, and
α = 0.93.

The last two parameters were measured by the ArgoNeuT experiment [13] at an electric field of 0.481 kV/cm. The modified box model is applied at MicroBooNE's electric field of 0.273 kV/cm.

PID In MicroBooNE

- For track-like particles, we rely on the Bragg peak
- Requires particles come to a stop in the detector
- PID all based off dE/dx vs Residual Range
- Pions and muons are functionally indistinguishable
- So PID is basically – is it a proton or not?
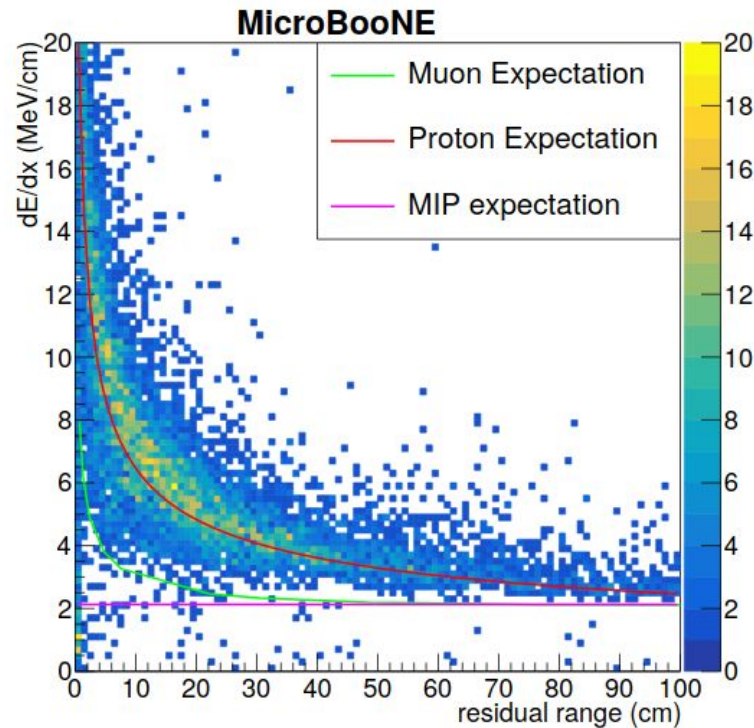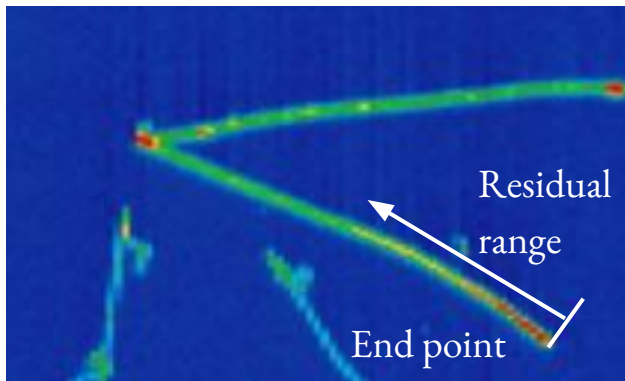
JINST 15, P03022 (2020)

PID In MicroBooNE

- We convert the dE/dx vs residual range into a single number, a summed average distance from proton expectation
- Low is proton-like, high is not proton-like

$$PID = \chi^2_{proton}/d.o.f. = \sum_{\text{Track hits}} \left(\frac{(dE/dx_{\text{measured}} - dE/dx_{\text{theory}})}{\sigma_{dE/dx}} \right)^2 / d.o.f.$$
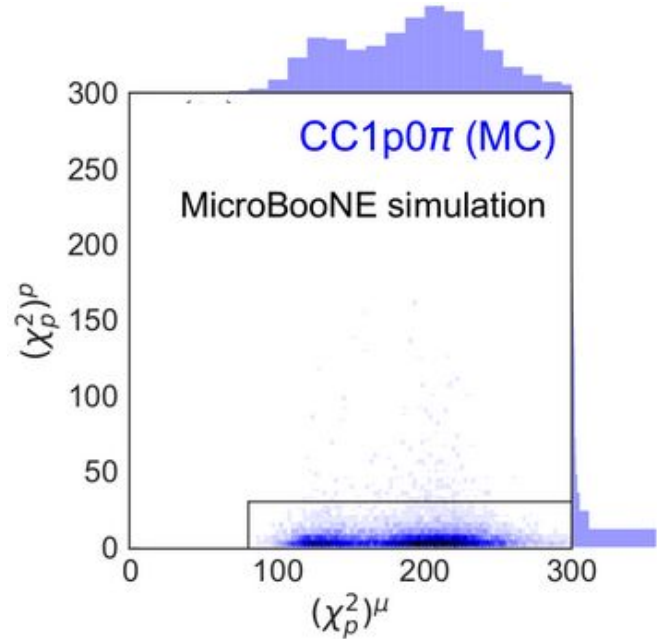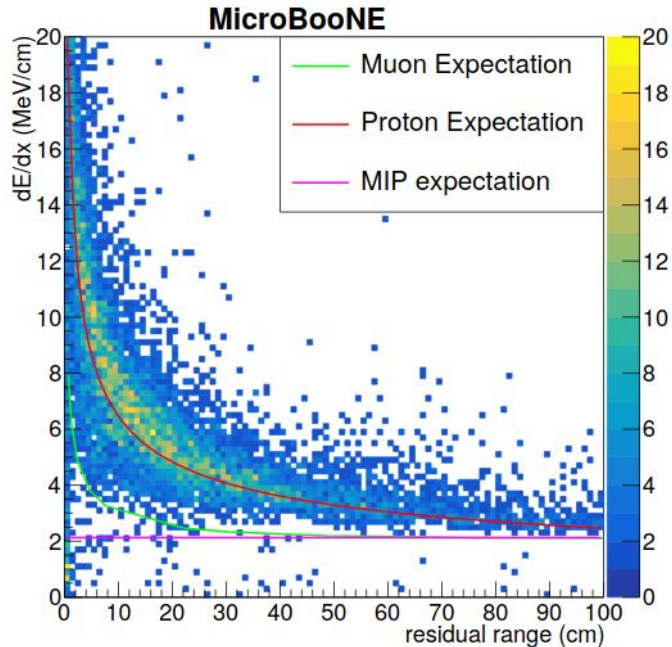
Reduction of cosmic background

is achieved using the Beam Spill Time

Neutrinos are delivered in spills of **1.6 μs**

The light information (prompt light O(ns))

can be used to identify neutrino interactions

during a spill
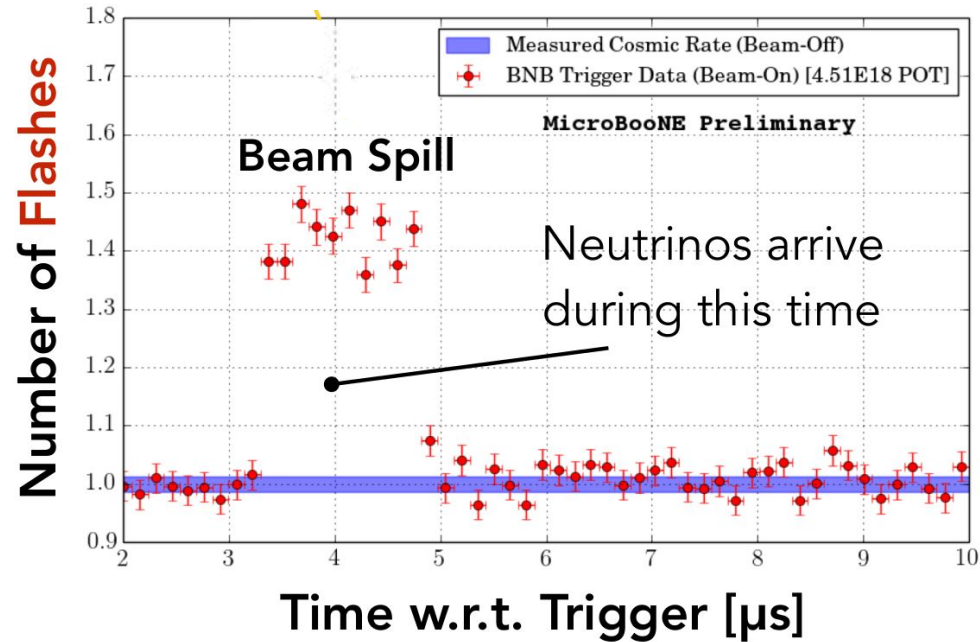
Detector Response

$$\chi^2_\mu > \chi^2_p$$

$$\chi^2_\mu > 80 \ \& \ \chi^2_p < 30$$

- **Energy deposition profile**

- Track length

- Scintillation light

- Non-collinearity
$$|\Delta\theta_{\mu p} - 90^o| < 55^o$$
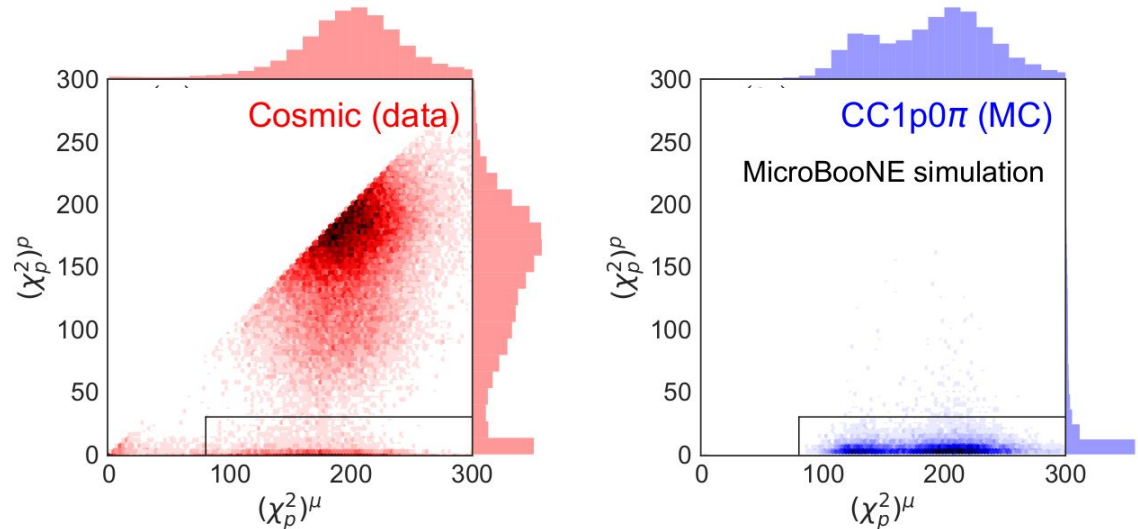
Detector Response

- Energy deposition profile

- **Track length**

- Scintillation light

- Non-collinearity

$$|\Delta\theta_{\mu p} - 90^o| < 55^o$$

$$l_\mu > l_p$$

Cosmic (data)

CC1p0π (MC)

MicroBooNE simulation

photoelectrons > 200
YZ vertex-flash distance < 2 m

- Energy deposition profile

- Track length

- **Scintillation light**

- Non-collinearity

$$|\Delta\theta_{\mu p} - 90^o| < 55^o$$

Cosmic (data)

CC1p0π (MC)

MicroBooNE simulation

- Energy deposition profile

- Track length

- Scintillation light

- **Non-collinearity**

$$|\Delta\theta_{\mu p} - 90^o| < 55^o$$

Broken track

Cosmic (data)

no cut
χ_p^2 cut
PMT cut
$l_\mu > l_p$ cut

pairs per bin [a.u.]

CC1p0π (MC)

MicroBooNE simulation

pairs per bin [a.u.]

θ_{12} [deg.]

104

- **Vertex activity**

U plane

$\Delta Q_{tracks}/\Delta Q_{total}$

$(20 \times 40) = 1.00$

$(50 \times 100) = 0.78$

$(150 \times 300) = 0.73$

Selection Cuts

	DATA	simulated signal	
criterion	cosmic	CC1p0π	purity
preselection			
preselection	155416(100.0%)	37228(100.0%)	13.1%
detector–response requirements			
dE/dx profile	8327(5.4%)	25016(67.2%)	38.8%
optical filter	2256(1.5%)	19208(51.6%)	43.6%
track lengths	1874(1.2%)	17623(47.3%)	46.5%
collinearity	839(0.54%)	16796(45.1%)	50.5%
kinematical requirements			
vertex activity	467(0.30%)	15034(40.4%)	62.1%
coplanarity only	189(0.12%)	11824(31.8%)	75.2%
p_T imbalance only	256(0.16%)	12261(32.9%)	69.3%
$\Delta\phi$ & p_T	104(0.07%)	10020(26.9%)	78.4%

Migration Matrices
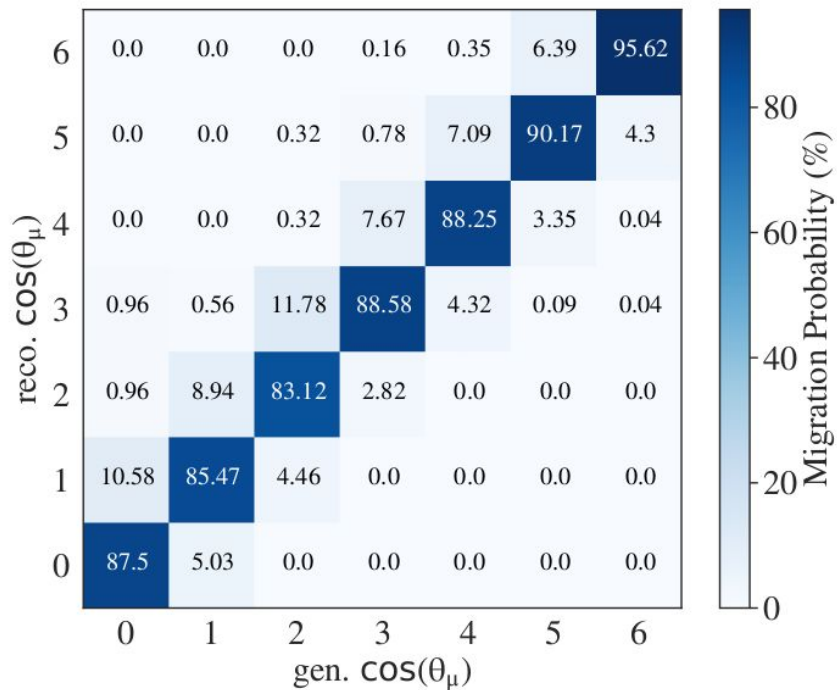
MicroBooNE Simulation

MicroBooNE Simulation

arXiv:2006.00108 [hep-ex] (2020)

Migration Matrices

MicroBooNE Simulation

MicroBooNE Simulation

arXiv:2006.00108 [hep-ex] (2020)
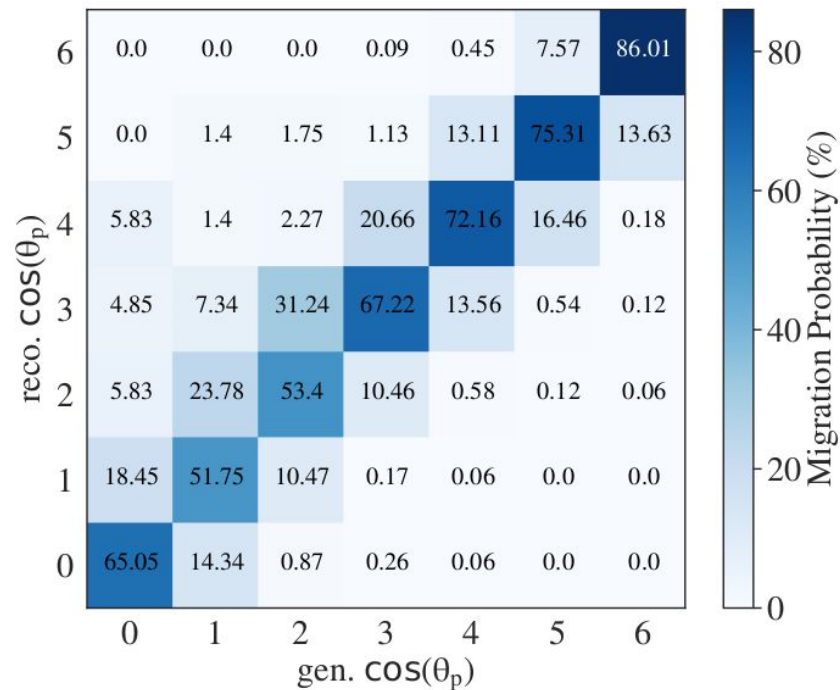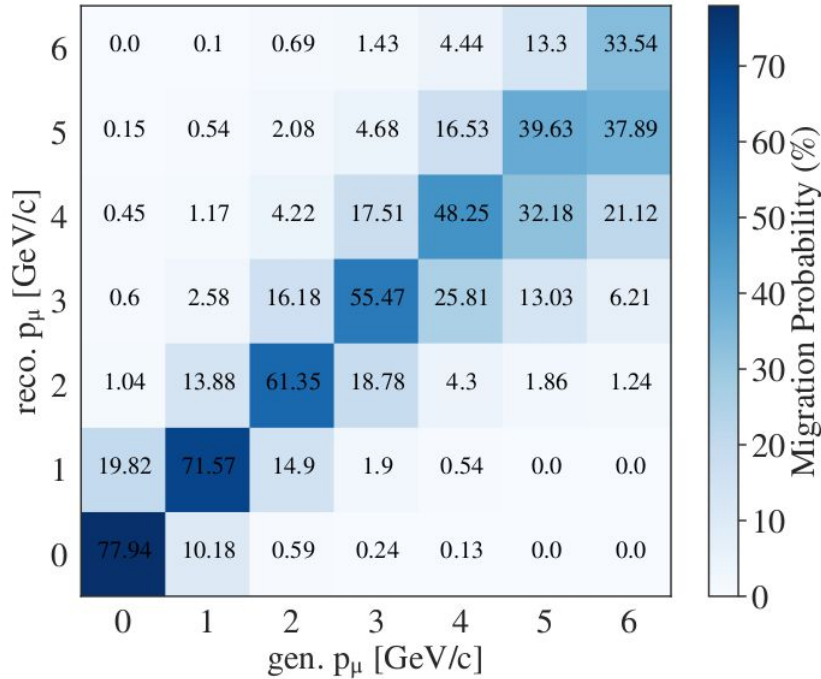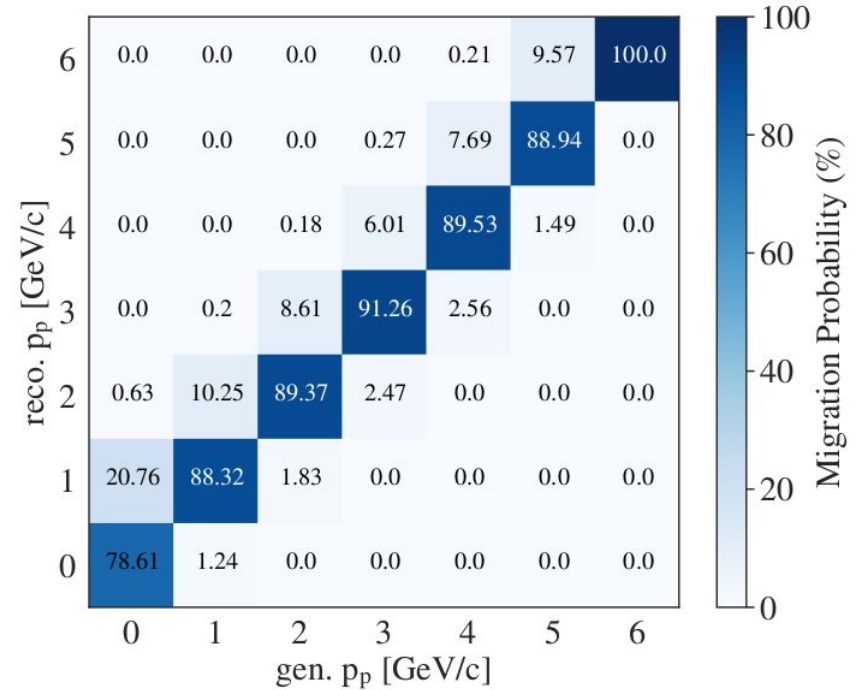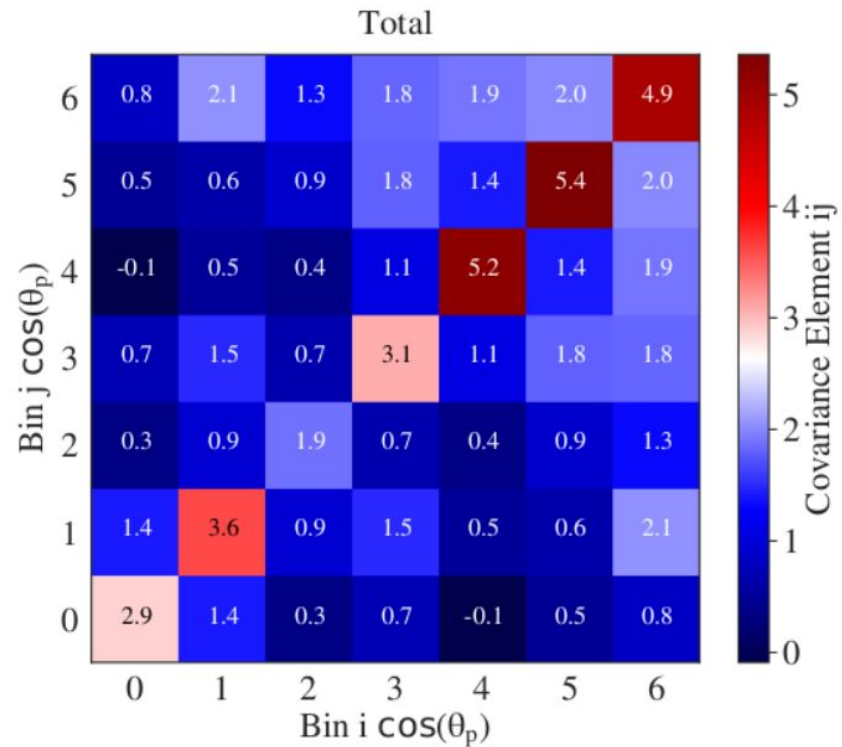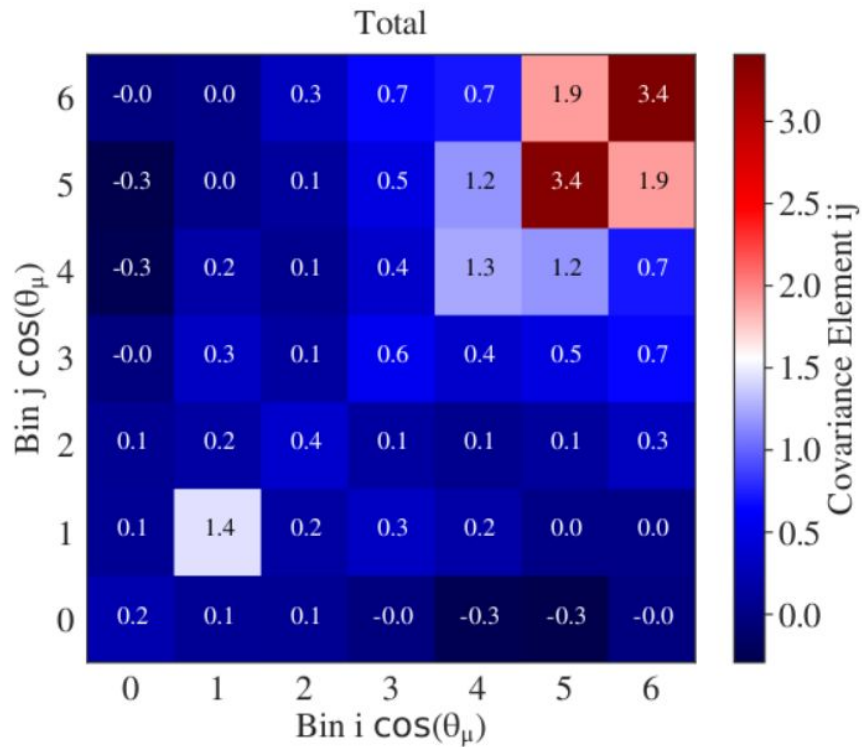
Covariance Matrices
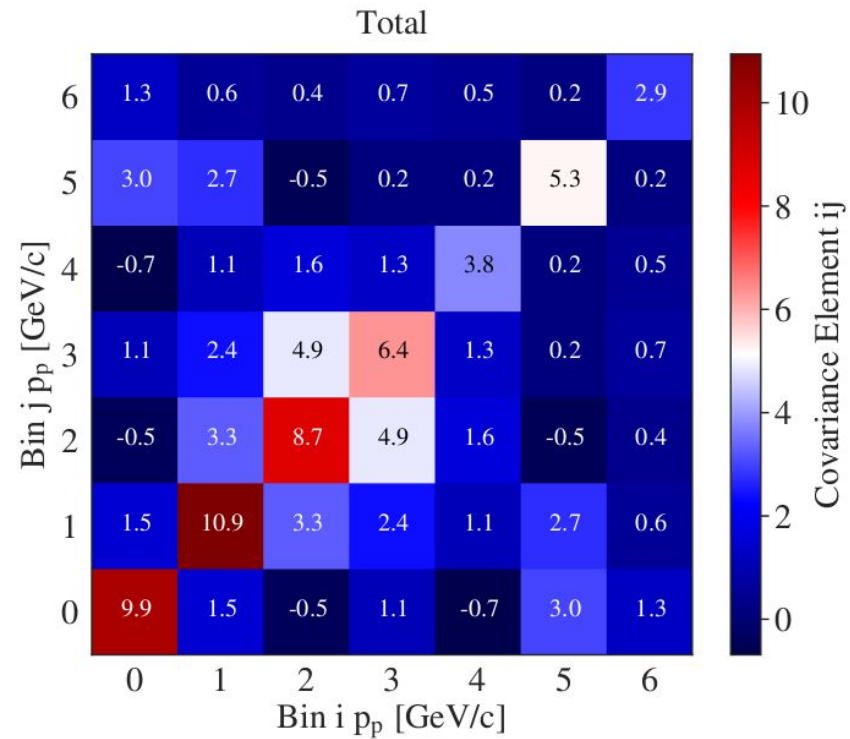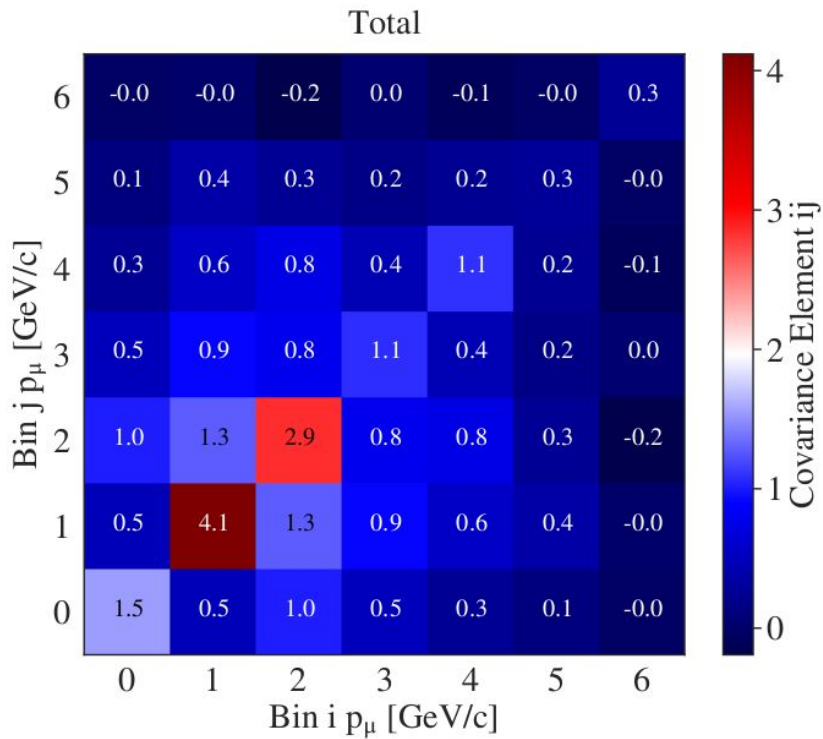
χ^2 Comparisons For Each Kinematic Variable

Data - GENIE Nominal comparisons

Kinematic Variable	$-0.65 < \cos(\theta_\mu) < 0.95$	$-0.65 < \cos(\theta_\mu) < 0.8$
P_μ	14.2/7	8.4/7
$\cos(\theta_\mu)$	33.8/7	7.3/6
P_p	2.8/7	5.1/7
$\cos(\theta_p)$	12.4/7	9.2/7

Agreement significantly improved if forward muon angles are excluded

GENIE Reweightable Cross Section Parameters

x_P	Description of P	$\delta P/P$
$x_{M_A^{NCEL}}$	Axial mass for NC elastic	$\pm 25\%$
$x_{\eta^{NCEL}}$	Strange axial form factor η for NC elastic	$\pm 30\%$
$x_{M_A^{CCQE}}$	Axial mass for CC quasi-elastic	$-15\%\ +25\%$
$x_{CCQE-Norm}$	Normalization factor for CCQE	
$x_{CCQE-PauliSup}$	CCQE Pauli suppression (via changes in Fermi level k_F)	$\pm 35\%$
$x_{CCQE-VecFF}$	Choice of CCQE vector form factors (BBA05 $\leftrightarrow$ Dipole)	-
$x_{CCRES-Norm}$	Normalization factor for CC resonance neutrino production	
$x_{NCRES-Norm}$	Normalization factor for NC resonance neutrino production	
$x_{M_A^{CCRES}}$	Axial mass for CC resonance neutrino production	$\pm 20\%$
$x_{M_V^{CCRES}}$	Vector mass for CC resonance neutrino production	$\pm 10\%$
$x_{M_A^{NCRES}}$	Axial mass for NC resonance neutrino production	$\pm 20\%$
$x_{M_V^{NCRES}}$	Vector mass for NC resonance neutrino production	$\pm 10\%$
$x_{M_A^{COHpi}}$	Axial mass for CC and NC coherent pion production	$\pm 50\%$
$x_{R_0^{COHpi}}$	Nuclear size param. controlling π absorption in RS model	$\pm 10\%$
$x_{R_{bkg}^{\nu p,CC1\pi}}$	Non-resonance bkg in νp $CC1\pi$ reactions	$\pm 50\%$
$x_{R_{bkg}^{\nu p,CC2\pi}}$	Non-resonance bkg in νp $CC2\pi$ reactions	$\pm 50\%$
$x_{R_{bkg}^{\nu n,CC1\pi}}$	Non-resonance bkg in νn $CC1\pi$ reactions	$\pm 50\%$
$x_{R_{bkg}^{\nu n,CC2\pi}}$	Non-resonance bkg in νn $CC2\pi$ reactions	$\pm 50\%$
$x_{R_{bkg}^{\nu p,NC1\pi}}$	Non-resonance bkg in νp $NC1\pi$ reactions	$\pm 50\%$
$x_{R_{bkg}^{\nu p,NC2\pi}}$	Non-resonance bkg in νp $NC2\pi$ reactions	$\pm 50\%$
$x_{R_{bkg}^{\nu n,NC1\pi}}$	Non-resonance bkg in νn $NC1\pi$ reactions	$\pm 50\%$
$x_{R_{bkg}^{\nu n,NC2\pi}}$	Non-resonance bkg in νn $NC2\pi$ reactions	$\pm 50\%$
$x_{A_{HT}^{BY}}$	A_{HT} higher-twist param in BY model scaling variable ξ_w	$\pm 25\%$

|		
$x_{C_{V1u}^{BY}}$	C_{V1u} u valence GRV98 PDF correction param in BY model	$\pm 30\%$
$x_{C_{V2u}^{BY}}$	C_{V2u} u valence GRV98 PDF correction param in BY model	$\pm 40\%$
x_{CCDIS}	Inclusive CC cross-section normalization factor	
$x_{CC\bar{\nu}/\nu}$	$\bar{\nu}/\nu$ CC ratio	
$x_{DIS-NuclMod}$	DIS nuclear modification (shadowing, anti-shadowing, EMC)	

Also included comparison to Nieves

CCQE & MEC models

GENIE Reweightable Hadronization & Resonant Parameters

| x_P	Description of P	$\delta P/P$
$x_{AGKY}^{pT1\pi}$	Pion transverse momentum (p_T) for $N\pi$ states in AGKY	-
$x_{AGKY}^{xF1\pi}$	Pion Feynman x (x_F) for $N\pi$ states in AGKY	-
x_{fz}	Hadron formation zone	$\pm 50\%$
$x_{\theta_\pi}^{\Delta \to \pi N}$	Pion angular distribution in $\Delta \to \pi N$ (isotropic $\leftrightarrow$ RS)	-
$x_{BR}^{R \to X+1\gamma}$	Branching ratio for radiative resonance decays	$\pm 50\%$
$x_{BR}^{R \to X+1\eta}$	Branching ratio for single-η resonance decays	$\pm 50\%$

GENIE Reweightable Hadron Transport Parameters

| x_P	Description of P	$\delta P/P$
x_{mfp}^N	Nucleon mean free path (total rescattering probability)	$\pm 20\%$
x_{cex}^N	Nucleon charge exchange probability	$\pm 50\%$
x_{el}^N	Nucleon elastic reaction probability	$\pm 30\%$
x_{inel}^N	Nucleon inelastic reaction probability	$\pm 40\%$
x_{abs}^N	Nucleon absorption probability	$\pm 20\%$
x_{π}^N	Nucleon π-production probability	$\pm 20\%$
x_{mfp}^{π}	π mean free path (total rescattering probability)	$\pm 20\%$
x_{cex}^{π}	π charge exchange probability	$\pm 50\%$
x_{el}^{π}	π elastic reaction probability	$\pm 10\%$
x_{inel}^{π}	π inelastic reaction probability	$\pm 40\%$
x_{abs}^{π}	π absorption probability	$\pm 20\%$
x_{π}^{π}	π π-production probability	$\pm 20\%$

Bin Migration Effects
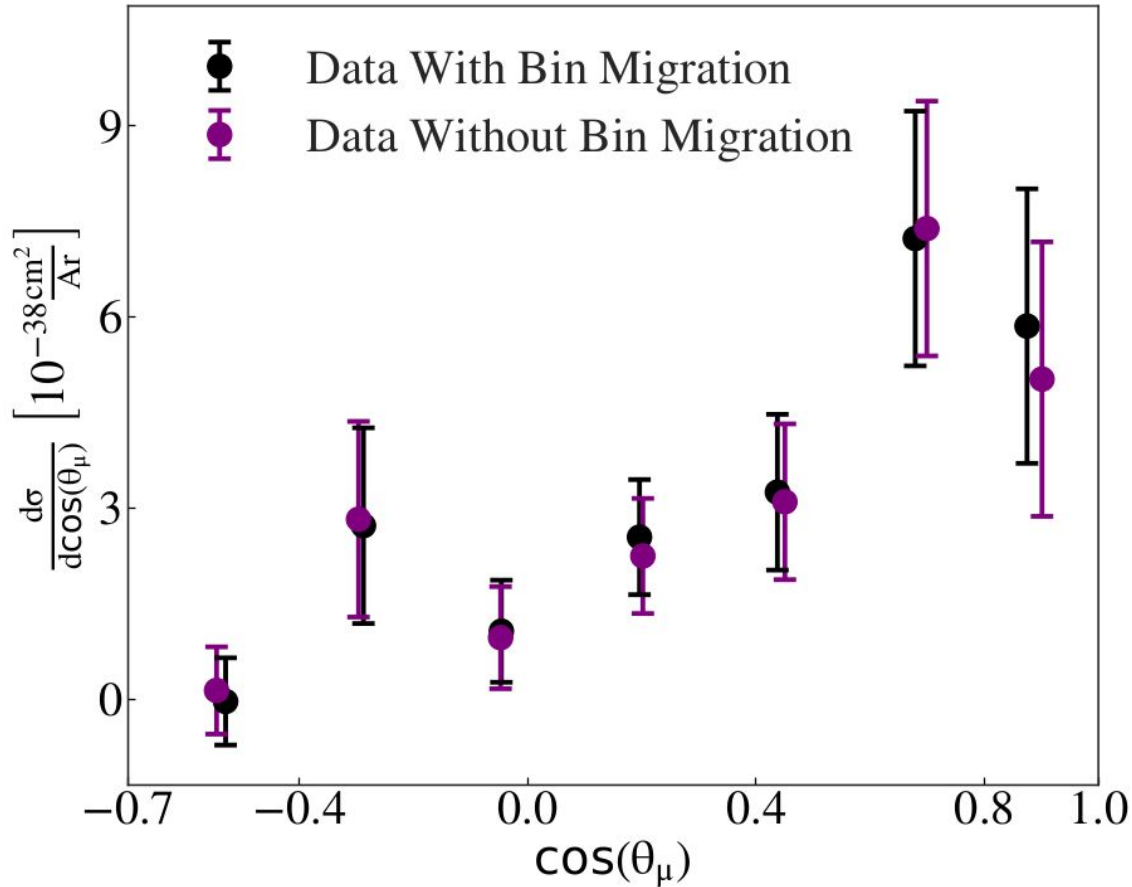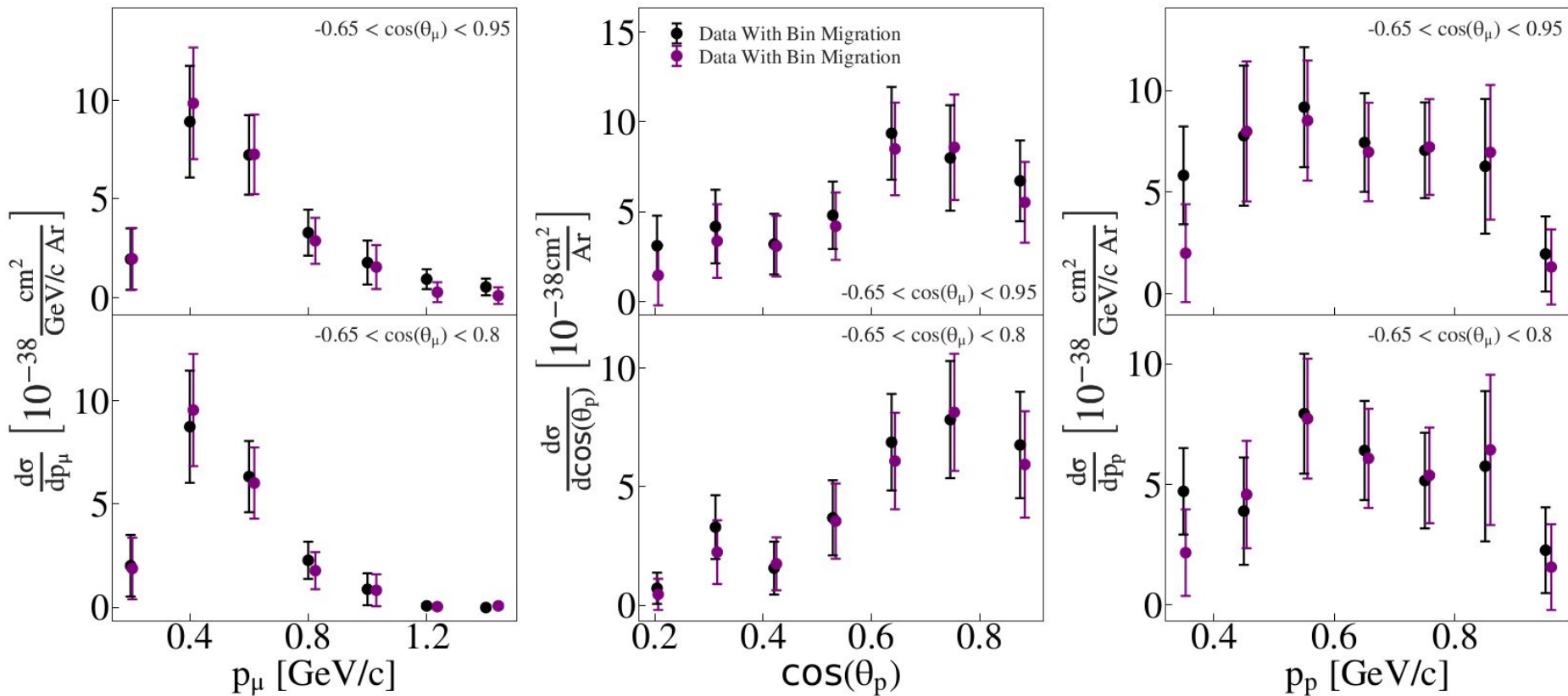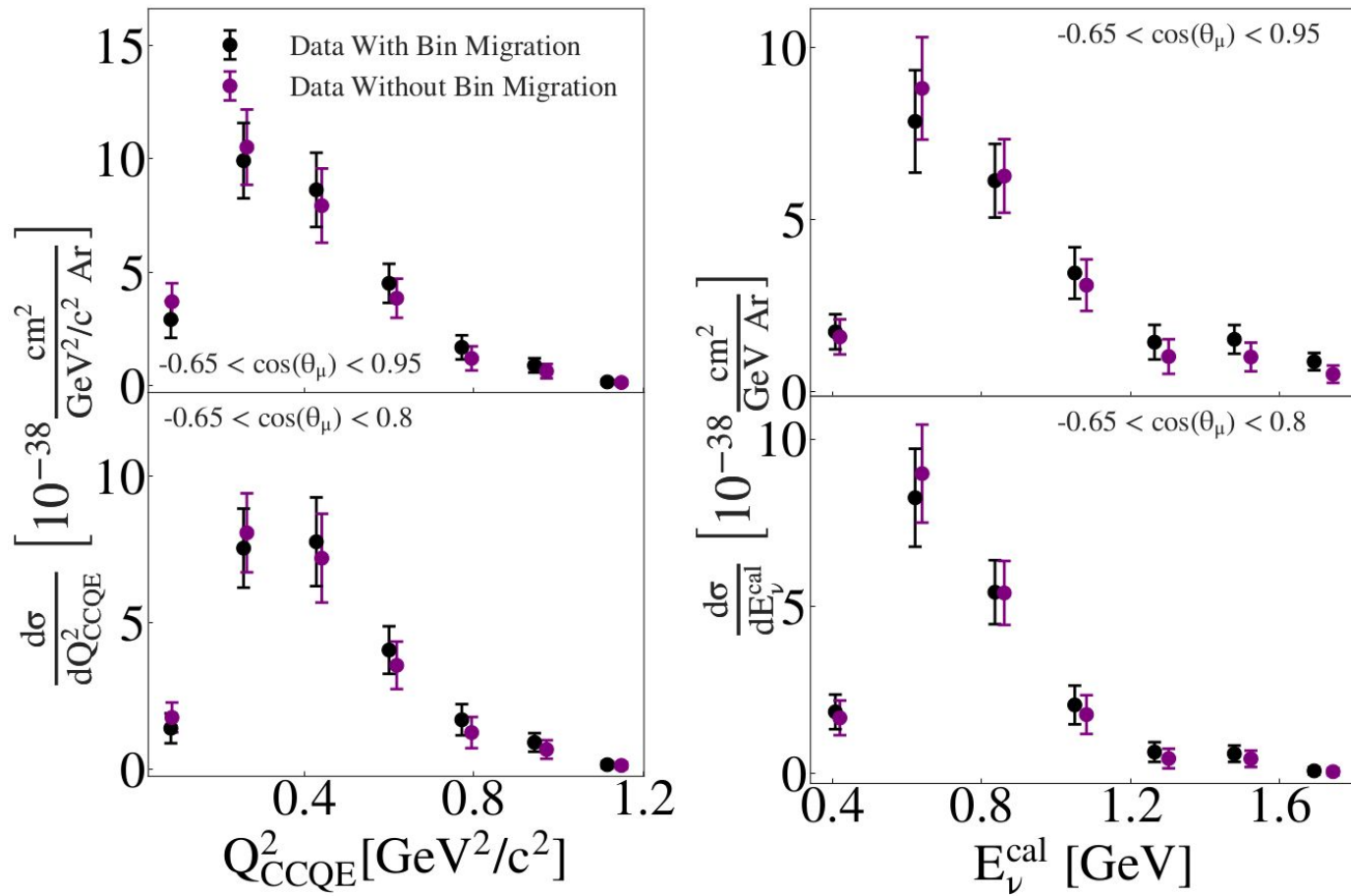
MicroBooNE Simulation

Interaction Mode	Fractional Contribution (%)
QE	87.9
MEC	10.6
RES	1.2
DIS	0.2

MicroBooNE Simulation

| Interaction Mode	Fractional Contribution (%)
QE	33.0
MEC	13.1
RES	44.1
DIS	9.9

Simulated Beam Related Background Breakdown

TABLE XIV: The number of simulated beam related background events from the other non μ–p pairs passing the analysis event selection cuts. The "beam–on" equivalent column lists the number of events scaled to the beam–on available POT.

background pairs	number of events	beam-on equivalent	fractional contribution to beam-on
broken tracks	13 ± 3.6	0.9 ± 0.2	$0.22 \pm 0.06\%$
$\mu^+ p$	11 ± 3.3	0.8 ± 0.2	$0.18 \pm 0.06\%$
pp	18 ± 4.2	1.2 ± 0.3	$0.30 \pm 0.07\%$
πp	109 ± 10.4	7.5 ± 0.7	$1.82 \pm 0.20\%$
ep	19 ± 4.4	1.3 ± 0.3	$0.32 \pm 0.07\%$
μD	1.0 ± 1.0	0.1 ± 0.1	$0.02 \pm 0.02\%$
others	1.0 ± 1.0	0.1 ± 0.1	$0.02 \pm 0.02\%$

Cos(θ_μ) Topological Breakdown
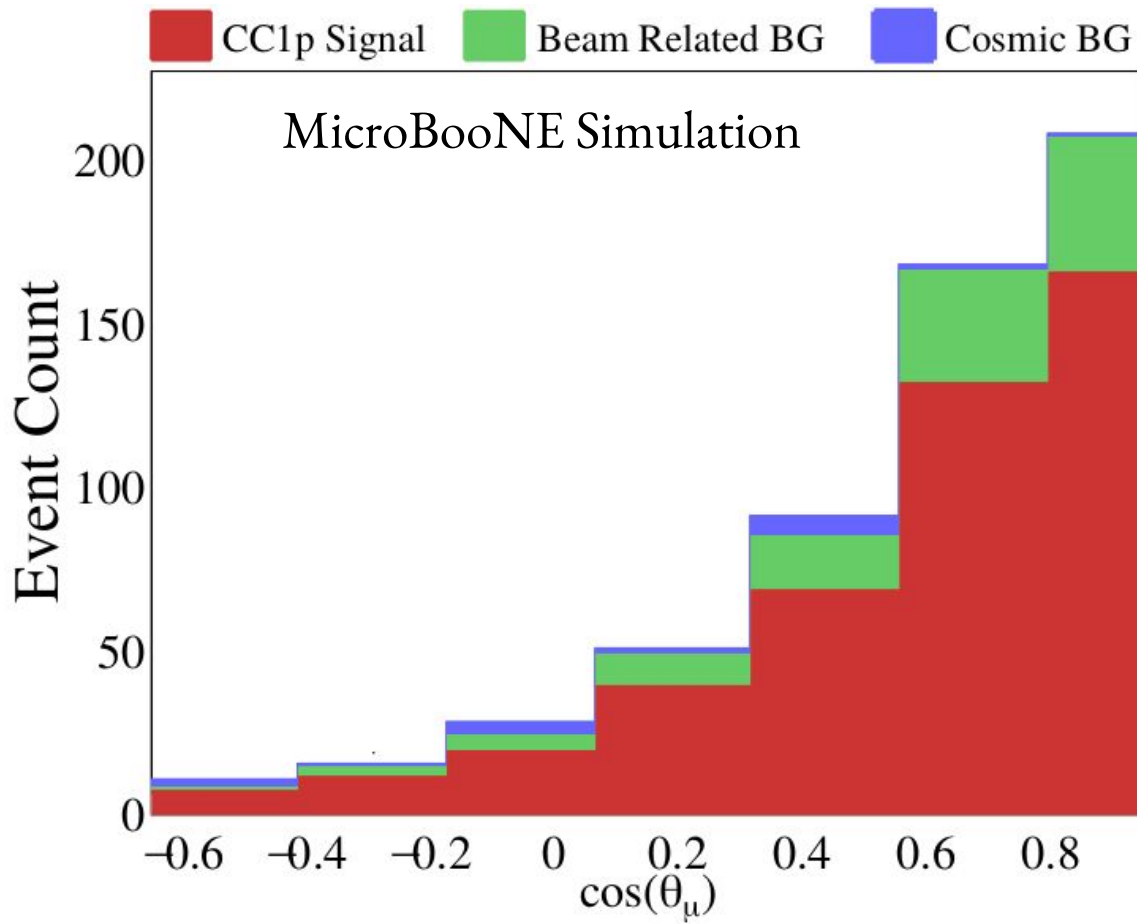
Effective Efficiency & Unfolding

$$\epsilon_n = \frac{N_{\text{reconstructed in bin n}}^{\text{true CC1p0}\pi}(\text{generated in any bin})}{N_{\text{generated in bin n}}^{\text{true CC1p0}\pi}}$$

$$= \frac{N_{\text{reconstructed in any bin}}^{\text{true CC1p0}\pi}(\text{generated in bin n})}{N_{\text{generated in bin n}}^{\text{true CC1p0}\pi}}$$
Standard efficiency

$$+ \frac{\sum_{j=1}^{N_{\text{bins}}} N_{\text{reconstructed in bin n}}^{\text{true CC1p0}\pi}(\text{generated in bin j}\neq n)}{N_{\text{generated in bin n}}^{\text{true CC1p0}\pi}}$$
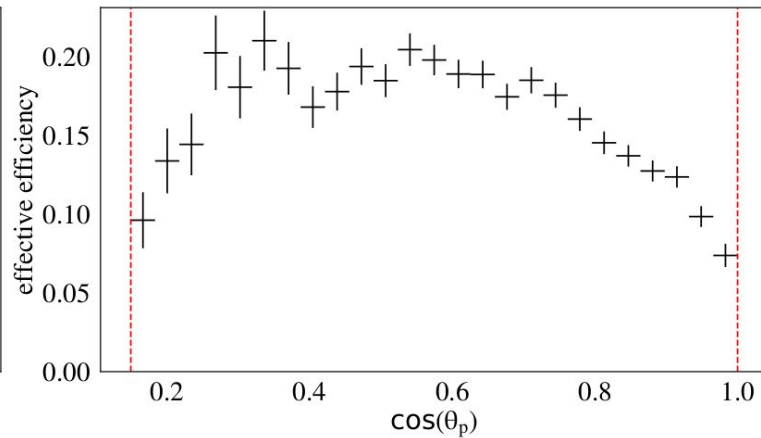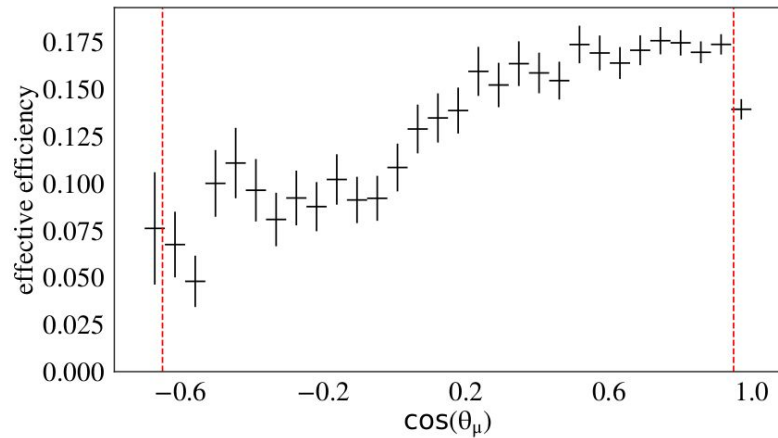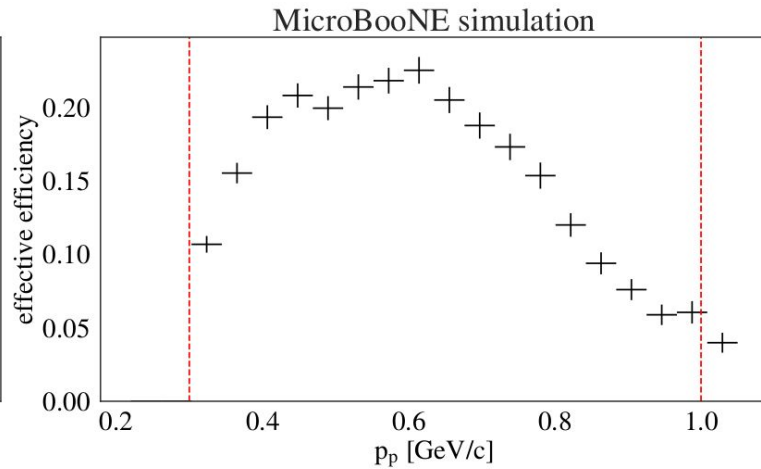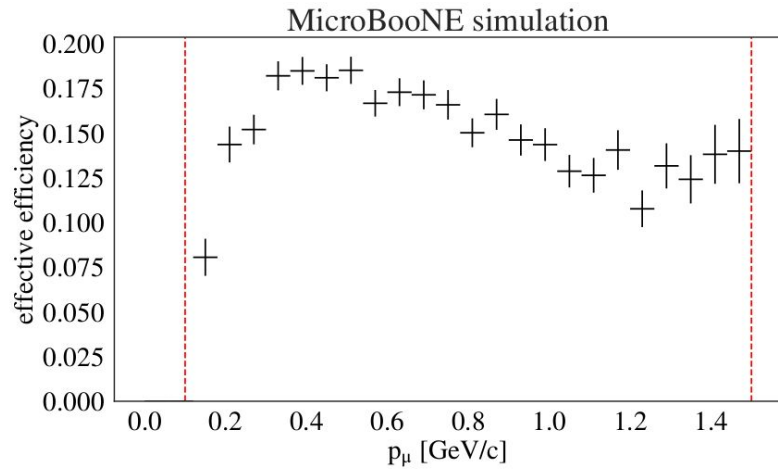
$$- \frac{\sum_{k=1}^{N_{\text{bins}}} N_{\text{reconstructed in bin k}\neq n}^{\text{true CC1p0}\pi}(\text{generated in bin n})}{N_{\text{generated in bin n}}^{\text{true CC1p0}\pi}}$$
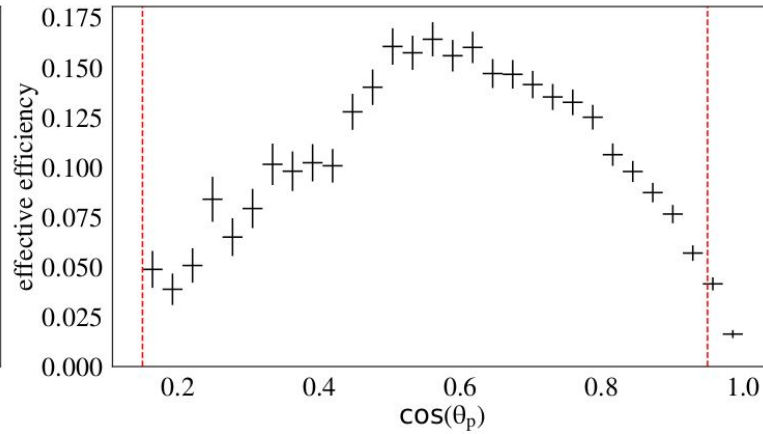
Bin migration effects

Results reported as a function of **true variables**

Effective Efficiencies

Effective Efficiencies
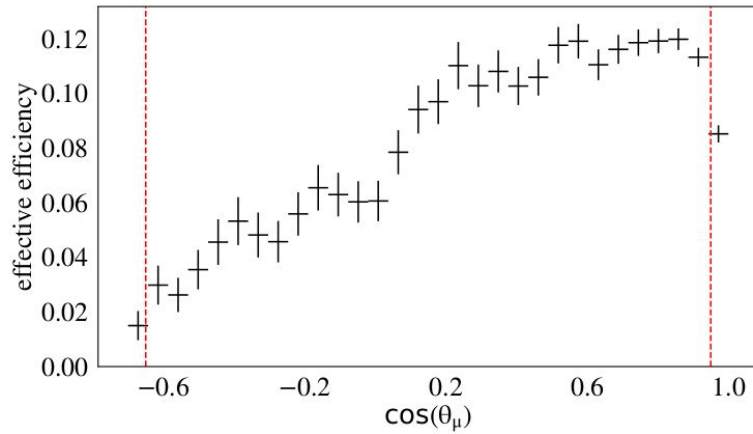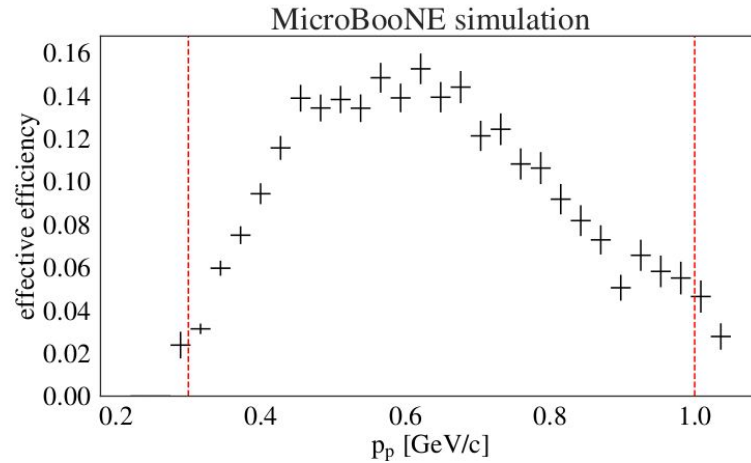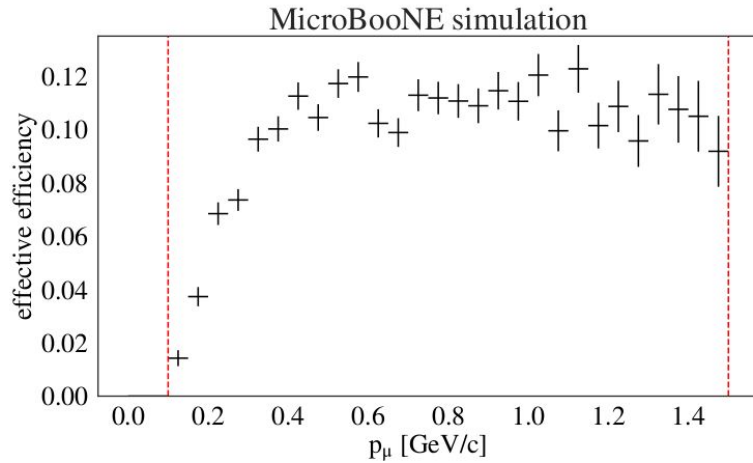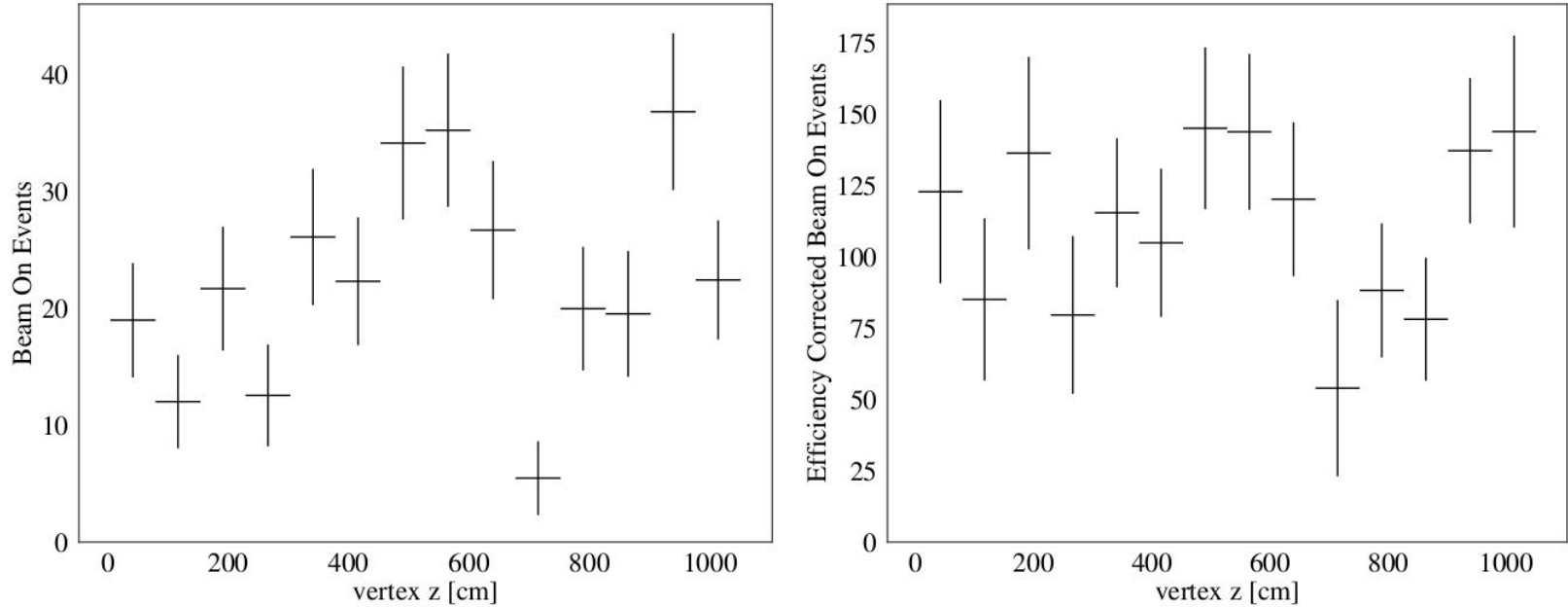
FIG. 19. Vertex z distribution for the measured events, after the beam related MC background has been subtracted, before (left) and after (right) detection efficiency corrections. No small-z enhancement is observed and, with efficiency corrections, the measured distribution is consistent with that of a uniform neutrino interaction vertex.
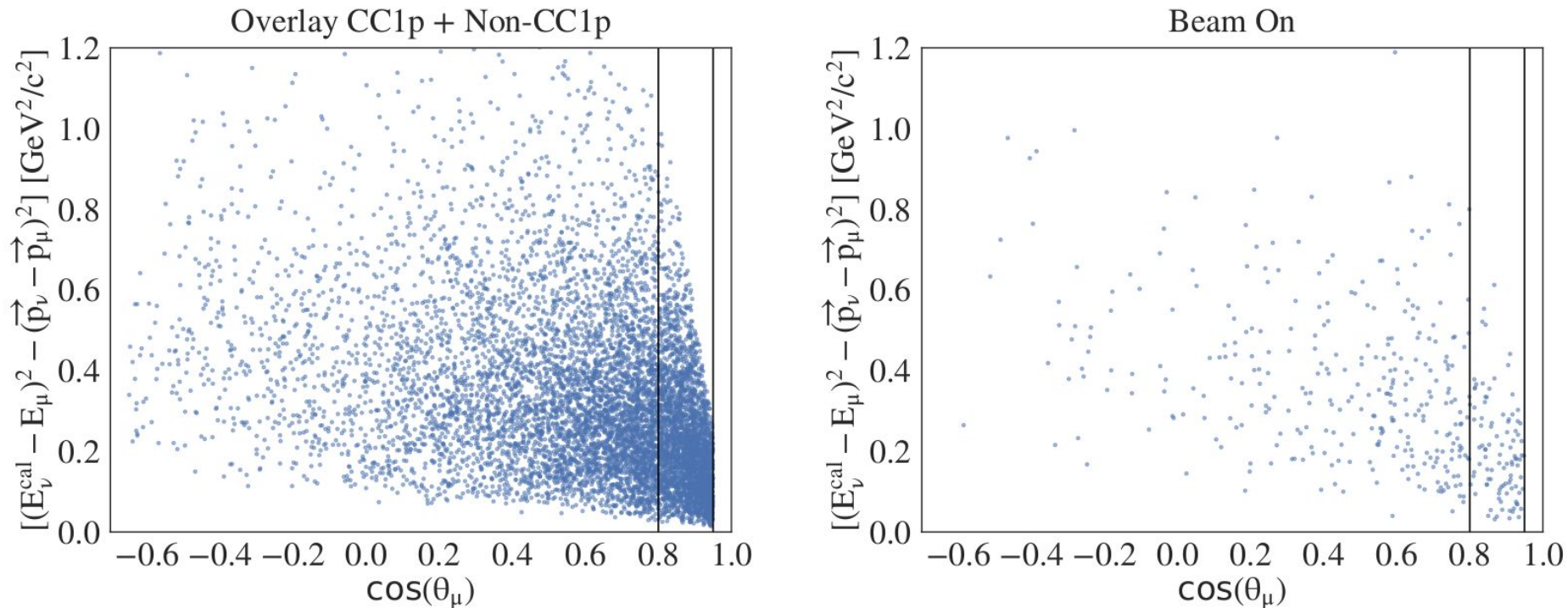
FIG. 5. Kinematic correlations between the high–level variable $Q^2_{CCQE} = (E^{cal}_\nu - E_\mu)^2 - (\vec{p}_\nu - \vec{p}_\mu)^2$ and $\cos(\theta_\mu)$ for the overlay sample (left) and beam on (right). The black vertical lines indicate the limits of the last $\cos(\theta_\mu)$ bin.

126

Systematic Uncertainties

$$E^{syst} = E^{flux} + E^{xsec} + E^{detector}$$

multisim

unisim

Generation of several MC replicas called "universes"

Changing one detector parameter at a time using the relevant uncertainty

Parameter variation within their uncertainties

Each variation requires a new MC generation

Performed via event reweighting

Take the difference between the central value cross section and the variation as the 1σ uncertainty on the cross section

One MC run required

Flux Systematic Uncertainties

1. uncertainties related to hadron production ($\pi^{\pm}, K^{\pm}, K^0$) that arise due to uncertainties in the production of secondary particles when protons collide with the beryllium target.

2. all other related uncertainties, which are here called "non-hadron". These uncertainties arise from errors in estimating the current that runs in the horn conductor, the depth by which such current penetrates the conductor ("skin effect") and the pion and nucleon cross sections (total, inelastic, and quasi-elastic) on aluminum and beryllium.

Flux Systematic Uncertainties
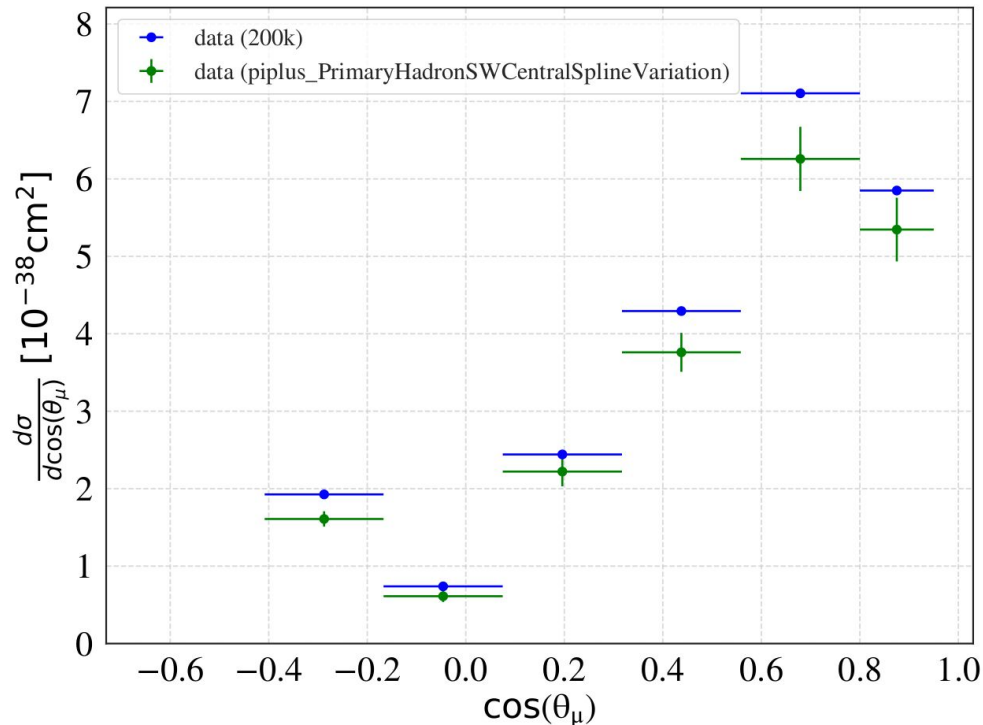
$$\text{Flux Systematic Uncertainty}_{bin\,i} = \sqrt{\frac{(\text{nominal}-\mu)^2_{bin\,i}}{12} + \sigma^2_{bin\,i}}$$

## 1.6 Genie Cross Section Uncertainty

The study of the uncertainties related to the genie cross sections followed. The EventWeight label that is relevant for this part of the analysis is "genie_all" and the knobs that tweaked within the context of this label are shown below starting from 200k events.

- genie_qema
- genie_ncelAxial
- genie_ncelEta
- genie_qevec
- genie_ccresAxial
- genie_ccresVector
- genie_ncresAxial
- genie_ncresVector
- genie_cohMA
- genie_cohR0
- genie_NonResRvp1pi
- genie_NonResRvbarp1pi
- genie_NonResRvp2pi

- genie_NonResRvbarp2pi
- genie_ResDecayGamma
- genie_ResDecayEta
- genie_ResDecayTheta
- genie_NC
- genie_DISAth
- genie_DISBth
- genie_DISCv1u
- genie_DISCv2u
- genie_AGKYxF
- genie_AGKYpT
- genie_FormZone
- genie_FermiGasModelKf

- genie_FermiGasModelSf
- genie_IntraNukeNmfp
- genie_IntraNukeNcex
- genie_IntraNukeNel
- genie_IntraNukeNinel
- genie_IntraNukeNabs
- genie_IntraNukeNpi
- genie_IntraNukePImfp
- genie_IntraNukePIcex
- genie_IntraNukePIel
- genie_IntraNukePIinel
- genie_IntraNukePIabs
- genie_IntraNukePIpi

130
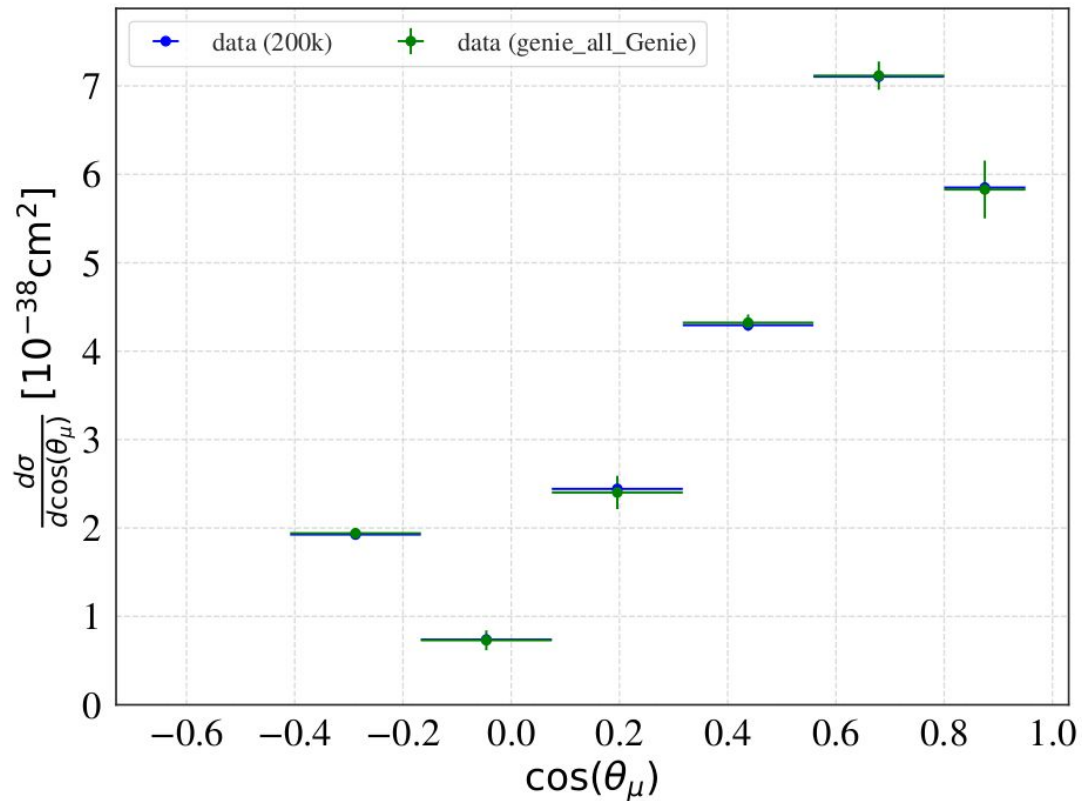
$$\text{Genie Systematic Uncertainty}_{bin\,i} = \sqrt{\frac{(\text{nominal}-\mu)^2_{bin\,i}}{12} + \sigma^2_{bin\,i}}$$

Detector Systematic Uncertainties

In order to assess the detector systematic uncertainties, several samples are generated, where one detector parameter is varied at a time, and the same neutrino events are generated on top of the same cosmic background. Each of the following detector parameters are varied by 1σ: longitudinal diffusion value, light yield outside the TPC, transverse diffusion, electron lifetime, recombination model and space charge map. The electronic response variation uses simulated neutrino events on top of a simulated cosmic background with CORSIKA [1]. The cross section is extracted using each one of those samples instead of the nominal simulation, where the relevant efficiencies, beam related background and data driven correction are rederived using the same procedures described in the paper. The uncertainty for each sample is obtained as the difference between the nominal cross section and the variation sample.
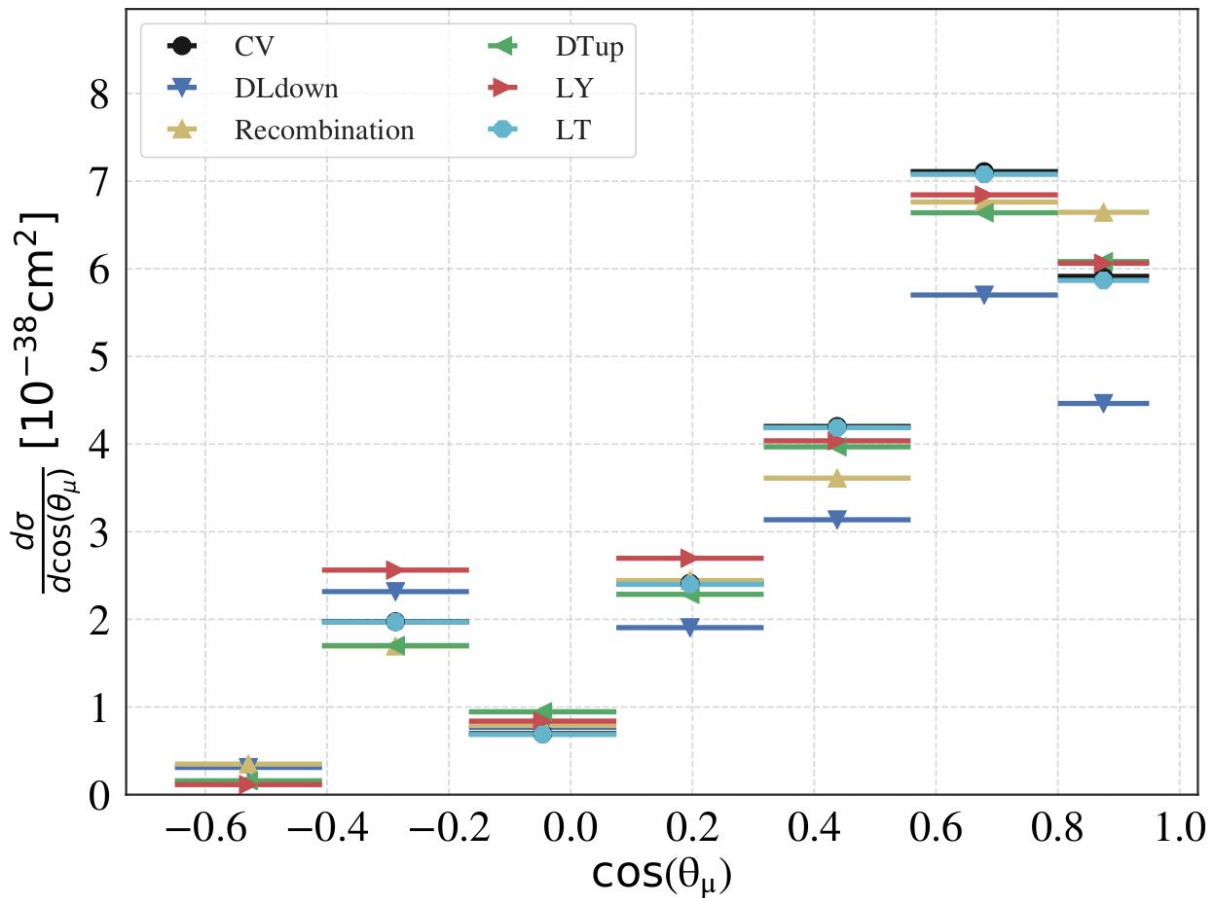
Dynamically Induced Charge

The extracted cross sections are expected to be independent of the azimuthal angle ϕ. However, the simple model used to simulate the effect of induced charge on neighboring TPC wires leads to a low reconstruction efficiency of tracks perpendicular to the wire planes ($\phi \approx 0$ and $\phi \approx \pm\pi$) that created an artificial ϕ dependence to the cross section. We correct for this effect using an iterative procedure. We first reweight events with a muon track falling in the $\phi \approx 0$ bin and $|\sin\theta| > 0.3$ to the weighted average of the cross sections in all other bins of ϕ_μ where $|\sin\theta| > 0.3$. Due to the coplanarity requirement, this reweighting affects the distribution of $\phi_p \approx \pm\pi$. We repeat the process starting from a proton track with $\phi_p \approx 0$ until the cross section change is less than 0.01%, typically after 5 iterations.

Dynamically Induced Charge

In order to address the deficit in the central ϕ bin due to the missing dynamically induced charge effects, we apply a data driven correction, as described in the paper. We estimate the uncertainty due to this procedure by producing a dedicated dynamically induced charge variation sample and by treating the sample as data. The difference between the cross section extracted using this variation as data and the nominal MC cross section results is assigned to be the uncertainty due to our data driven correction.

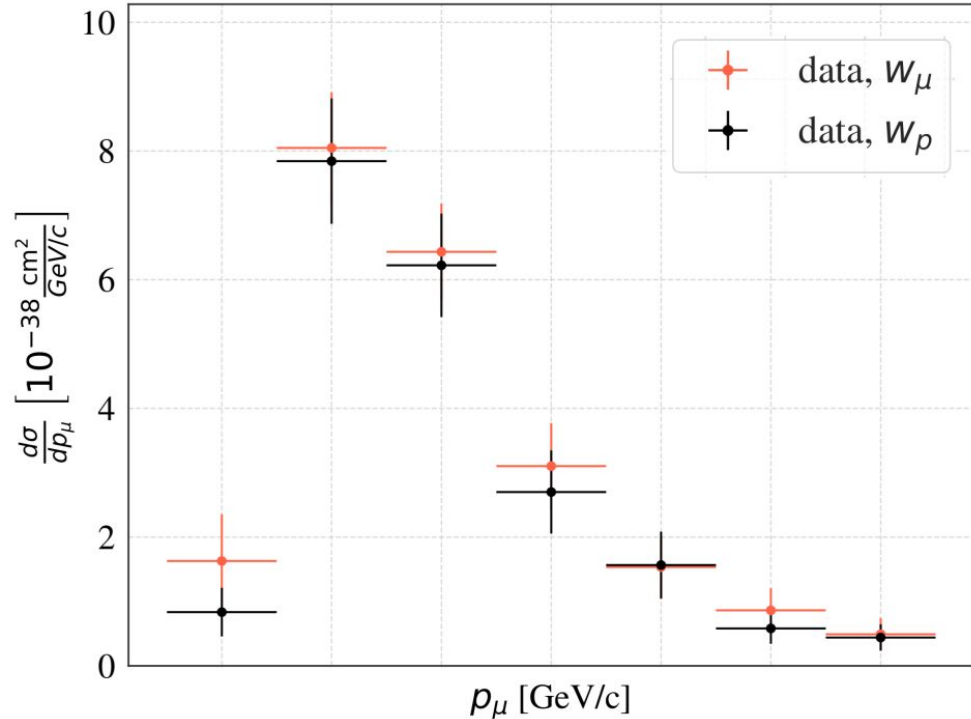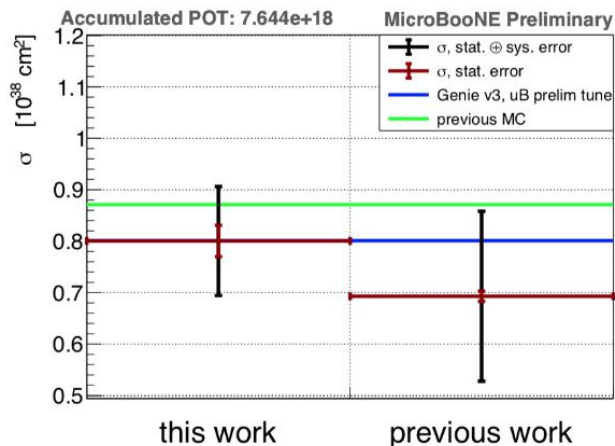# Data Driven Correction
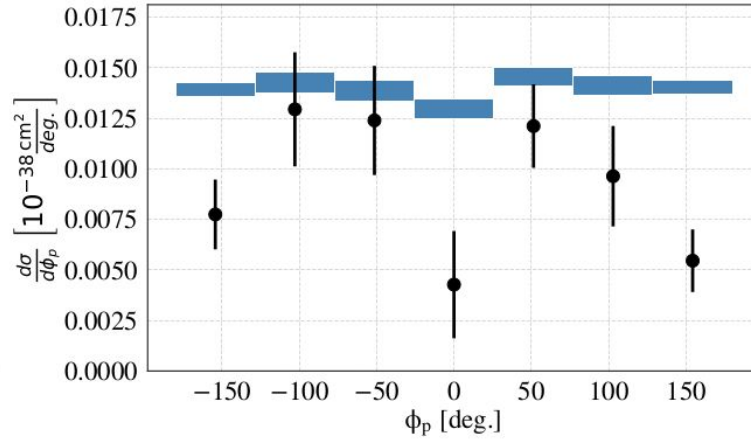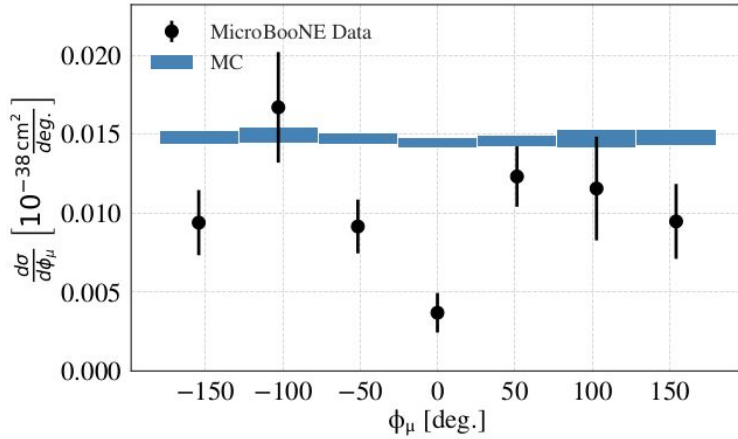
Before
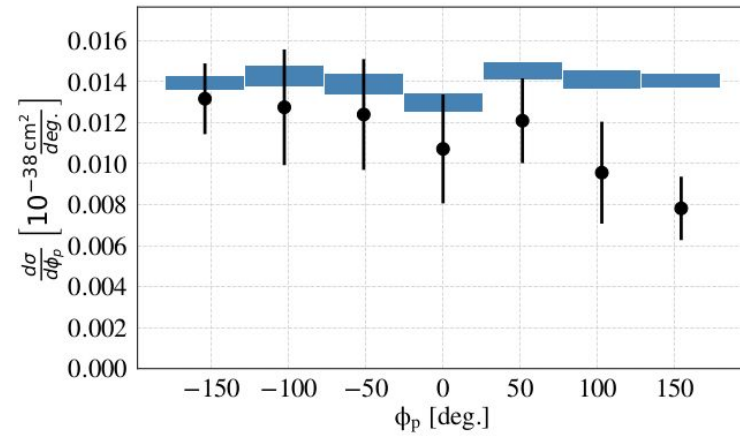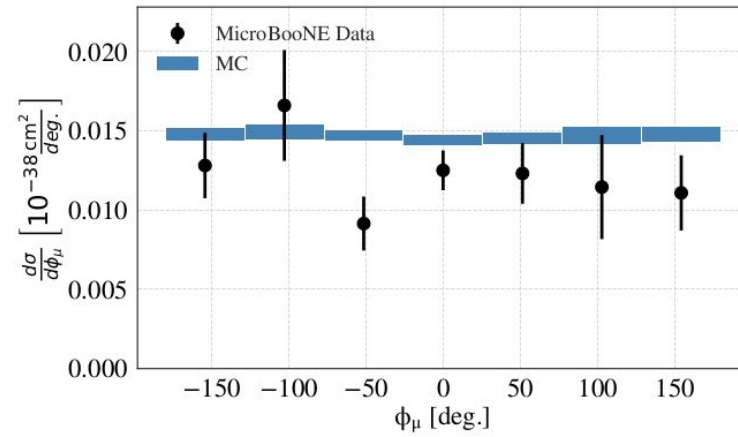
After

Due to the limited MC and data statistics, we divide the data into two three-dimensional (3D) bins and extract the differential cross–sections in each of the decoupled 3D spaces. This is justified in the limit that the muon and proton efficiencies are decoupled. This is not the case in our exclusive measurement.

$$\Delta^{2\times3D}_{\mathrm{sys}} = \frac{1}{2} \left| \frac{d\sigma}{dp_\mu}(w_\mu) - \frac{d\sigma}{dp_\mu}(w_p) \right|$$

Drastically Reduced Systematic Uncertainties

Accumulated POT: 7.644e+18 **MicroBooNE Preliminary**

- σ, stat. $\oplus$ sys. error
- σ, stat. error
- Genie v3, uB prelim tune
- previous MC

σ [10^{38} cm^2]

this work   previous work

Flux-integrated cross section
consistent with previous measurement
Drastically reduced systematic uncertainties

Instead of cosmic ray simulation, now use overlay: simulated neutrino interactions overlaid on real cosmic data → no uncertainty in cosmic ray model

| Source	Uncertainty	
	Previous Analysis	This Analysis
Detector response	16.2%	3.3%
Cross section	3.9%	2.7%
Flux	12.4%	10.5%
Dirt background	10.9%	3.3%
Cosmic ray background	4.2%	N/A
POT counting	2.0%	2.0%
CRT	N/A	1.7%
Total Sys. Error	23.8%	12.1%
Statistics	1.4%	3.8%
Total (Quadratic Sum)	**23.8%**	**12.7%**

PRL 123, 131801 (2019)

μBooNE

The Ingredients
Leveraging Correlations to Minimize Systematics
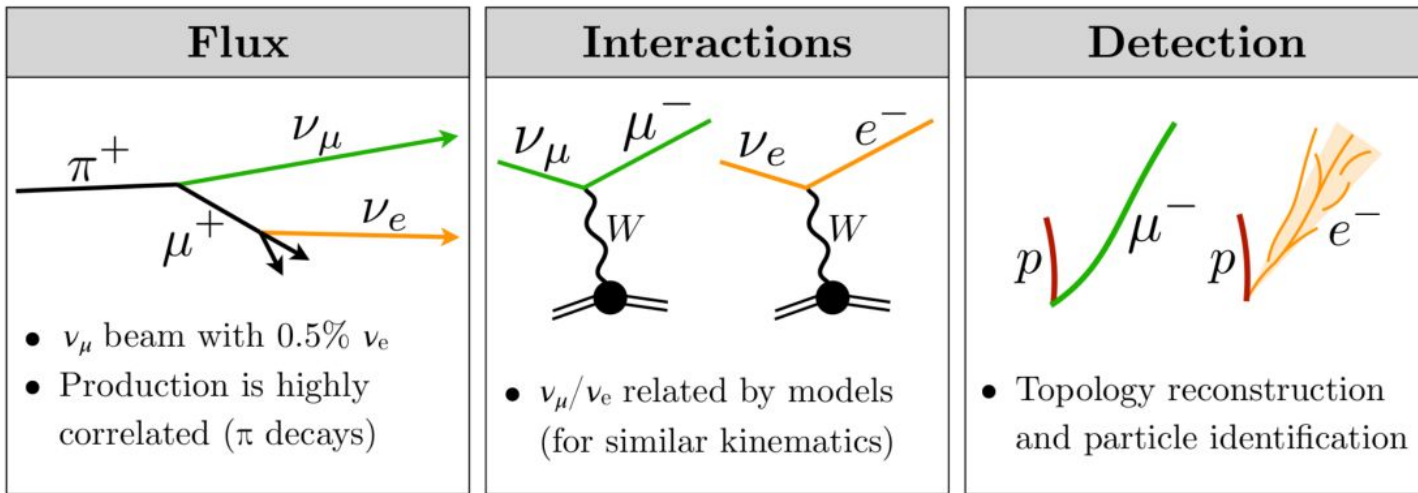
Given the small appearance probability of ~0.15%, we are looking for **an excess** of ν_e interactions on top of the 0.5% **intrinsic to the beam**
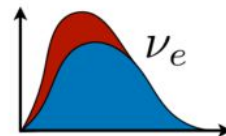
A key to MicroBooNE's single-detector appearance measurement is using ν_μ events to constrain the small ν_e flux intrinsic to the beam
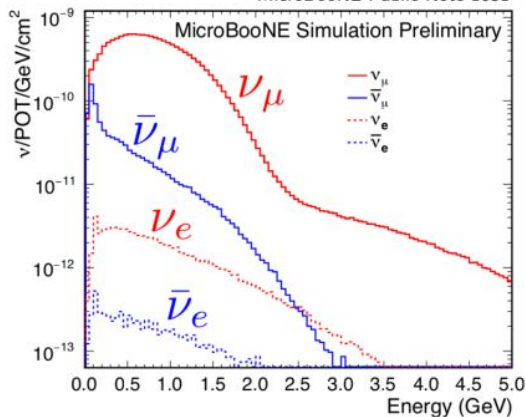
Credit A.Mastbaum

Flux	Interactions	Detection
• ν_μ beam with 0.5% ν_e • Production is highly correlated (π decays)	• ν_μ/ν_e related by models (for similar kinematics)	• Topology reconstruction and particle identification

Neutrino Flux

Flux Modeling & Uncertainties
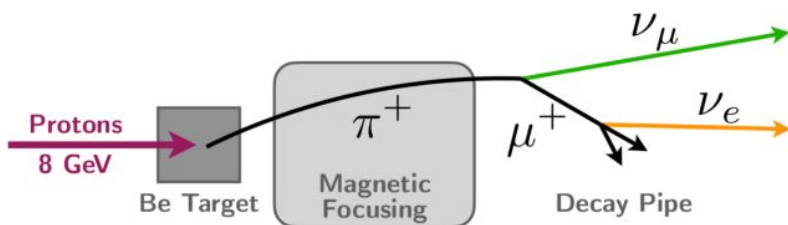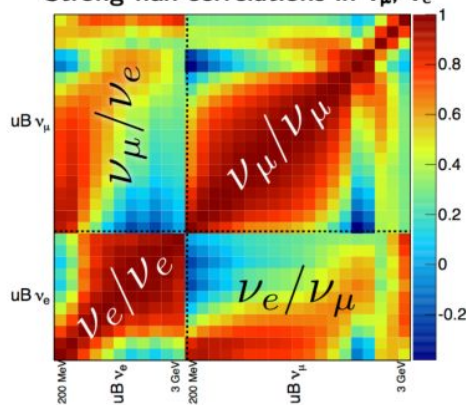
- **Fermilab Booster Neutrino Beam**
  - ‣ 8 GeV protons on a Be target
  - ‣ Primarily a ν_μ beam, with 0.5% ν_e
- **MiniBooNE-based flux uncertainties**
  - ‣ Beamline modeling in Geant4
  - ‣ π, K production (HARP, SciBooNE)
  - ‣ π, nucleon interactions
  - ‣ ~12% integral flux uncertainty
- **Leverage strong ν_μ/ν_e correlations** $\rightarrow$

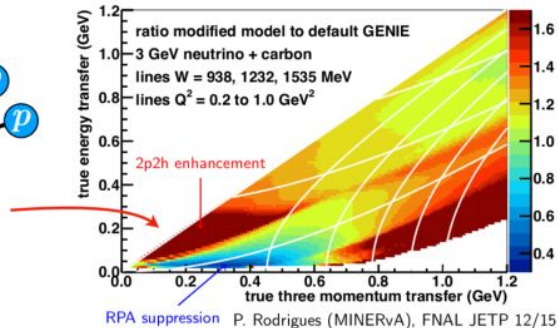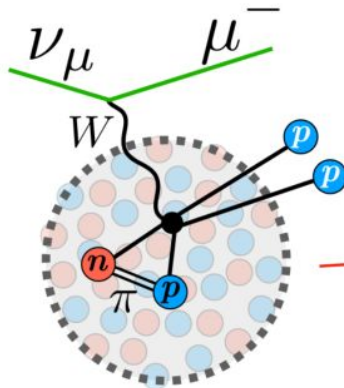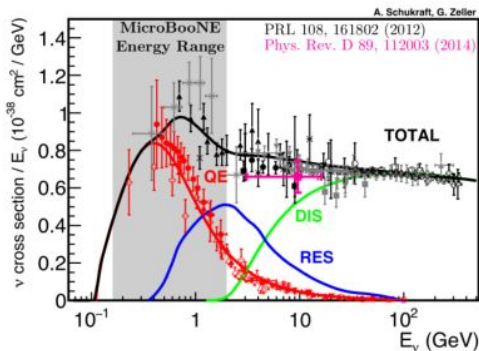MicroBooNE Public Note 1031

MicroBooNE Simulation Preliminary

Credit A.Mastbaum

Strong flux correlations in ν_μ, ν_e

Neutrino Interactions

Interaction Modeling & Uncertainties

µBooNE

A. Schukraft, G. Zeller
PRL 108, 161802 (2012)
Phys. Rev. D 89, 112003 (2014)

MicroBooNE Energy Range

TOTAL

QE

DIS

RES

Searching for possible new physics in a regime with poor *a priori* constraints

(ν-Ar interactions at 200 MeV)

ν_μ μ^-

W

p
p

n
π p

Nuclear physics effects

e.g. interactions with correlated nucleon pairs (*2p2h*, or MEC)

ratio modified model to default GENIE
3 GeV neutrino + carbon
lines W = 938, 1232, 1535 MeV
lines Q^2 = 0.2 to 1.0 GeV^2

2p2h enhancement

RPA suppression   P. Rodrigues (MINERvA), FNAL JETP 12/15

Credit A.Mastbaum

Genie

- Latest **theory-driven models**
- New **tunes** including T2K CC0π data
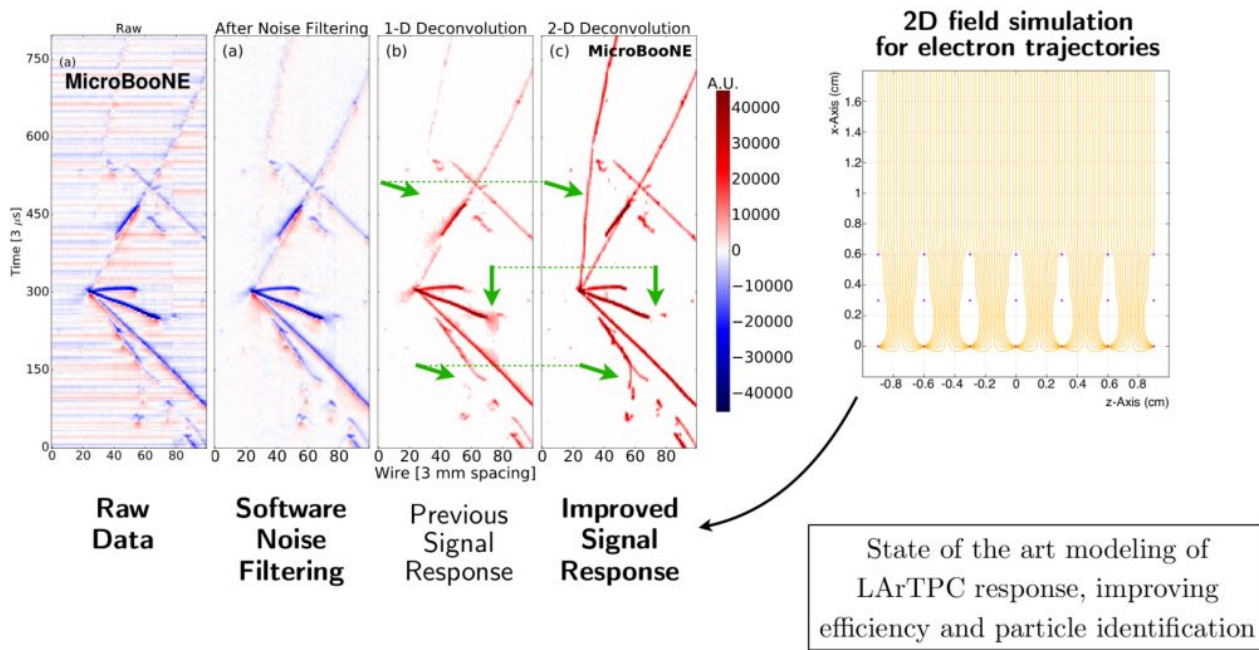 - MICROBOONE-NOTE-1074-PUB
- Integrating Ar targets, (e,e') data
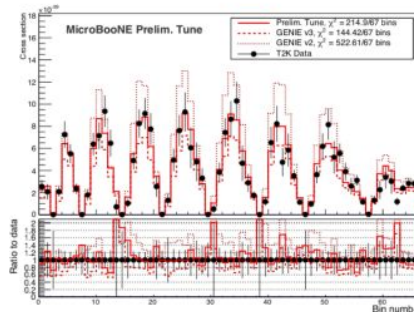
MicroBooNE Prelim. Tune

Detector Modeling

µBooNE

Detailed modeling of **particle propagation**, **electron drift** & **detector response**, and **photon propagation**

1. Signal processing (MicroBooNE Collaboration, JINST 13 P07007, 2018 and JINST 13 P07007, 2018)
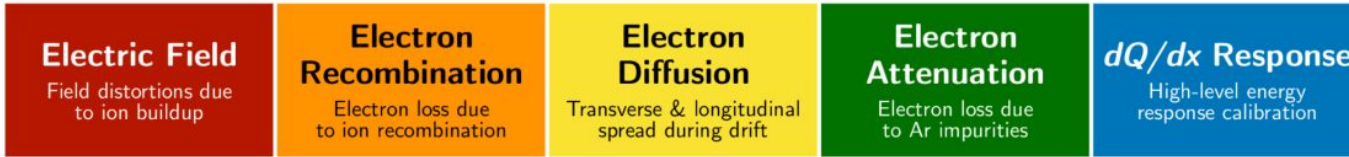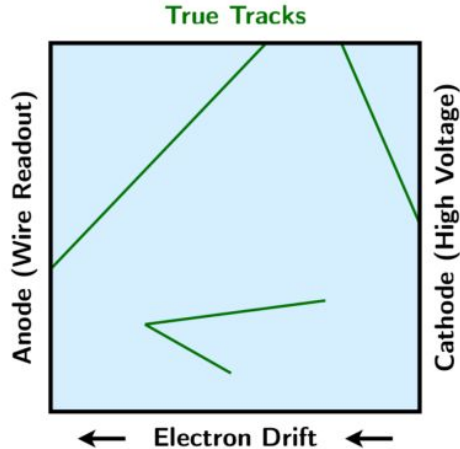

Credit A.Mastbaum

State of the art modeling of LArTPC response, improving efficiency and particle identification
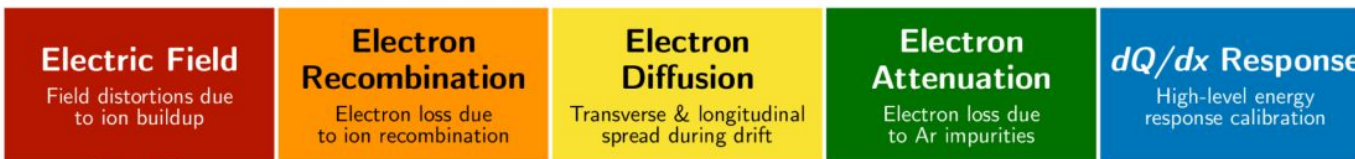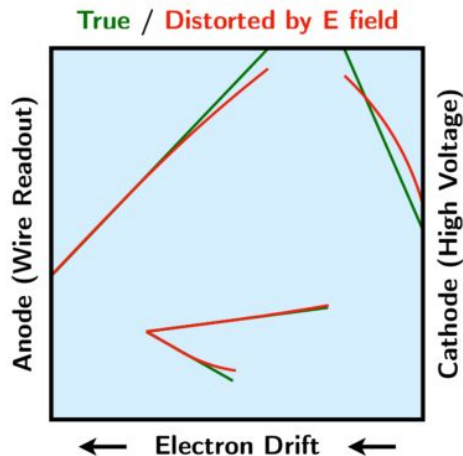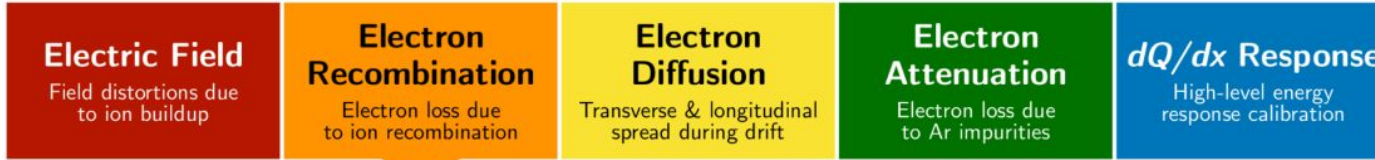
Detector Modeling

Detailed modeling of **particle propagation**, **electron drift** & **detector response**, and **photon propagation**

1. **Signal processing** (MicroBooNE Collaboration, JINST 13 P07007, 2018 and JINST 13 P07007, 2018)

2. **Response Calibration** *or* How Things Go Wrong

Electric Field	**Electron Recombination**	**Electron Diffusion**	**Electron Attenuation**	**dQ/dx Response**
Field distortions due to ion buildup	Electron loss due to ion recombination	Transverse & longitudinal spread during drift	Electron loss due to Ar impurities	High-level energy response calibration

Credit A.Mastbaum

True Tracks

Anode (Wire Readout) — Cathode (High Voltage)

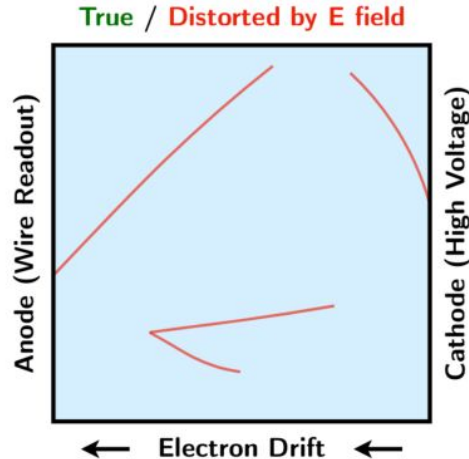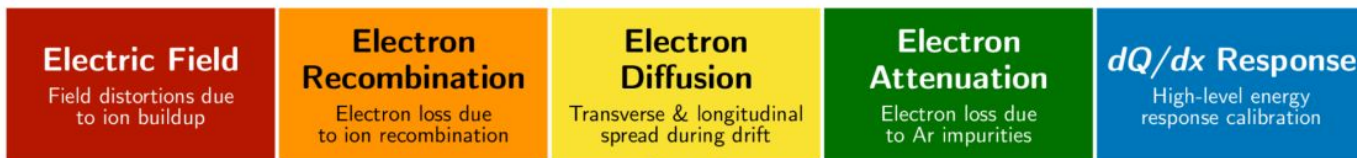← **Electron Drift** ←
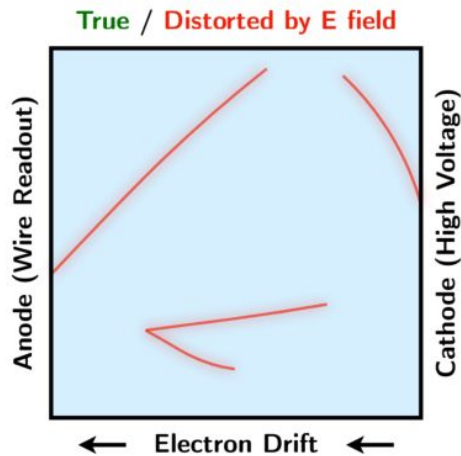
Detector Modeling

µBooNE

Detailed modeling of **particle propagation**, **electron drift** & **detector response**, and **photon propagation**

1. **Signal processing** (MicroBooNE Collaboration, JINST 13 P07007, 2018 and JINST 13 P07007, 2018)

2. **Response Calibration** *or* How Things Go Wrong

Electric Field	Electron Recombination	Electron Diffusion	Electron Attenuation	dQ/dx Response
Field distortions due to ion buildup	Electron loss due to ion recombination	Transverse & longitudinal spread during drift	Electron loss due to Ar impurities	High-level energy response calibration

Credit A.Mastbaum

True / Distorted by E field

Anode (Wire Readout) — Cathode (High Voltage)
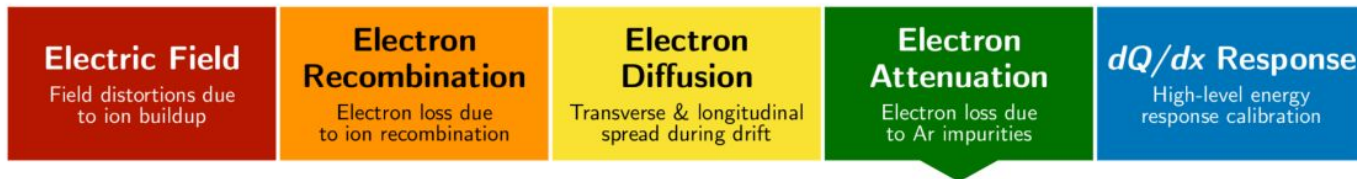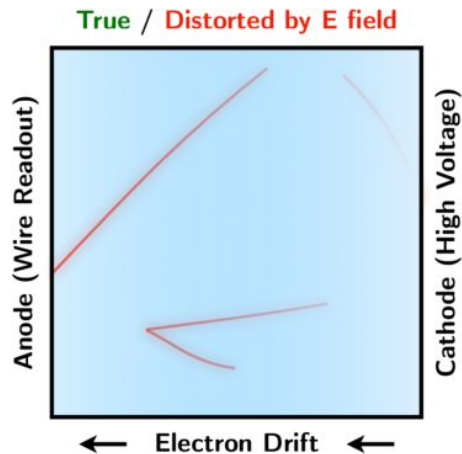
← **Electron Drift** ←

144

Detector Modeling

Detailed modeling of **particle propagation**, **electron drift** & **detector response**, and **photon propagation**

1. **Signal processing** (MicroBooNE Collaboration, JINST 13 P07007, 2018 and JINST 13 P07007, 2018)

2. **Response Calibration** *or* How Things Go Wrong

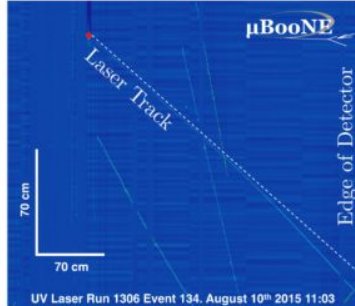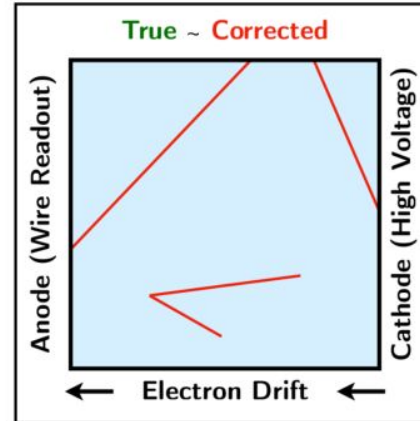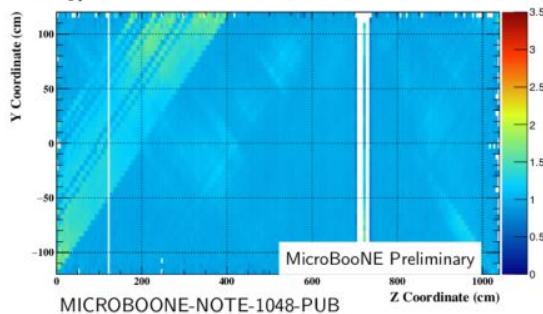| **Electric Field** Field distortions due to ion buildup	**Electron Recombination** Electron loss due to ion recombination	**Electron Diffusion** Transverse & longitudinal spread during drift	**Electron Attenuation** Electron loss due to Ar impurities	*dQ/dx* **Response** High-level energy response calibration

Credit A.Mastbaum

True / Distorted by E field

Anode (Wire Readout)

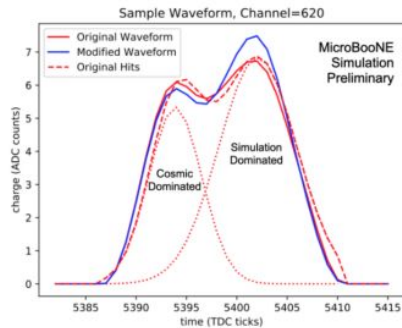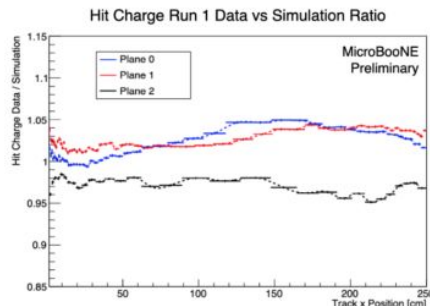Cathode (High Voltage)

← **Electron Drift** ←

Detector Modeling

μBooNE

Detailed modeling of **particle propagation**, **electron drift** & **detector response**, and **photon propagation**

1. **Signal processing** (MicroBooNE Collaboration, JINST 13 P07007, 2018 and JINST 13 P07007, 2018)

2. **Response Calibration** *or* How Things Go Wrong

Electric Field	Electron Recombination	Electron Diffusion	Electron Attenuation	dQ/dx Response
Field distortions due to ion buildup	Electron loss due to ion recombination	Transverse & longitudinal spread during drift	Electron loss due to Ar impurities	High-level energy response calibration

Credit A.Mastbaum

True / Distorted by E field

Anode (Wire Readout)

Cathode (High Voltage)

← Electron Drift ←

146

Detector Modeling

μBooNE

Detailed modeling of **particle propagation**, **electron drift** &
detector response, and **photon propagation**

1. **Signal processing** (MicroBooNE Collaboration, JINST 13 P07007, 2018 and JINST 13 P07007, 2018)

2. **Response Calibration** *or* How Things Go Wrong

Electric Field Field distortions due to ion buildup	**Electron Recombination** Electron loss due to ion recombination	**Electron Diffusion** Transverse & longitudinal spread during drift	**Electron Attenuation** Electron loss due to Ar impurities	**dQ/dx Response** High-level energy response calibration

Credit A.Mastbaum

True / Distorted by E field

Anode (Wire Readout)

Cathode (High Voltage)

← Electron Drift ←

Detector Modeling

μBooNE

Detailed modeling of **particle propagation**, **electron drift** & **detector response**, and **photon propagation**

1. **Signal processing** (MicroBooNE Collaboration, JINST 13 P07007, 2018 and JINST 13 P07007, 2018)

2. **Response Calibration** *or* How Things Go Wrong

Electric Field Field distortions due to ion buildup	**Electron Recombination** Electron loss due to ion recombination	**Electron Diffusion** Transverse & longitudinal spread during drift	**Electron Attenuation** Electron loss due to Ar impurities	**dQ/dx Response** High-level energy response calibration

Credit A.Mastbaum

In Situ Laser System

μBooNE

Laser Track

Edge of Detector

70 cm

70 cm

UV Laser Run 1306 Event 134. August 10th 2015 11:03

MICROBOONE-NOTE-1018-PUB

dQ/dx Calibration with Cosmic Muons

Y Coordinate (cm)

MicroBooNE Preliminary

MICROBOONE-NOTE-1048-PUB

Z Coordinate (cm)

True ~ Corrected

Anode (Wire Readout)

Cathode (High Voltage)

← **Electron Drift** ←

148

Detector Modeling

Detailed modeling of **particle propagation**, **electron drift &
detector response**, and **photon propagation**

1. **Signal processing** (MicroBooNE Collaboration, JINST 13 P07007, 2018 and JINST 13 P07007, 2018)

2. **Response Calibration** *or* How Things Go Wrong

3. **Systematic Uncertainties**

- Highest precision measurements yet performed with LArTPC technology
- Many subtle and correlated effects in the detector response model
- **First iteration:** Vary parameters according to *in situ* measurements and re-run full MC and analysis
- **Latest approach:** Capture waveform-level data/ MC differences in response as a function of x, yz, angle, etc. as a correction and residual detector modeling systematic *(MICROBOONE-NOTE-1075-PUB)*

Credit A.Mastbaum

Hit Charge Run 1 Data vs Simulation Ratio

MicroBooNE Preliminary

Sample Waveform, Channel=620

MicroBooNE Simulation Preliminary

MICROBOONE-NOTE-1075-PUB

Coverage of MCC8 Detector Variations μBooNE

Want to make sure that MCC8 detector variations will be covered by the approach to simulation and detector systematics in MCC9

Some are covered by the move to cosmic data overlay for the MC

The rest are covered by this method, SCE variations, and light

Credit L.Yates

Covered by...	Detector Variations
x	Longitudinal & transverse diffusion, electron lifetime, SCE
(y, z)	Wire response, SCE
angles	Induced charge
dE/dx	Recombination
SCE variation	SCE (esp. spatial distortions)
light variations	Light model, light yield
overlay MC	Wire noise, PMT noise, saturated channels, dead channels

Association between
simulated energy deposits
and the wire waveforms

Selections for each of the
measurements:
x, (y, z), (θ, ϕ), dE/dx

Fits for R_Q, R_σ for each
of the measurements

Code that modifies wires based
on truth information, R_Q and R_σ

Events with modified wires
based on functions R_Q, R_σ

Systematic uncertainties for
high-level physics analyses

Credit L.Yates

151
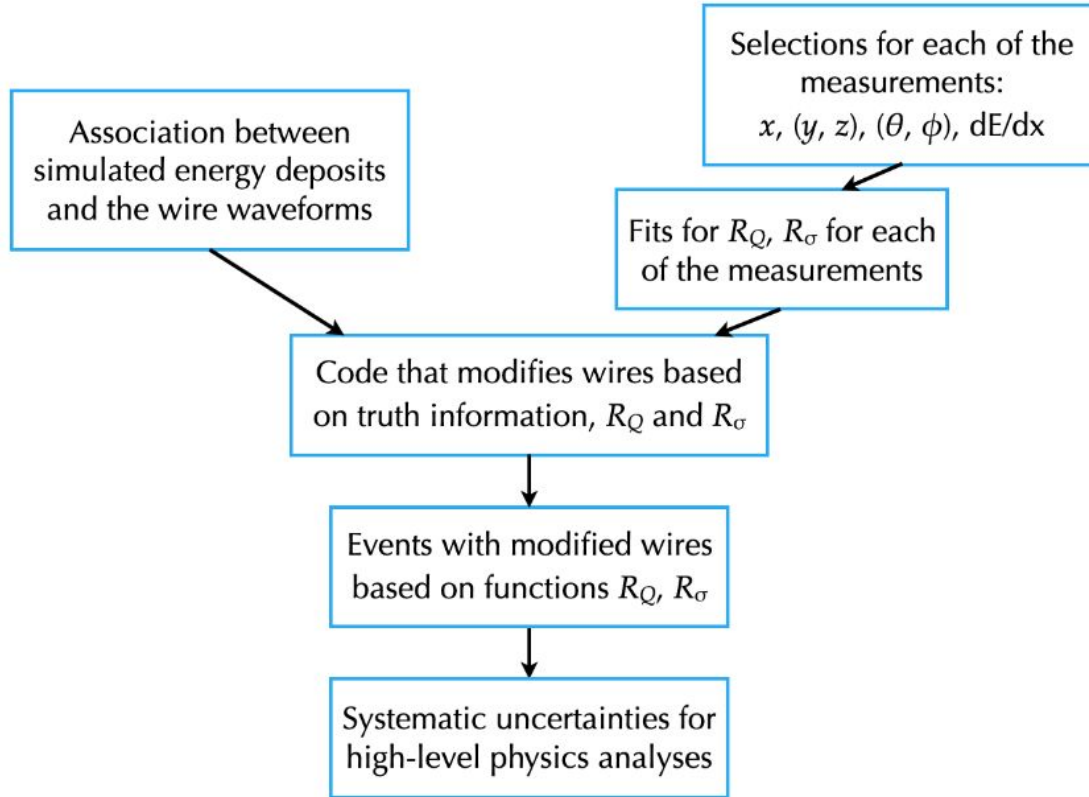
MCC8 Detector Variations

SCE

In the variation sample, a simple data-driven correction is applied to the central value simulation of these effects in order to better match what is measured in data. The central value space charge simulation includes spatial migration of charge and electron-ion recombination variations due to electric field distortions in the detector. The variation is defined by a set of corrections to the spatial migration and the electric field distortion. The spatial migration is altered by applying a scale factor, $F(x)$, which is dependent on the drift direction only, such that the spatial distortions observed at the top and bottom of the detector match between data and MC. This scale factor is applied to the distortions throughout the detector in MC. Additionally, the electric field distortions are reduced in the unisim to 70% of the nominal value in order to reflect the fact that space charge effects are less severe in data than they are in the nominal MC samples.

Longitudinal Diffusion
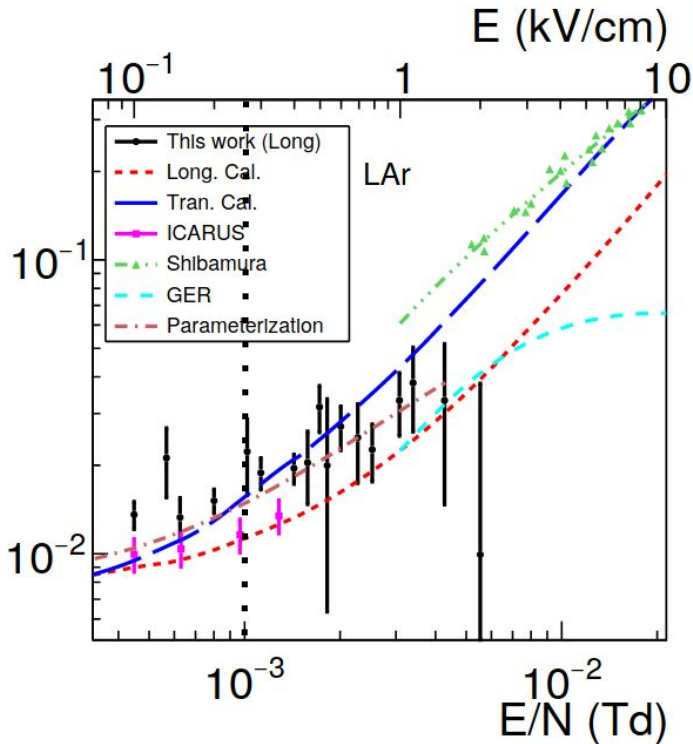
In the variation samples, the longitudinal diffusion constant is increased (`DLup`) or decreased (`DLdn`) relative to the MCC8 central value. We chose these variations by to span the range of previous measurements of longitudinal diffusion in liquid argon, using Fig. 11 (plot on the right side) in this reference.[3] We looked at the data bands at the MicroBooNE field strength, 0.273 kV/cm. We used the upper extent of those bands for the `DLup` variation and the lower extent of those bands for the `DLdn` variation. The MCC8 central value for this constant is between these values.

Electron Energy in LAr: Data + Theory of Artazhev

These variations were defined by extrapolation from the measurements shown on p. 9 in DocDB 412. Unlike in the case of longitudinal diffusion, the available world data points do not cover the MicroBooNE field strength. Instead, we looked at a theoretical extrapolations (red curves on p. 9 of previously referenced document).

For the DTdn variation, we used the transverse diffusion constant coming from the data-scaled theory (red dashed curve on that plot) at 0.273 kV/cm. For the DTup variation, we used the constant coming from the unscaled theory (red solid curve) at 0.273 kV/cm; this was a relatively arbitrary choice intended to give a reasonable value above our best guess of the CV. The central value MCC8 uses a transverse diffusion constant corresponding to a nominal MicroBooNE electric field magnitude of 0.5 kV/cm, not the actual field of 0.273 kV/cm. This means that both the DTdn and DTup variations are actually below the CV.
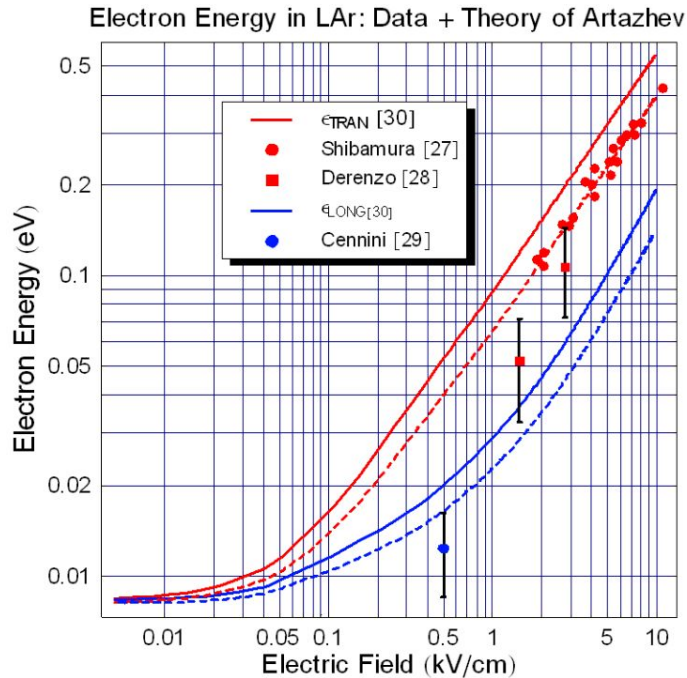
Dynamically Induced Charge

Description of variation: In central value MCC8, induction is simulated only on the wire closest to the drifting charge.

In this variation, the central value MCC8 model for charge induction is replaced by a model that includes longer-range charge induction. This model simulations induction on the closest wire, plus the 10 neighboring wires on each side. The new model is more realistic than the central value MCC8 model, but it is still imperfect in, for example, lacking smooth inter-wire treatment. An improved model developed by the WireCell team will be included in MCC9.

JINST 13, P07007 (2018)

Data/Sim. Response Comparison: U Plane, Normal Region
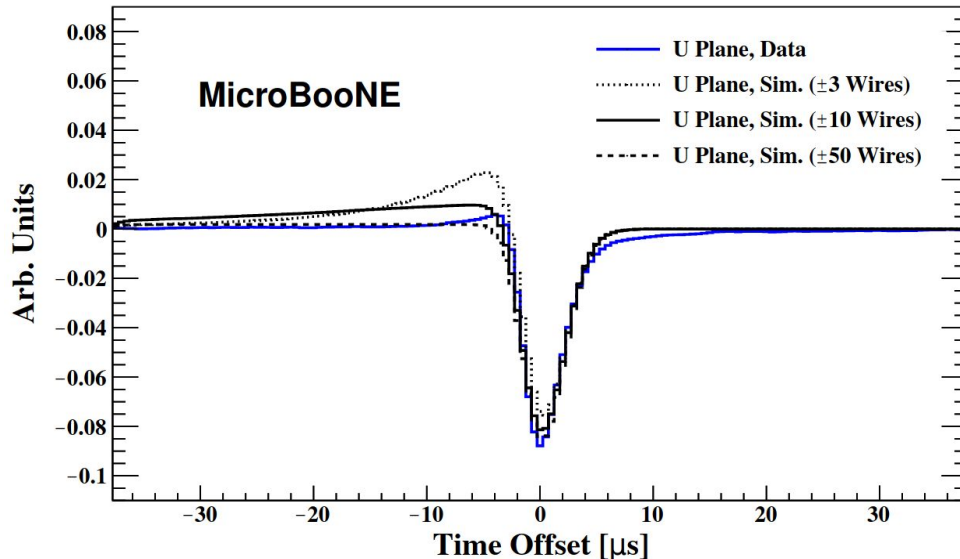
Wire Response Function

Description of variation: Charge induction on the TPC wires is simulated using a set of response functions, bipolar on the U and V planes and unipolar on the Y plane. The same functions are later used to deconvolve the wire signals. The derivation of these functions is described in full in the MicroBooNE Signal Processing II paper.[5]

In this variation, the wire response function of each plane is squeezed by 20%. This represents the approximate uncertainty on the functions, as shown on slides 23–24 of DocDB 9419, according to detector expert Mike Mooney. These squeezed functions are used to simulate the charge induction; the central value functions are still used to deconvolute the signals. We squeezed each plane's response functions for the nominal, shorted-U, and shorted-Y regions of the detector and properly time-alined all of the squeezed functions.

Credit M.Mooney

Wire Response Function

♦ Check accuracy/precision of technique by comparing response estimated from MC to the true simulated response

    • Using the old MCC7 ("v0.1") responses for this check

♦ Find: **~1 μs** residual smearing

Credit M.Mooney

Wire Response Function

♦ Check accuracy/precision of technique by comparing response estimated from MC to the true simulated response

    • Using the old MCC7 ("v0.1") responses for this check

♦ Find: ~1 μs residual smearing

Credit M.Mooney

U Plane After Truth Smearing

V Plane After Truth Smearing

Y Plane After Truth Smearing
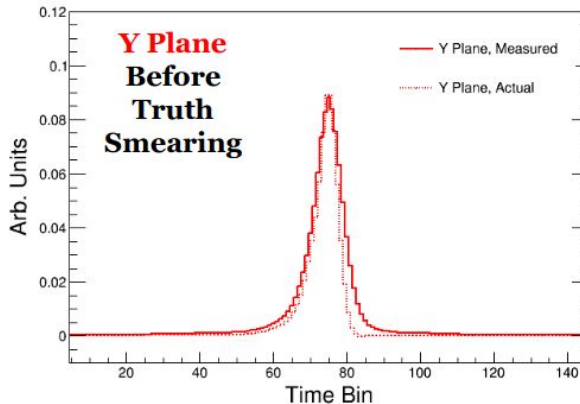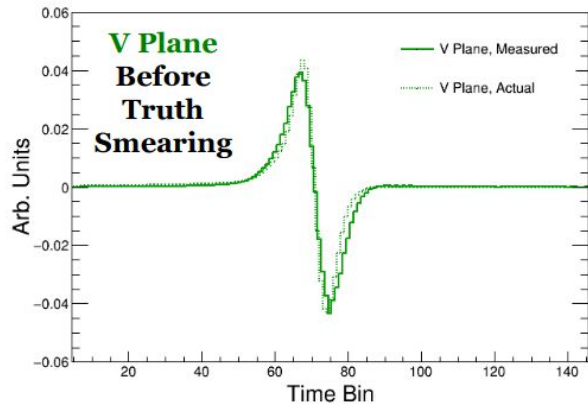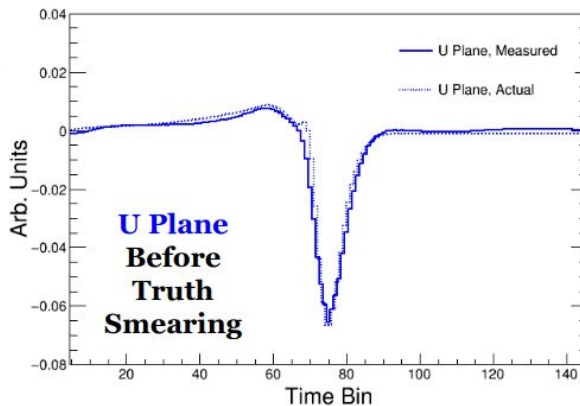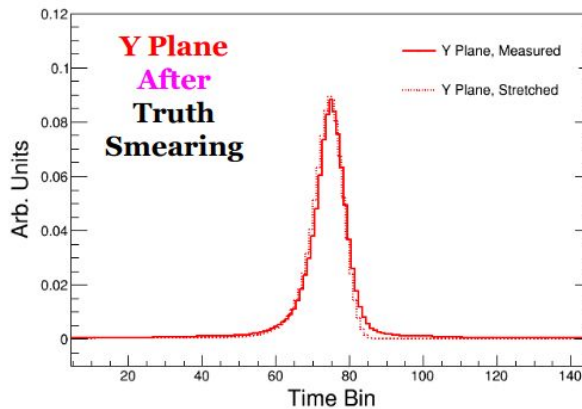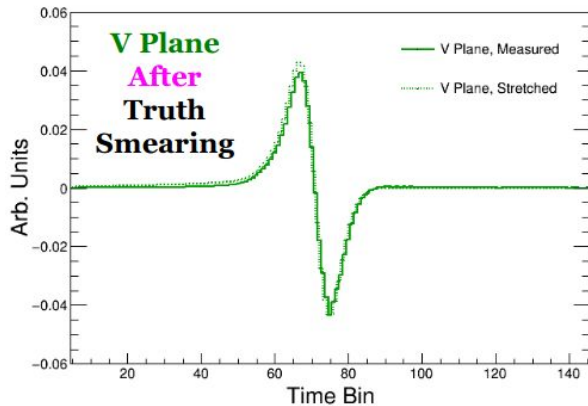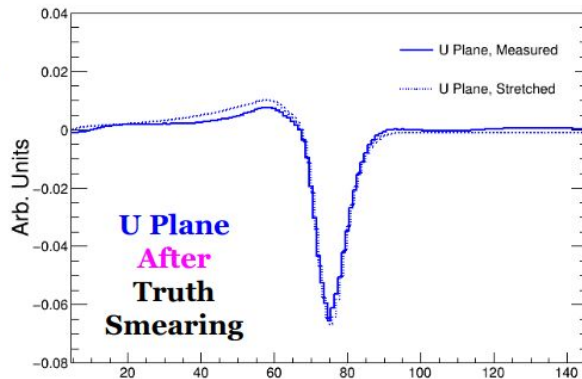
Description of variation: Light production outside the TPC may be imprecisely modeled. In this variation, we increase the light yield outside the TPC by 50%.
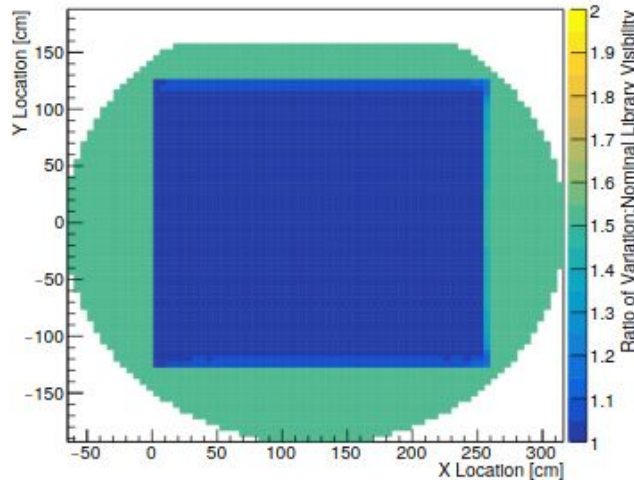
Figure 4: The ratio of systematically varied photon visibility library over our nominal photon visibility library projected onto the xy plane. The core of the TPC is fixed at 1 while the outer volume shifts to 1.5. The blank region at the top of the cryostat is the ullage where no scintillation light is simulated. Plot from Joseph Zennamo.

160

Description of variation: The central value MCC8 models the electron lifetime in liquid argon as infinite. In this variation, we reduce the lifetime to 10 ms, representative of the electron lifetime in the lowest-purity runs included in the good run list.
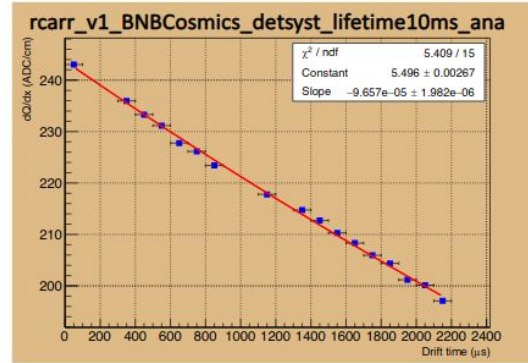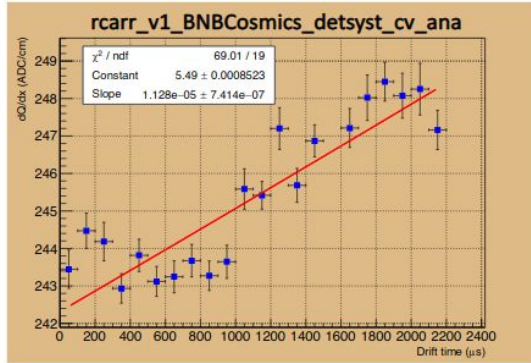
Electron lifetime : -88 619 +/-5.822
QA/QC = 1.025 +/- 0.003 (amount charge left after @ 2.2 ms/amount of initial charge @ 0 ms)

Unphysical e liftme so QA/QC is more ideal

Electron lifetime : 10.355 +/-0.212
QA/QC = 0.809 +/- 0.006 (amount charge left after @ 2.2 ms/amount of initial charge @ 0 ms)

Figure 3: Left, from central value MC: dQ/dx of anode- or cathode-piercing tracks, as a function of drift distance. An estimate of the electron lifetime can be extracted from this plot, following the method in DocDB 6318. The estimate for this sample comes out to be an unphysical value, indicating that the lifetime is effectively infinite. Right, from the sample with an electron lifetime of 10 ms: The same type of plot, showing that for this sample, the extracted lifetime is the expected 10 ms. Plots from Varuna Meddage.

161

Recombination

Description of variation: The central value MC models electron-ion recombination using the modified box model with parameters fit to ArgoNeuT data. This variation substitutes the Birks model with parameters tuned to ICARUS data.

Future Prospects

- Higher statistics

- New simulation

- New signal processing

- Completely new detector uncertainties

- 3-plane PID

- Working on various derived variables

Future Experiments

Long-Baseline Neutrino Facility (LBNF) and
Deep Underground Neutrino Experiment (DUNE)

Conceptual Design Report
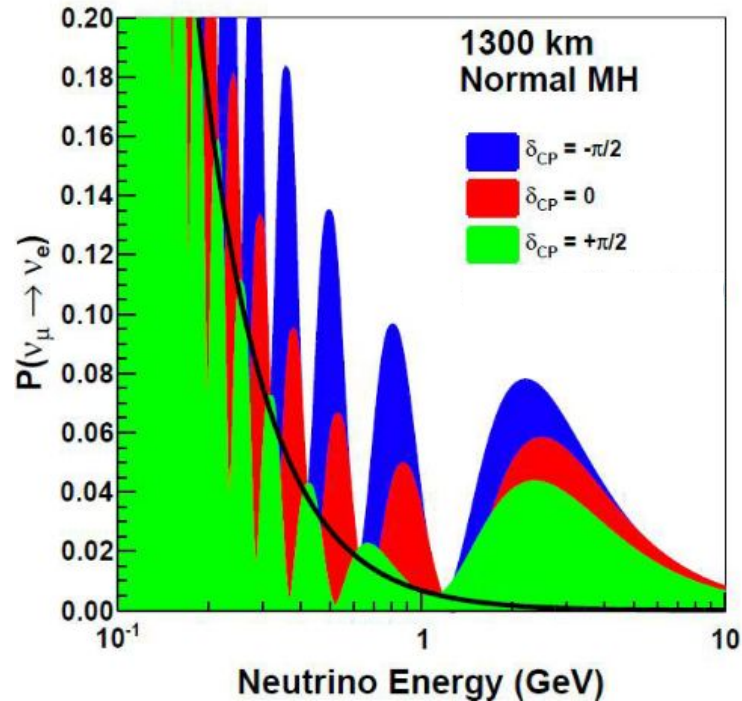
"Uncertainties on the oscillation analysis indicate that uncertainties exceeding 1% for signal and 5% for backgrounds may result in substantial degradation of the sensitivity to CP violation and mass hierarchy"

Incident & Inferred Fluxes
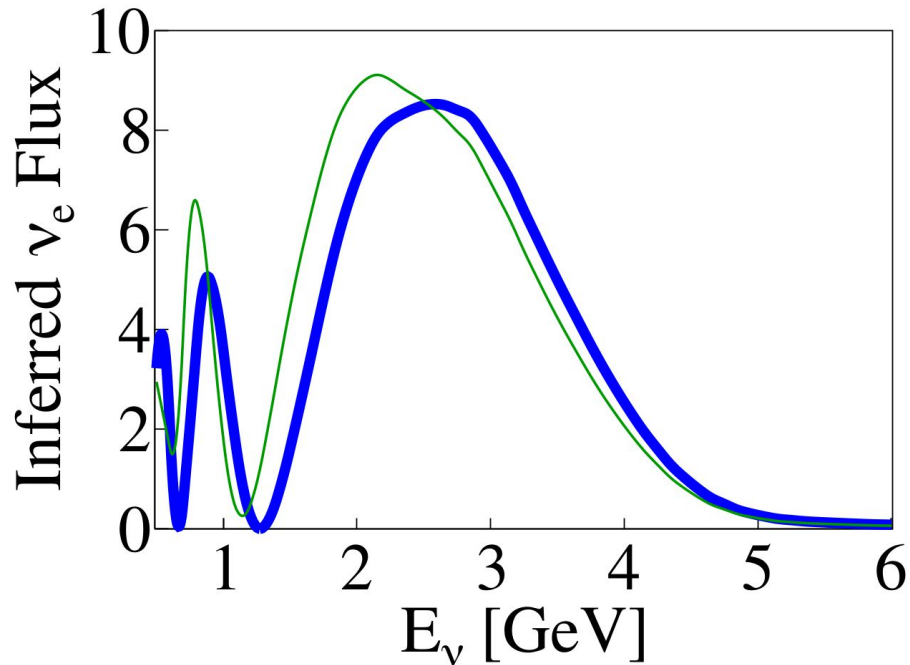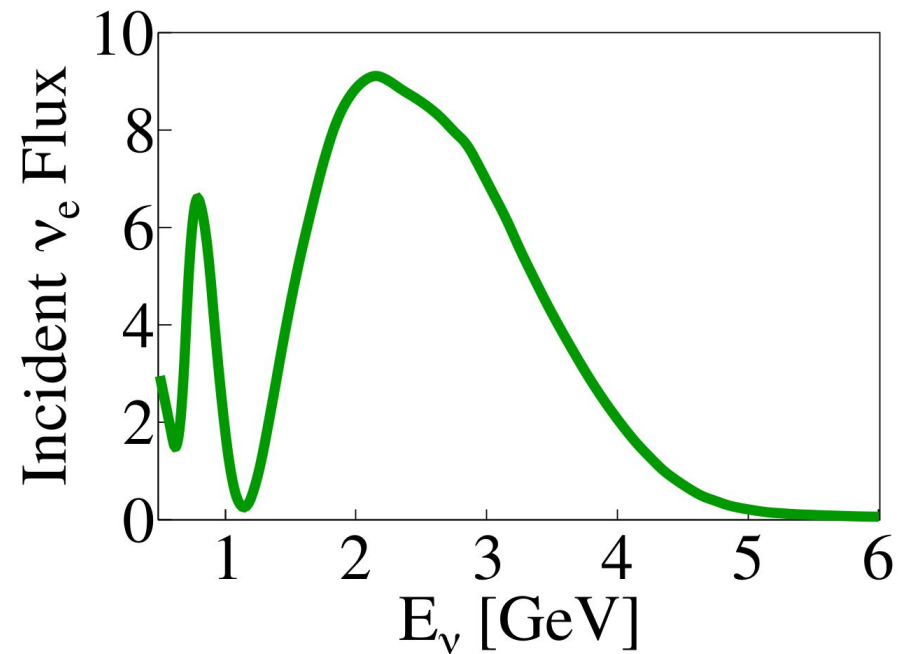
PHYSICS PROCESS

Particles shoot out

Interacts with the nucleus

Neutrino comes in

167

PHYSICS PROCESS
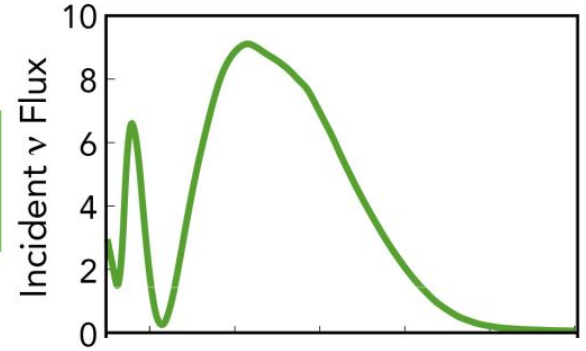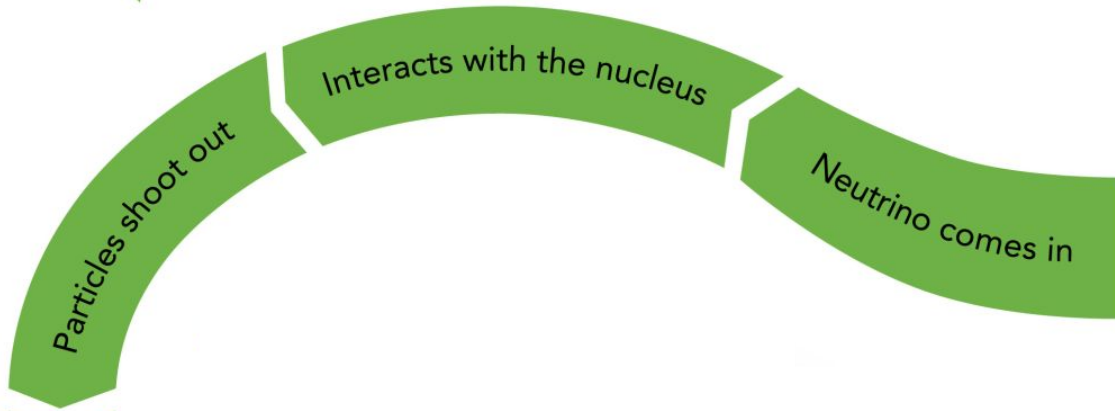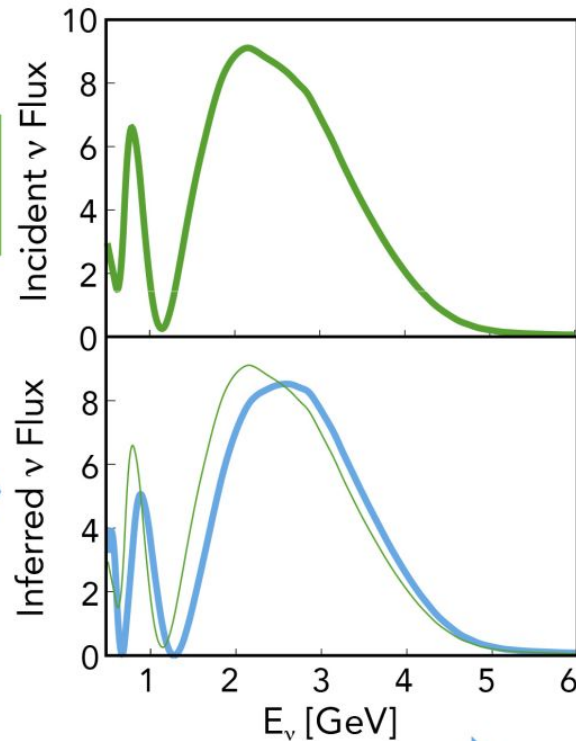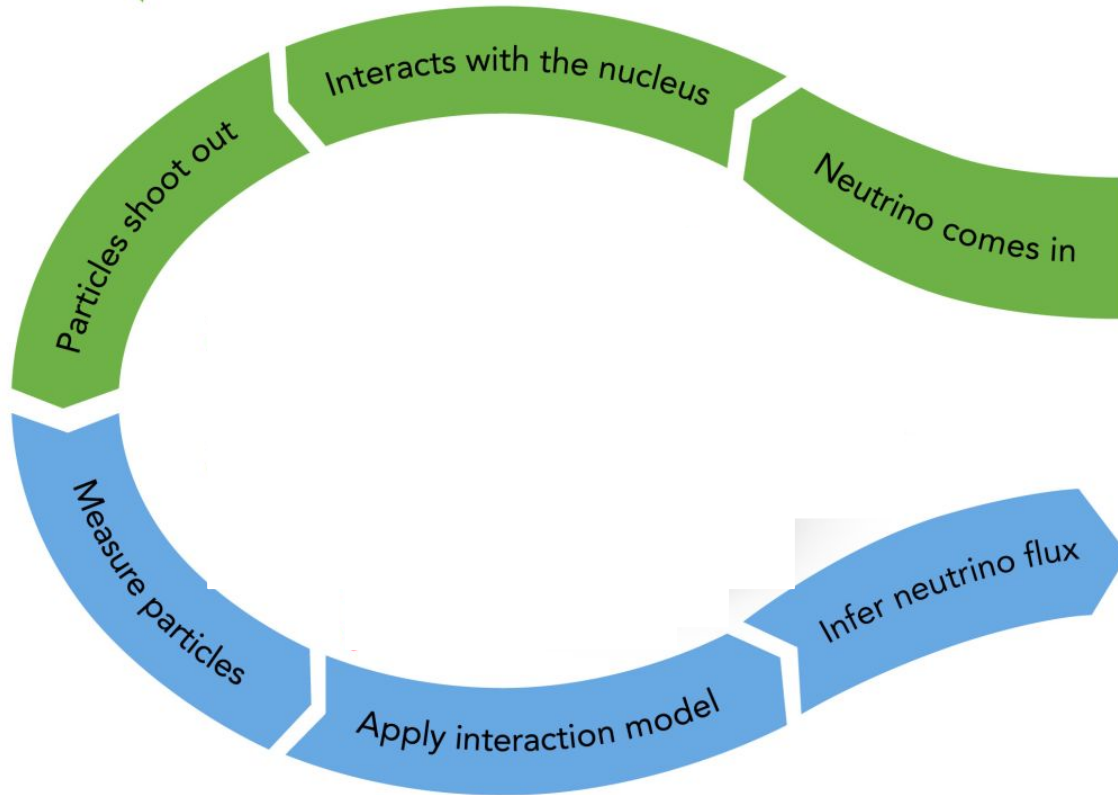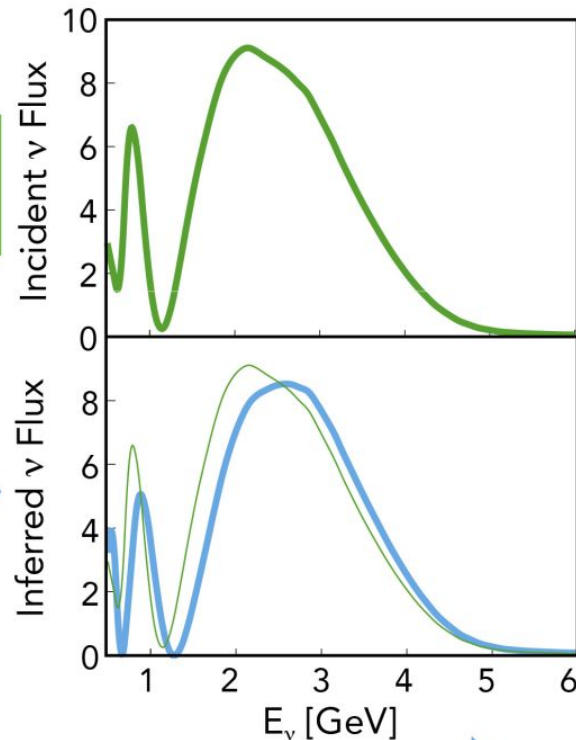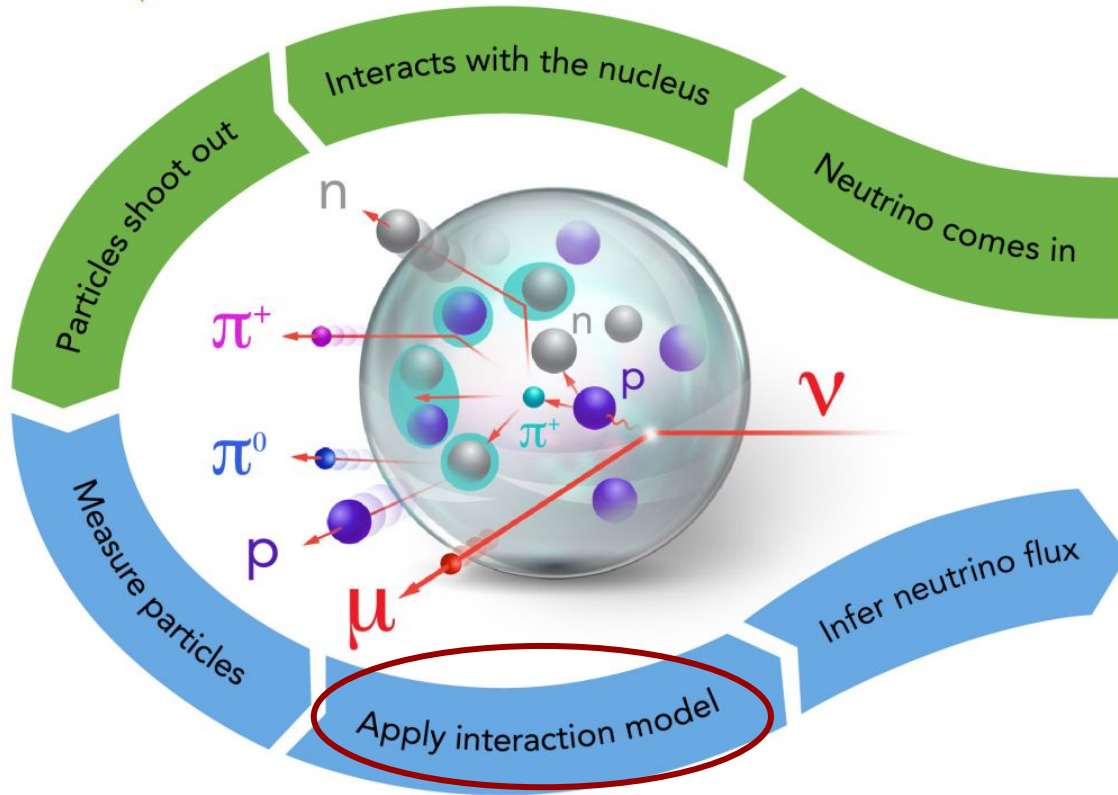
Neutrino comes in
Interacts with the nucleus
Particles shoot out
Measure particles
Apply interaction model
Infer neutrino flux

EXPERIMENTAL ANALYSIS

Incident ν Flux

Inferred ν Flux

E_ν [GeV]

EXPERIMENTAL ANALYSIS

169

Event Rate

$$N(E_{rec}, L) \sim \Sigma_i \int \Phi(E_\nu, L) \, \sigma_i(E_\nu) \, f_{\sigma i}(E_{rec}, E_\nu) dE$$

Neutrino Flux Prediction

Neutrino Cross Section Model

Smearing Matrix
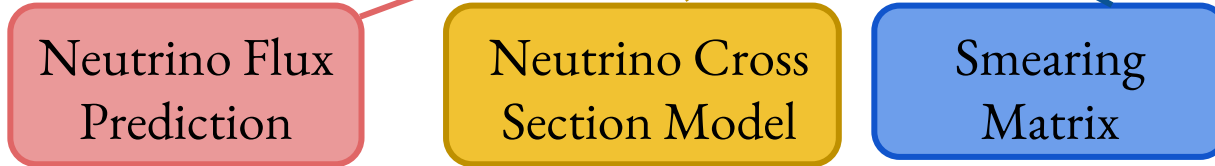
Wide Energy Spectra

- Use final state particles to reconstruct ν energy & direction
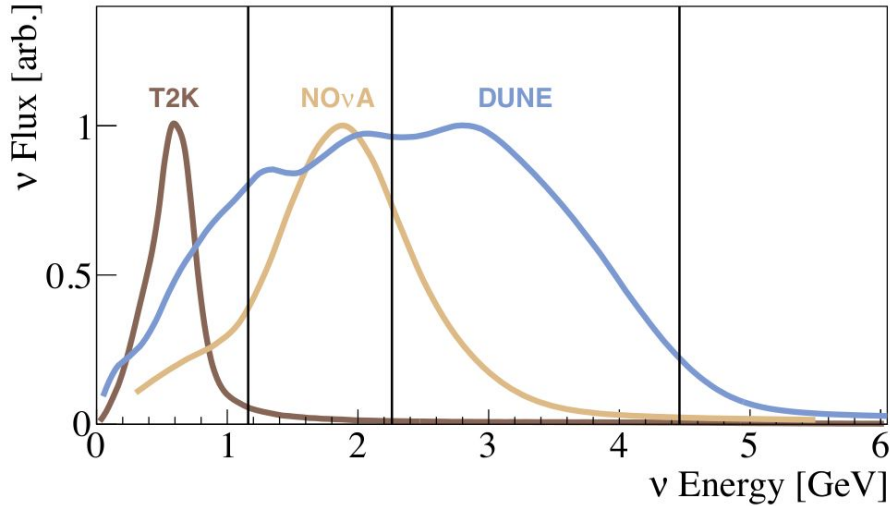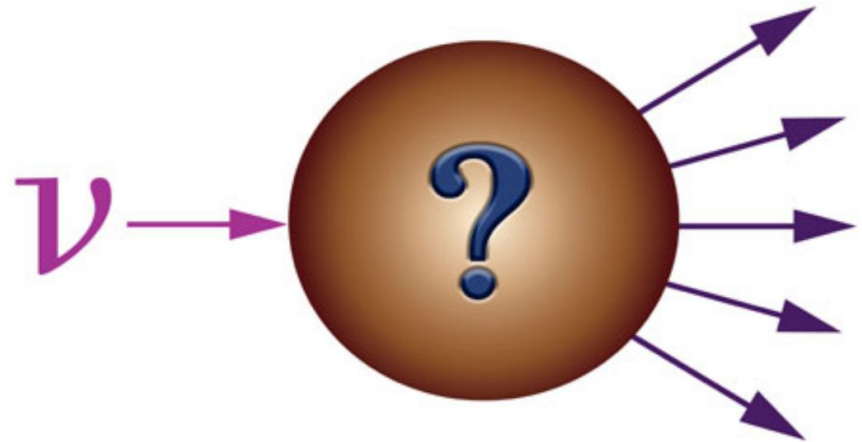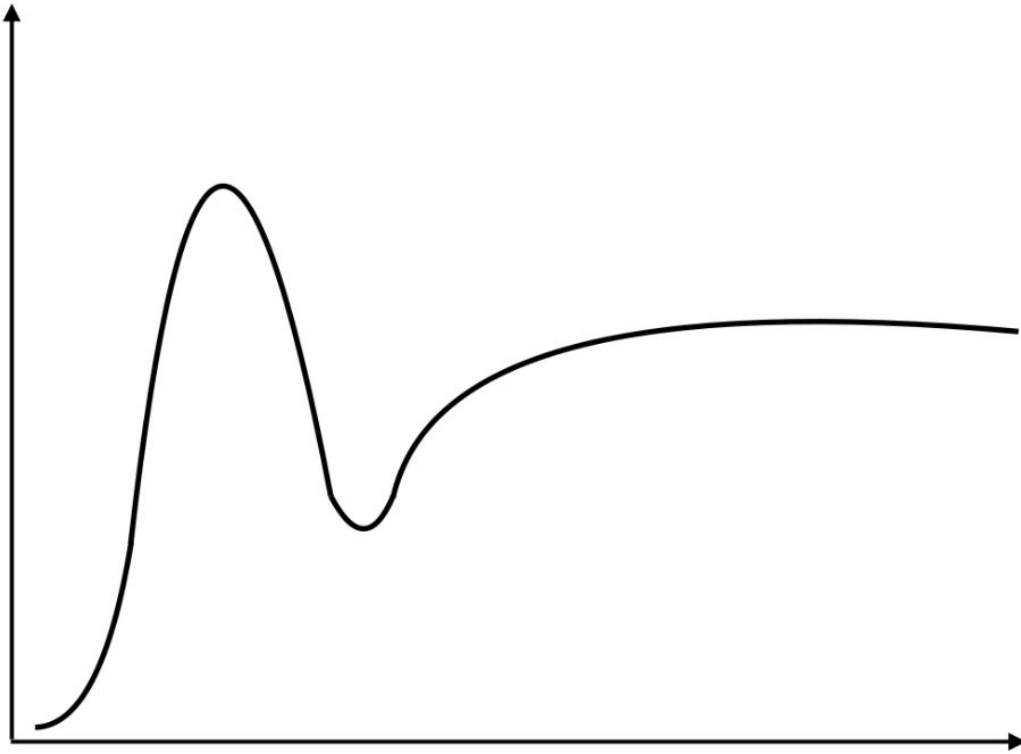
- Very challenging due to nuclear effects & final state interactions

Energy Transfer = $E_l - E_{l'}$

QE

MEC

RES

DIS

Quasi Elastic

Resonance

Deep Inelastic Scattering

Meson Exchange

Energy Transfer = $E_l - E_{l'}$

Free Nucleon

Initial Nuclear State

Extra Nuclear Effects
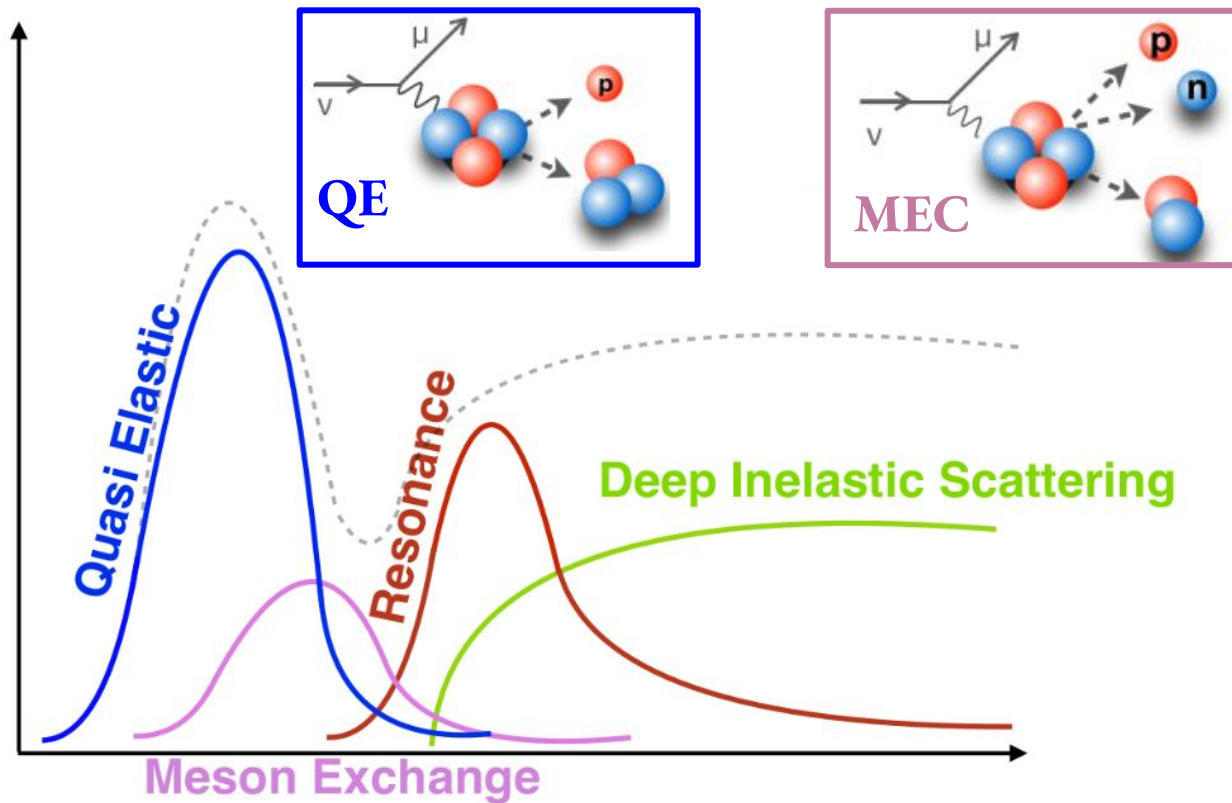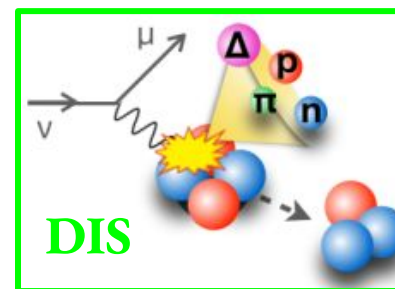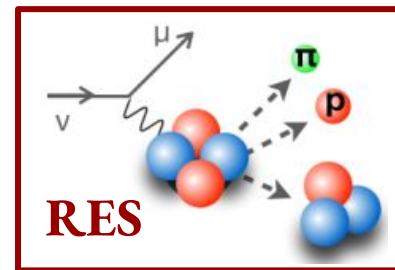
Final State Interactions (FSI)
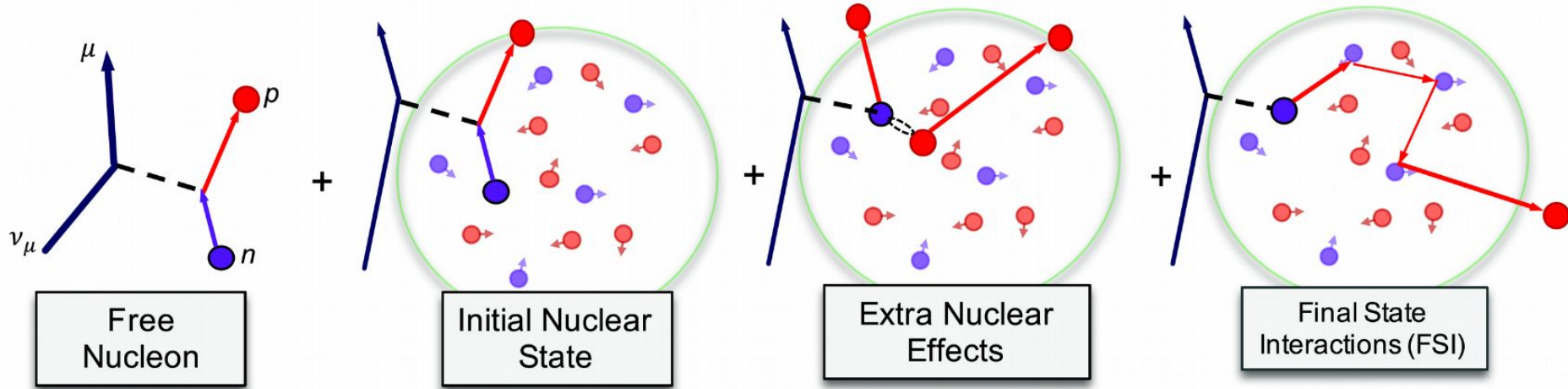
Final state particle content does not isolate initial interaction type!

CCQE

CCRES

2p2h

CC0π
(CCQE-like)

CC1π
(CCRES-like)
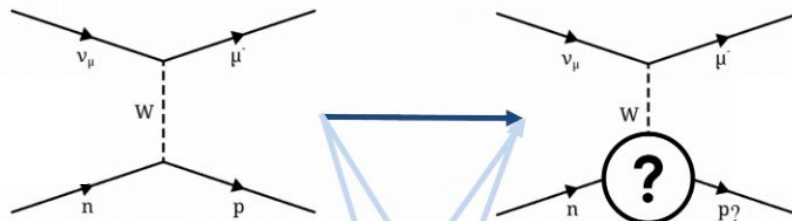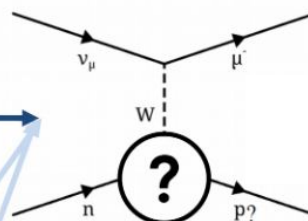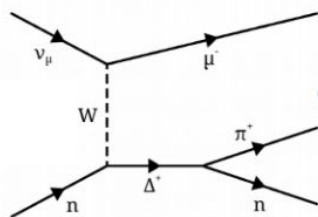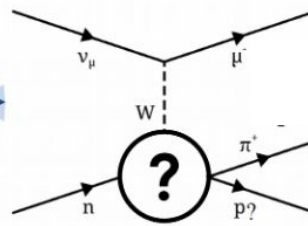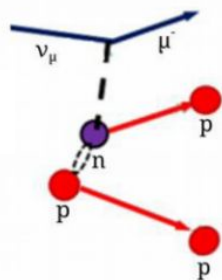
CC0π+Np
(N > 0)
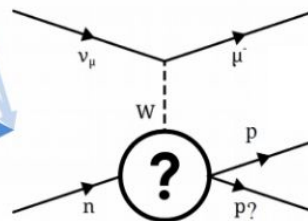
Miss-modelling might impact mixing parameters
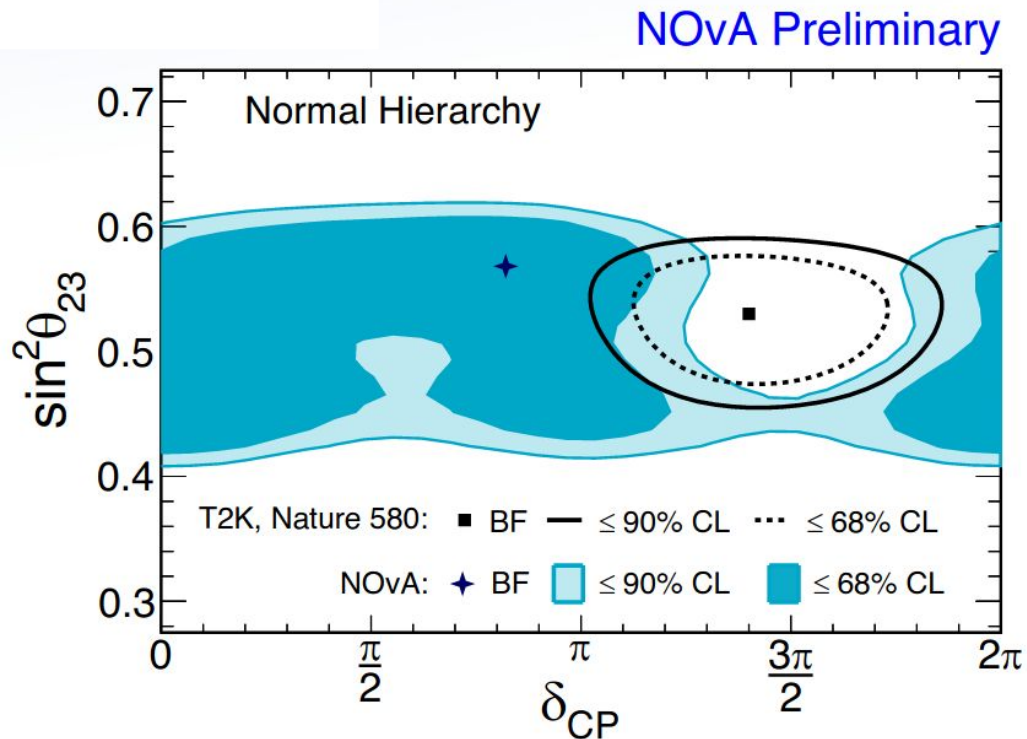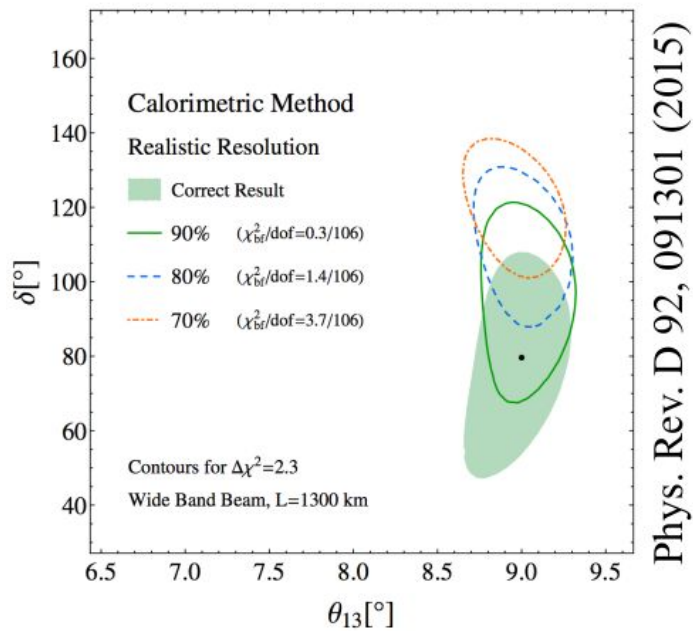
Background Subtraction

Non-QE interactions lead to multi-hadron final states
Gaps make them look like (e,e'p) events
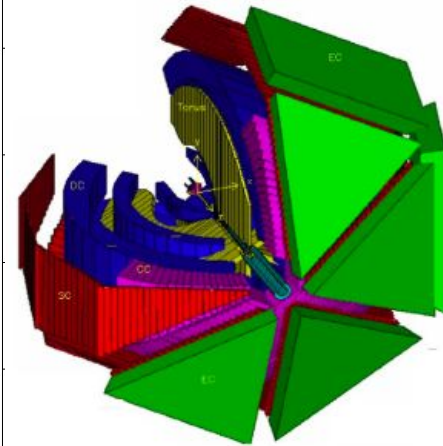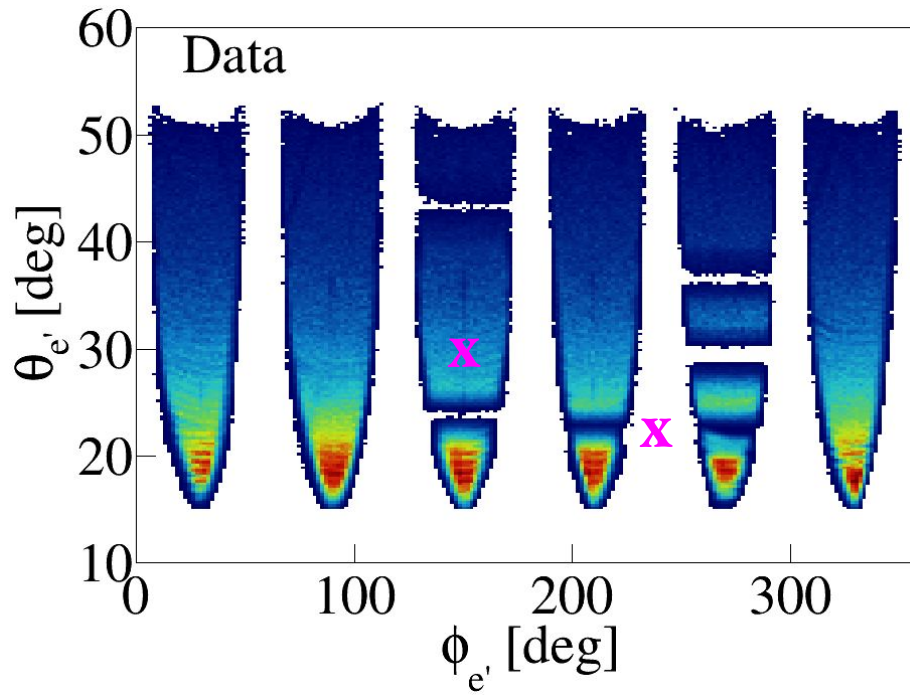
Data Driven Correction

Non-QE interactions lead to multi-hadron final states
Gaps make them look like (e,e'p) events

- Use measured (e,e'pπ) events

- Rotate p, π around q to
determine π detection efficiency

- Subtract undetected (e,e'pπ)

- Repeat for higher hadron multiplicities

A.Papadopoulou
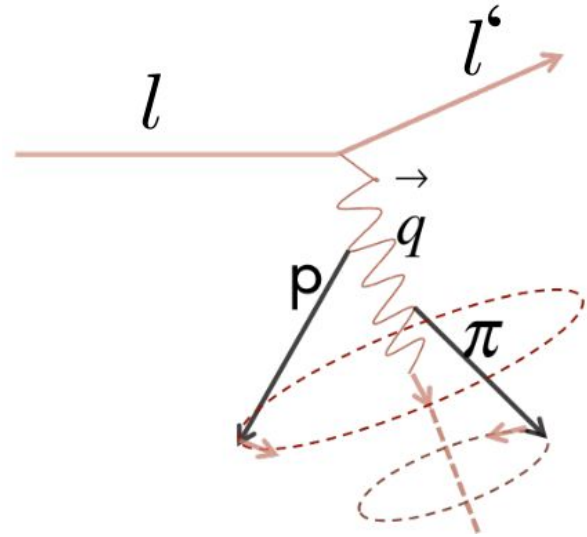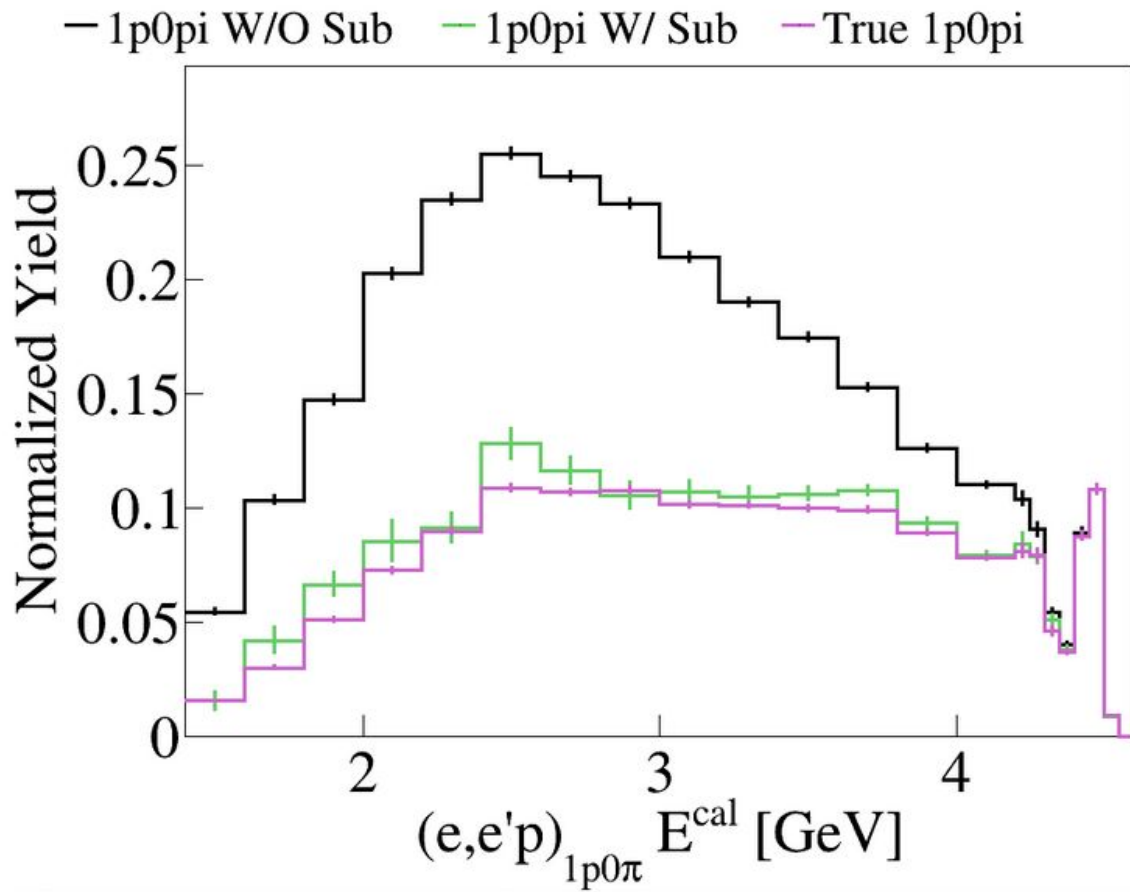
e & ν Similarities (Inclusive Channel)
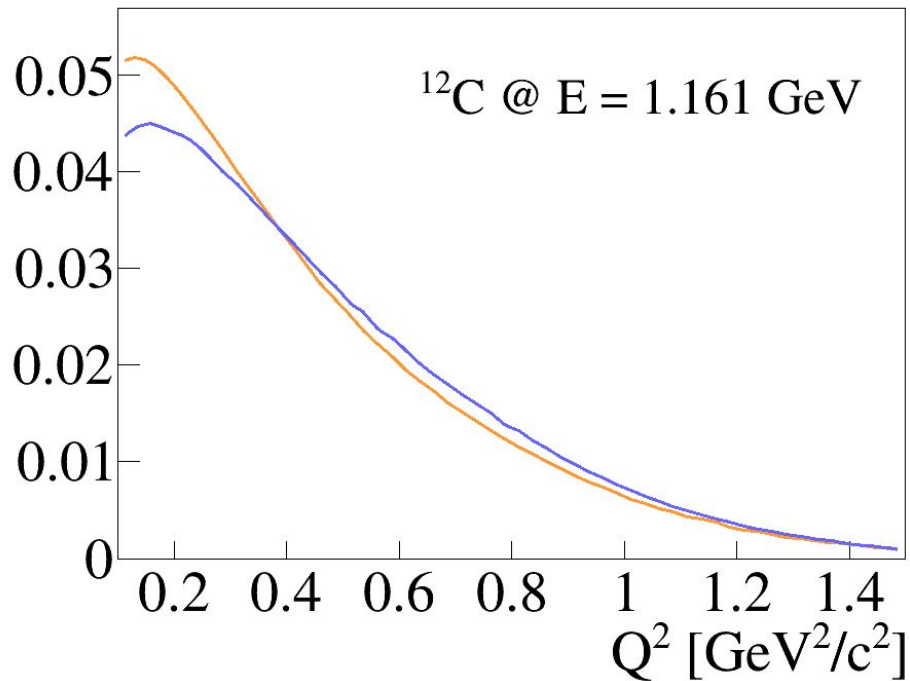
Area Normalized

ν SuSav2   e SuSav2   ν SuSav2   e SuSav2

^{12}C @ E = 1.161 GeV

Area Normalized

$\delta\phi_T$ (degrees)

^{12}C @ E = 1.161 GeV

$Q^2 > 0.1$ GeV^2 / c^2

P_T [GeV/c]
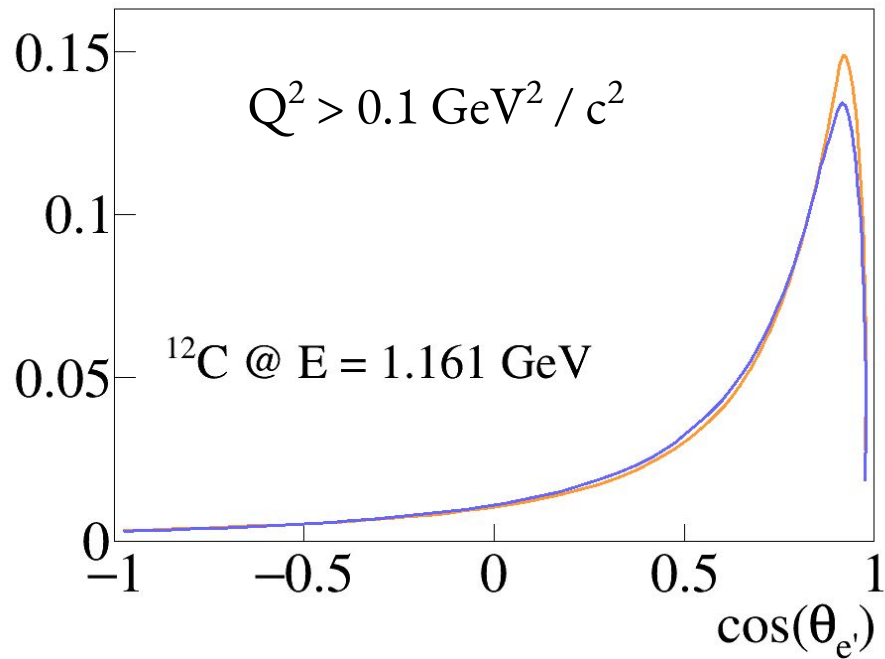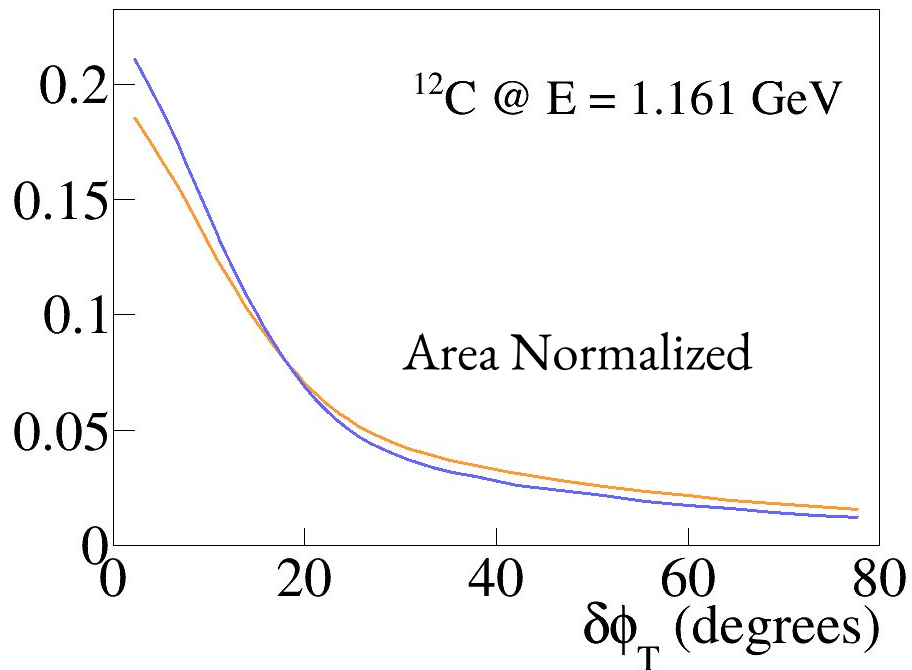
- 1 proton > 300 MeV / c

- 0 $\pi^{+/-}$ > 70 MeV / c

- 0 π^0 or γ
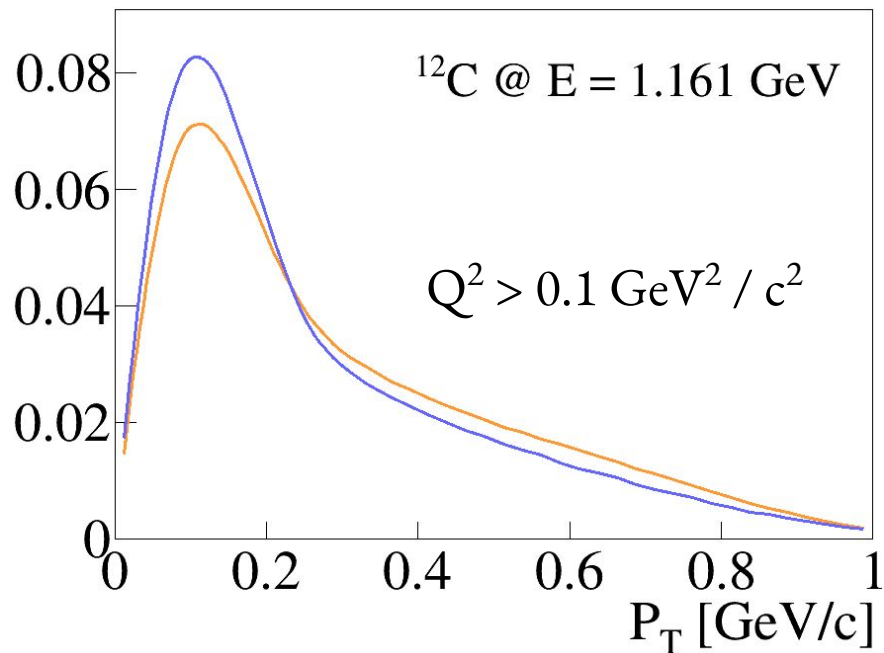
- any number of n
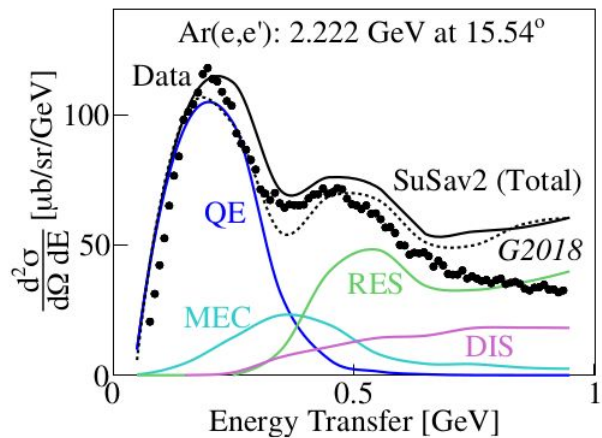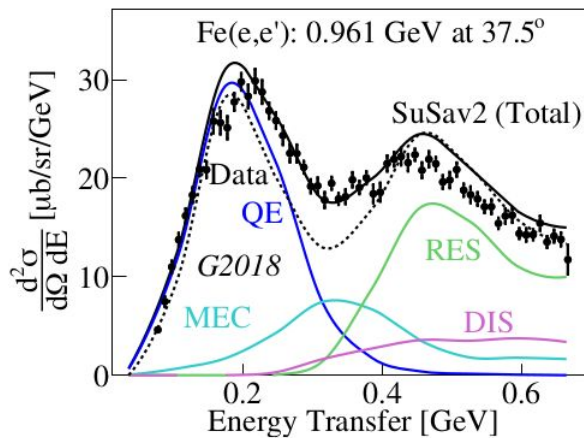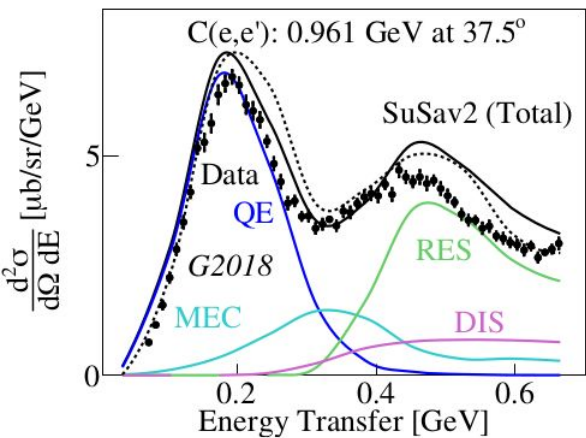
G2018 = G18_10a_02_11a
(default MicroBooNE GENIE tune)

SuSav2 = Superscaling model

Phys. Rev. D 94, 013012 (2016)

(First time that QE & MEC events use the same model for e & ν scattering in GENIE)

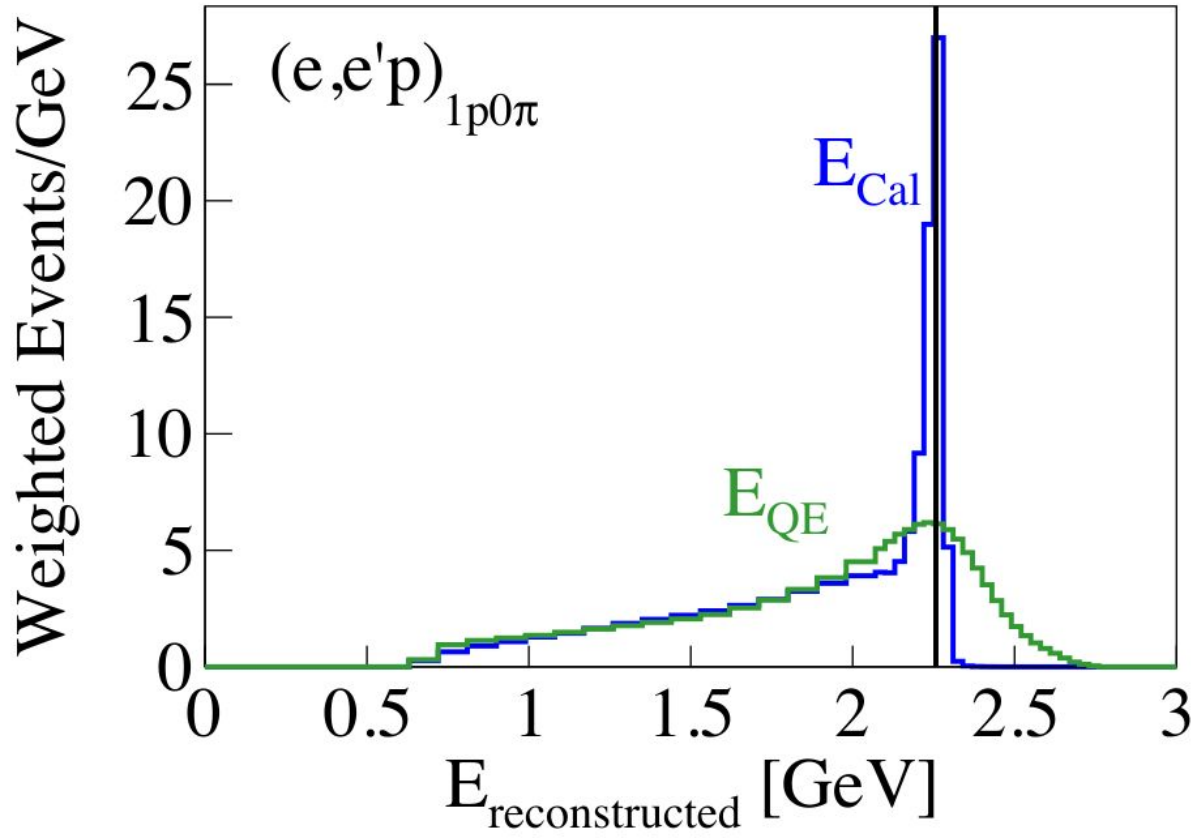More inclusive comparisons arXiv:2009.07228 [nucl-th]
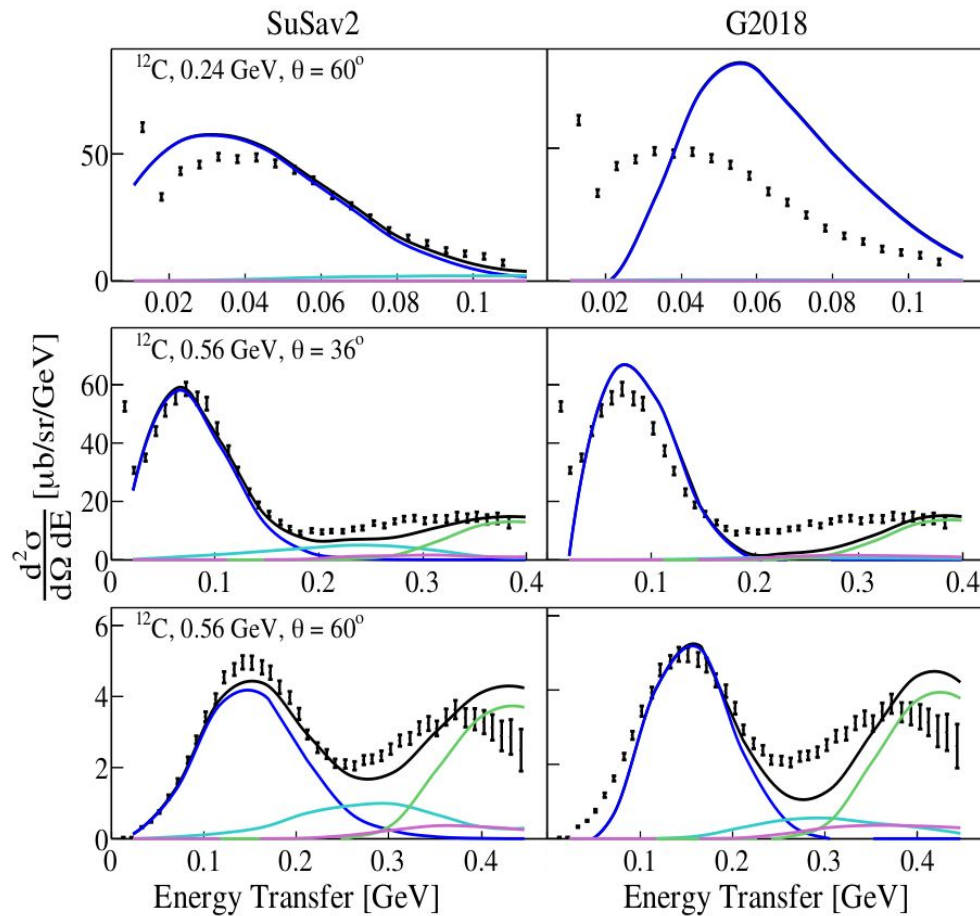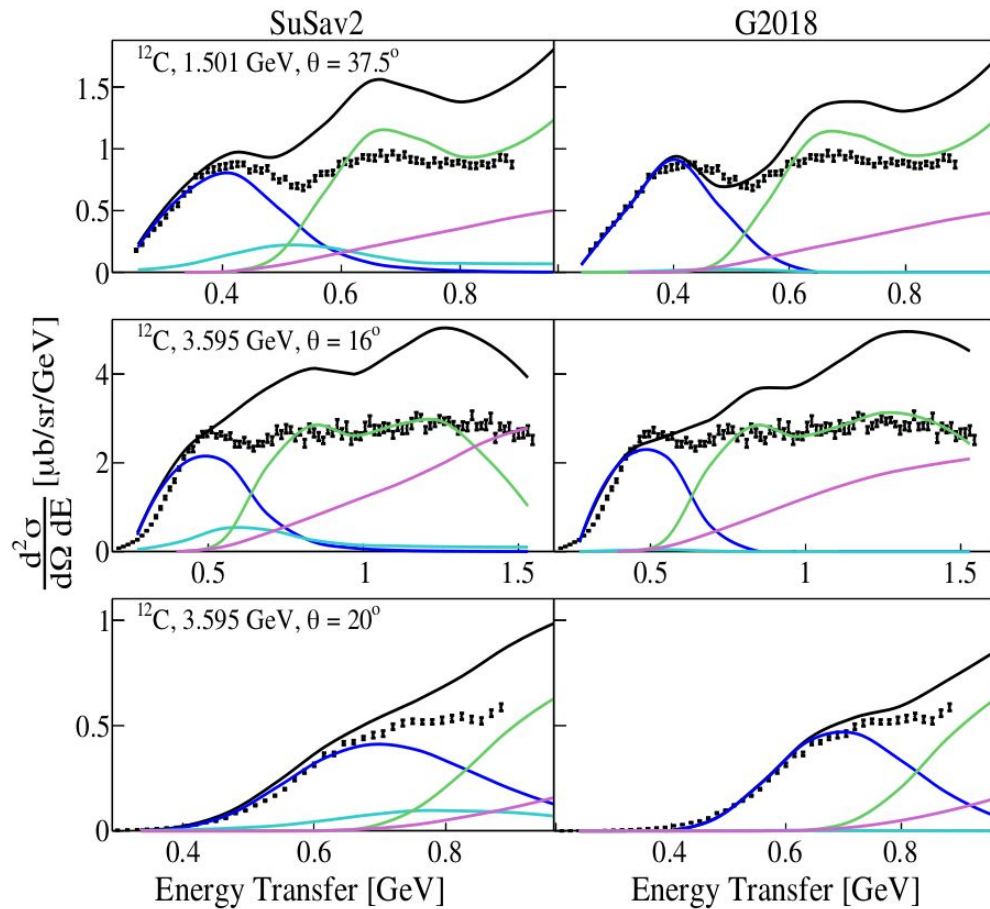
Systematic Uncertainty

- Cross section sector variation (6%)
- Overall normalization (20% ?????)
- Acceptance correction (G2018 vs SuSav2) (20% ?????)
-
-
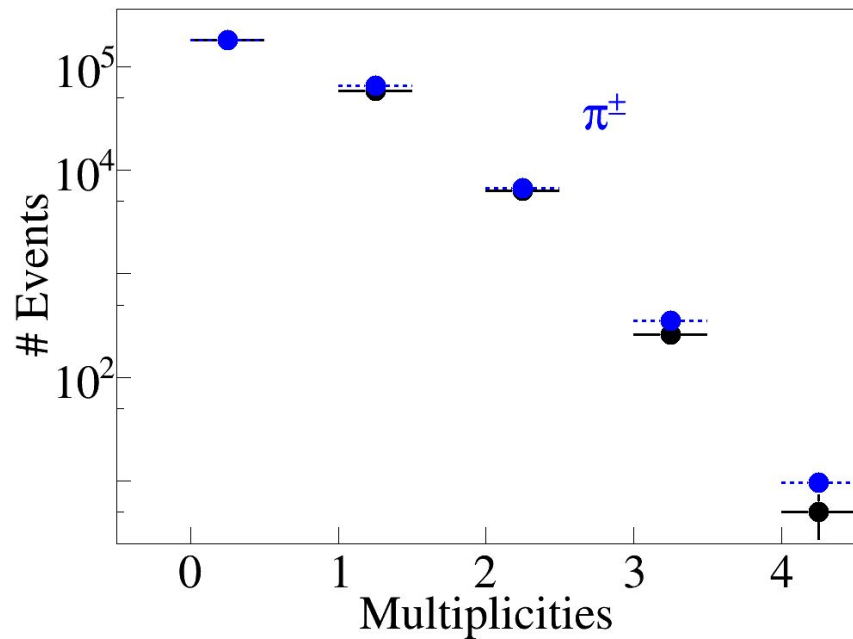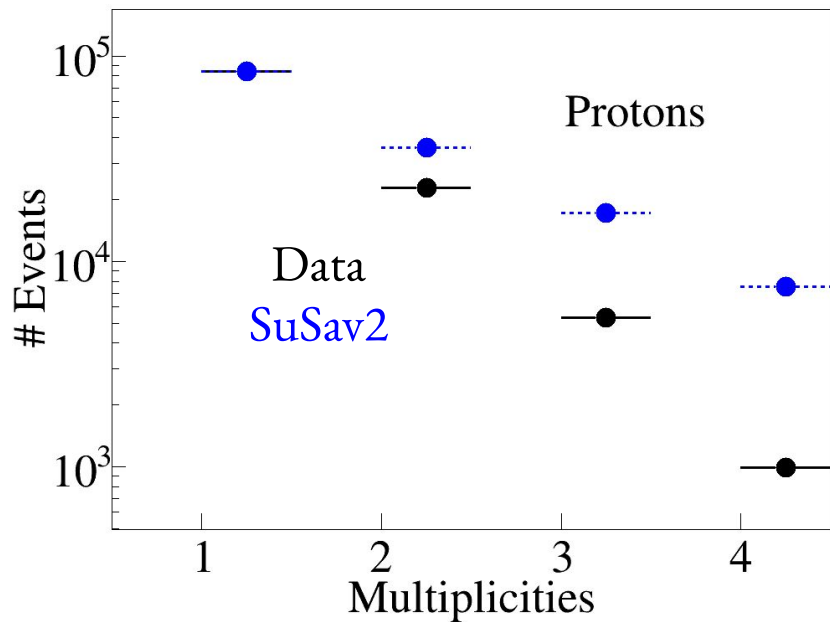
2.257 GeV ^{12}C

$(e,e'p)_{1p0\pi}$

E_{Cal}

E_{QE}

Weighted Events/GeV

$E_{reconstructed}$ [GeV]

2.257 GeV

^{4}He
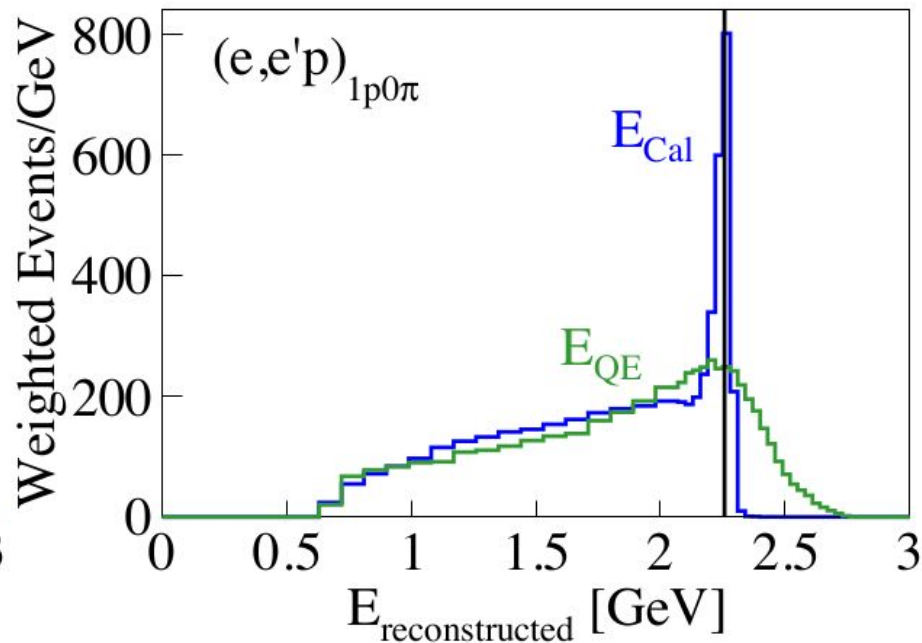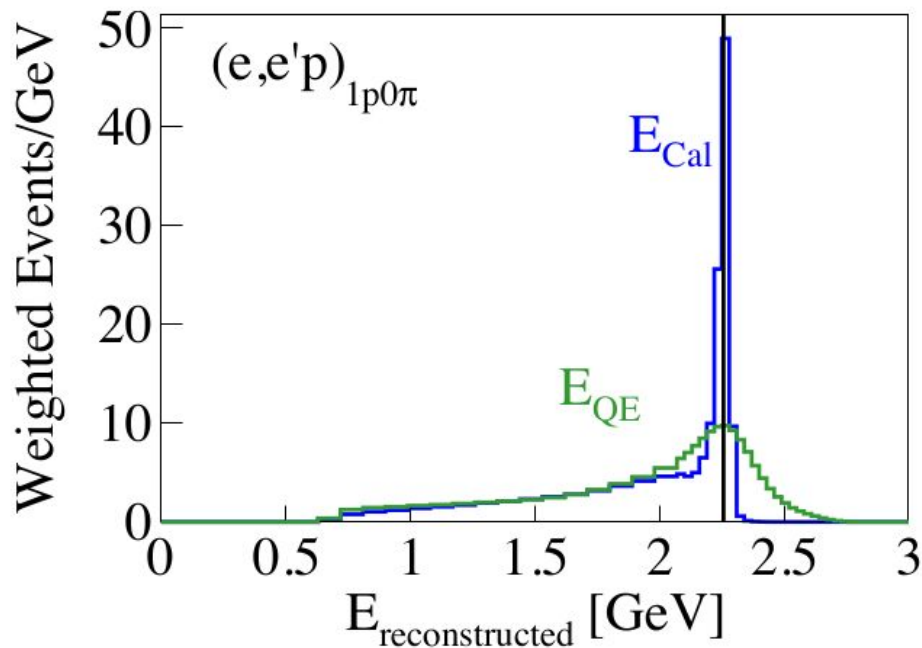
^{56}Fe

^{56}Fe

2.257 GeV
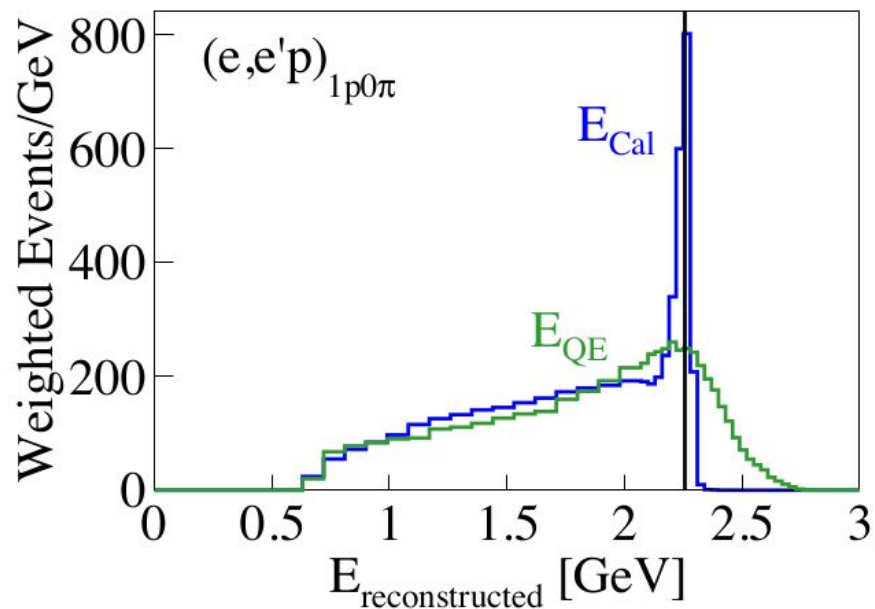
4.453 GeV
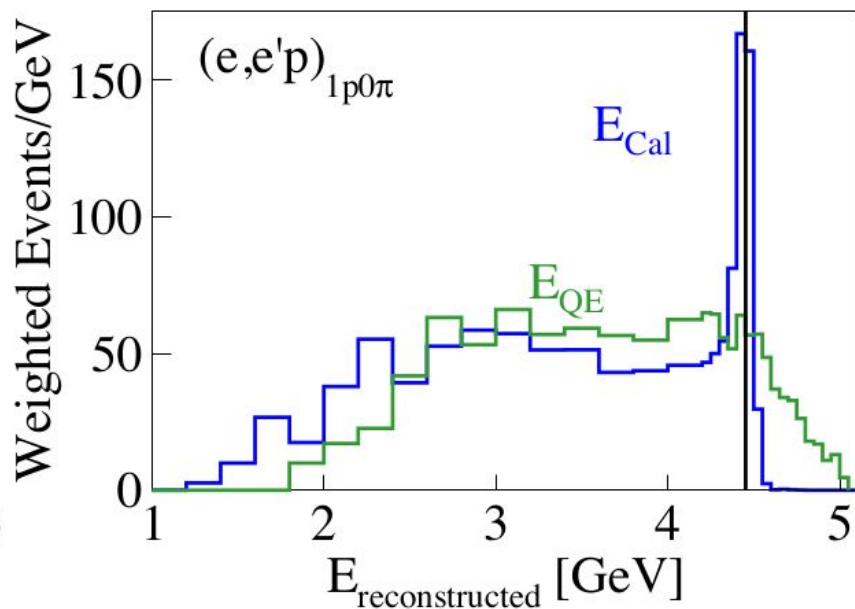
Transverse Missing Momentum

$C(e,e'p)_{1p0\pi}$ @ E = 2.257 GeV

- ◆ Data
- — SuSav2 (Total)
- ···· G2018
- — QE
- — RES
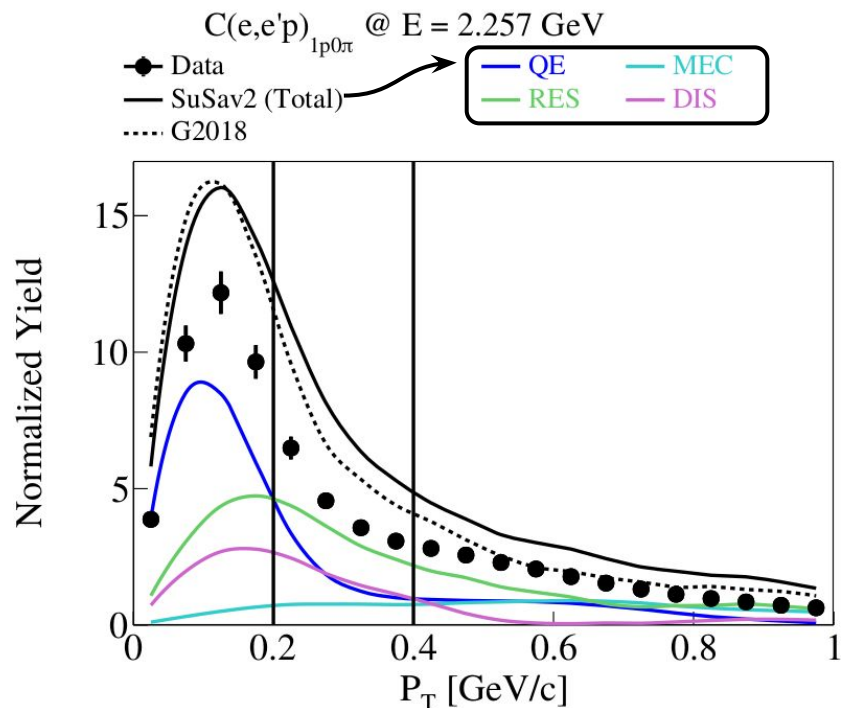- — MEC
- — DIS
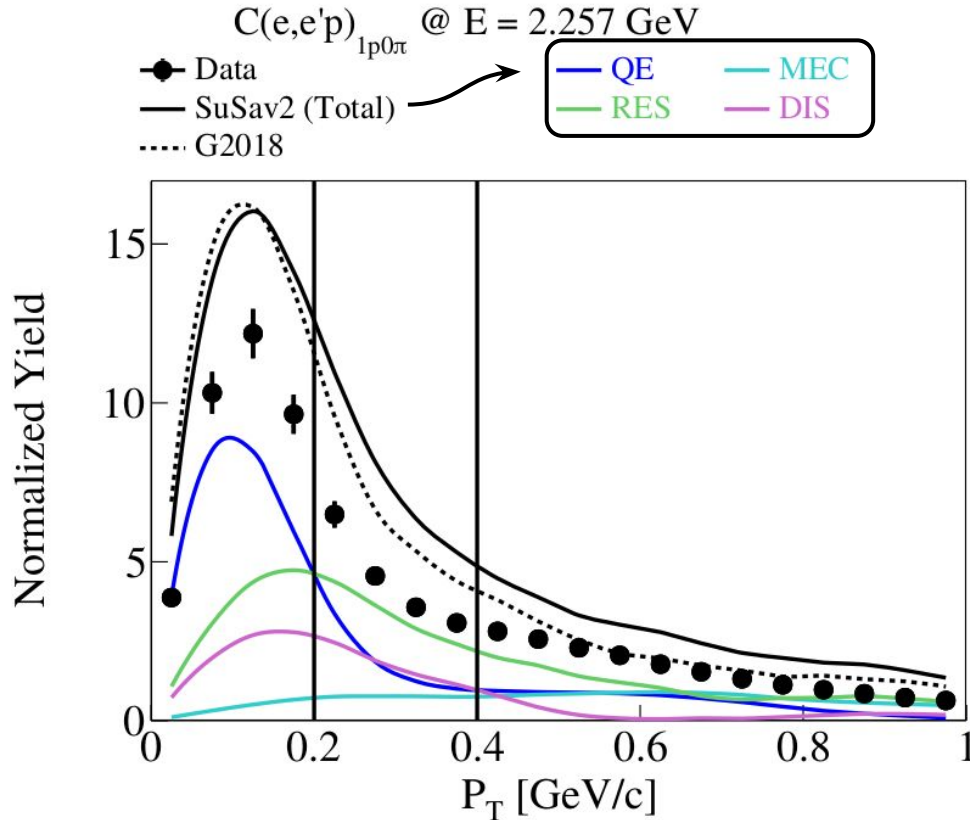
$$\vec{P}_T = \vec{P}_T^{\,e'} + \vec{P}_T^{\,p}$$
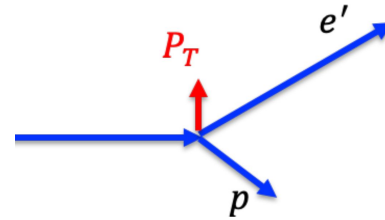
Simulation overpredicts strength
However, overall good shape agreement

Equivalent MicroBooNE Single
Transverse Variable analysis will follow

$C(e,e'p)_{1p0\pi}$ @ E = 2.257 GeV

- Data
- SuSav2 (Total)
- G2018
- QE
- RES
- MEC
- DIS

Normalized Yield

P_T [GeV/c]

$0 < P_T < 200$ [MeV/c]

$200 < P_T < 400$ [MeV/c]

$P_T > 400$ [MeV/c]

Normalized Yield
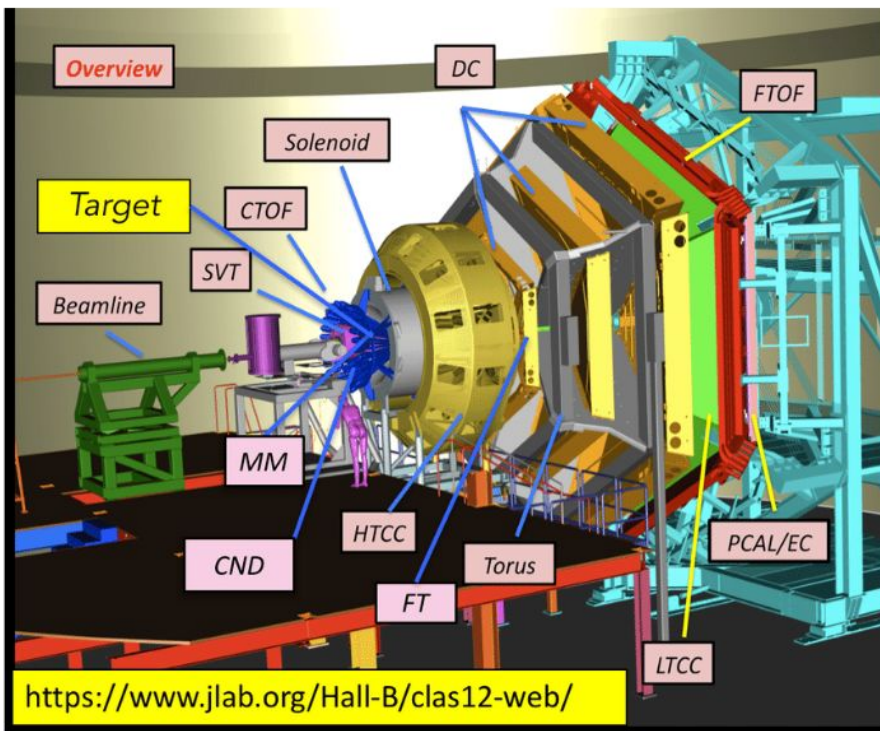
$(e,e'p)_{1p0\pi}$ E_{cal} [GeV]

Splitting phase space in P_T slices

Data/MC disagreement in E_{cal} for higher P_T
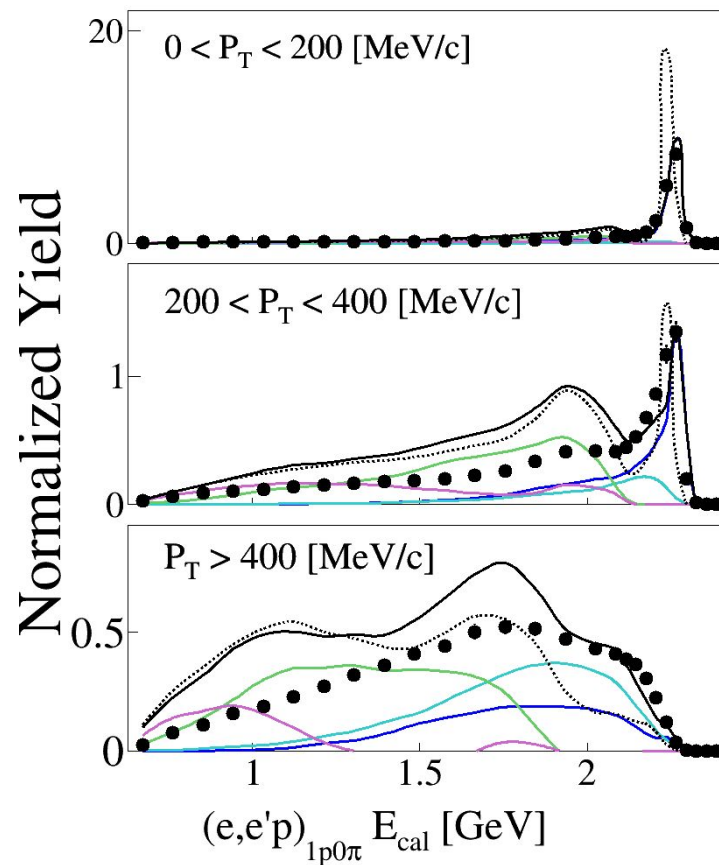
CLAS 12

Jefferson Lab

Forward Detector

- Torus Magnet
- Drift Chamber (DC)
- Forward Time of Flight (FTOF)
- High-threshold Cherenkov Counter (HTCC)
- Low-threshold Cherenkov Counter (LTCC)
- Ring Imaging Cherenkov Detector (RICH)
- Preshower + Electromagnetic Calorimeter (PCAL/EC)
- Forward Tagger (FT)
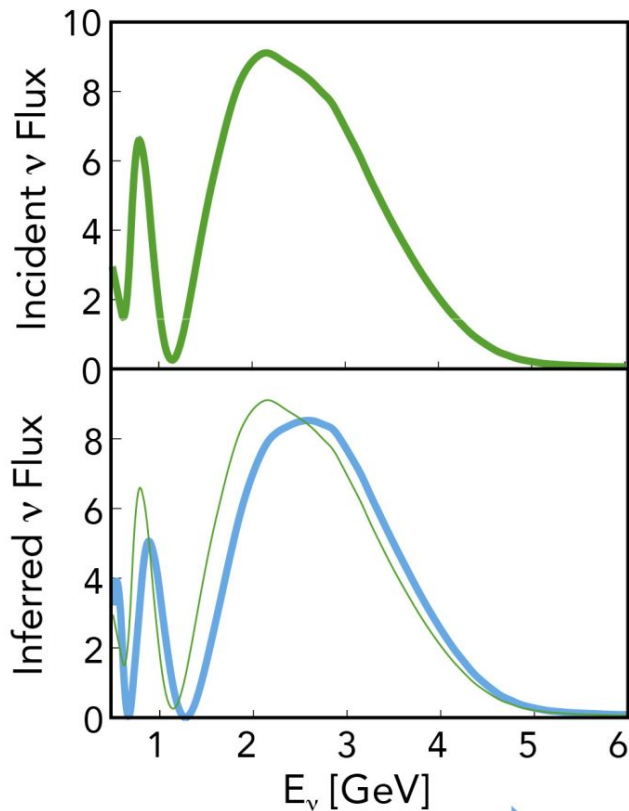
■ **Longitudinally Polarized Electron Beam**
  - E = 10.6 GeV
  - P = 86–89%

■ **Unpolarized Liquid H_2 Fixed Target**

■ Torus magnet → electrons inbending

https://www.jlab.org/Hall-B/clas12-web/

C. Dilks

16

$$N(E_{rec}, L) \sim \Sigma_i \int \Phi(E_\nu, L)\, \sigma_i(E_\nu)\, f_{\sigma i}(E_{rec}, E_\nu)\, dE$$

Smearing Matrix

Oscillated incident energy spectrum

Smear with GENIE-derived feed-down matrix

Reconstruct with data-derived feed-dow matrix

Improvement of event generators needed !

Smearing Matrix